TECHNICAL REPORT STANDARD TITLE PAGE

1. Report No.	2. Government Accession No.	3. Recipient's Catalog No.
FHWA/TX-86/14+417-1F		

4. Title and Subtitle	5. Report Date
A Low-Maintenance, Energy-Absorbing Bridge Rail	October 1986
	6. Performing Organization Code

7. Author(s)	8. Performing Organization Report No.
W. Lynn Beason, J. C. Cain and T. J. Hirsch	Research Report 417-1F

9. Performing Organization Name and Address	10. Work Unit No.
Texas Transportation Institute The Texas A&M University System College Station, Texas 77843	11. Contract or Grant No. Study No. 2-5-83-417
	13. Type of Report and Period Covered Final - September 1982 October 1986
12. Sponsoring Agency Name and Address Texas State Department of Highways and Public Transportation; Transportation Planning Division P. O. Box 5051 Austin, Texas 78763	14. Sponsoring Agency Code

15. Supplementary Notes

Research performed in cooperation with DOT, FHWA.
Research Study Title: Energy-Absorbing Traffic Rail

16. Abstract

A low-maintenance, energy-absorbing bridge rail has been developed for use in high traffic volume situation where the cost of repairing conventional bridge rails has become prohibitively expansive. The new bridge rail is designed to meet or exceed current bridge rail design guidelines. The new bridge rail incorporates structural steel tube railings and posts and high strength rubber energy absorbers. The new bridge rail is designed to be installed on new or existing standard bridge decks. Results of crash tests show that the bridge rail can smoothly redirect a 4500 lb (2043 kg) automobile impacting with a velocity of 60 mph (96.6 km/hr) and an angle of 25° and remain in service with no maintenance. If exposed to a more severe impact, the bridge rail may have to be repaired, but the bridge deck will remain undamaged. Finally, the new energy-absorbing rail occupies less bridge deck area than conventional bridge rails.

17. Key Words	18. Distribution Statement
Bridge Rail, Energy Absorbing, Crash Test(s), Retrofit, Bridge Deck, Safety.	No restrictions. This document is available to the public through the National Technical Information Service 5825 Port Royal Road Springfield, Virginia 22161

19. Security Classif. (of this report)	20. Security Classif. (of this page)	21. No. of Pages	22. Price
Unclassified	Unclassified	94	

Form DOT F 1700.7 (8-69)

A LOW-MAINTENANCE, ENERGY-ABSORBING BRIDGE RAIL

by

W. Lynn Beason
J. C. Cain
T. J. Hirsch

Research Report 417-1F
on
Research Study No. 2-5-83-417
Energy-Absorbing Traffic Rail

Sponsored by
State Department of Highways and Public Transportation
in cooperation with
U.S. Department of Transportation
Federal Highway Administration

October 1986

Texas Transportation Institute
The Texas A&M University System
College Station, Texas

METRIC CONVERSION FACTORS

Approximate Conversions to Metric Measures

Symbol	When You Know	Multiply by	To Find	Symbol
	LENGTH			
in	inches	*2.5	centimeters	cm
ft	feet	30	centimeters	cm
yd	yards	0.9	meters	m
mi	miles	1.6	kilometers	km
	AREA			
in^2	square inches	6.5	square centimeters	cm^2
ft^2	square feet	0.09	square meters	m^2
yd^2	square yards	0.8	square meters	m^2
mi^2	square miles	2.6	square kilometers	km^2
	acres	0.4	hectares	ha
	MASS (weight)			
oz	ounces	28	grams	g
lb	pounds	0.45	kilograms	kg
	short tons (2000 lb)	0.9	tonnes	t
	VOLUME			
tsp	teaspoons	5	milliliters	ml
Tbsp	tablespoons	15	milliliters	ml
fl oz	fluid ounces	30	milliliters	ml
c	cups	0.24	liters	l
pt	pints	0.47	liters	l
qt	quarts	0.95	liters	l
gal	gallons	3.8	liters	l
ft^3	cubic feet	0.03	cubic meters	m^3
yd^3	cubic yards	0.76	cubic meters	m^3
	TEMPERATURE (exact)			
°F	Fahrenheit temperature	5/9 (after subtracting 32)	Celsius temperature	°C

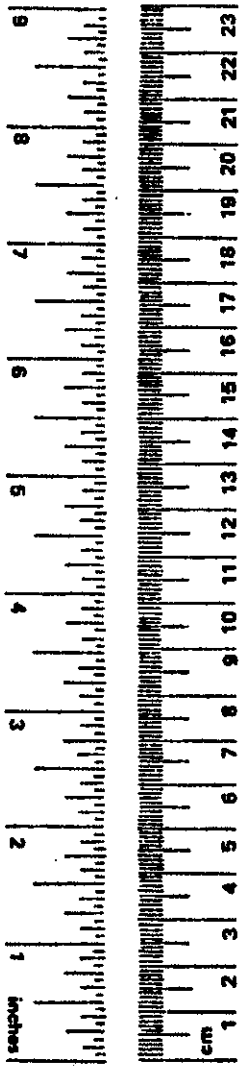

*1 in = 2.54 (exactly). For other exact conversions and more detailed tables, see NBS Misc. Publ. 286, Units of Weights and Measures, Price $2.25, SD Catalog No. C13.10:286.

Approximate Conversions from Metric Measures

Symbol	When You Know	Multiply by	To Find	Symbol
	LENGTH			
mm	millimeters	0.04	inches	in
cm	centimeters	0.4	inches	in
m	meters	3.3	feet	ft
m	meters	1.1	yards	yd
km	kilometers	0.6	miles	mi
	AREA			
cm^2	square centimeters	0.16	square inches	in^2
m^2	square meters	1.2	square yards	yd^2
km^2	square kilometers	0.4	square miles	mi^2
ha	hectares (10,000 m^2)	2.5	acres	
	MASS (weight)			
g	grams	0.035	ounces	oz
kg	kilograms	2.2	pounds	lb
t	tonnes (1000 kg)	1.1	short tons	
	VOLUME			
ml	milliliters	0.03	fluid ounces	fl oz
l	liters	2.1	pints	pt
l	liters	1.06	quarts	qt
l	liters	0.26	gallons	gal
m^3	cubic meters	35	cubic feet	ft^3
m^3	cubic meters	1.3	cubic yards	yd^3
	TEMPERATURE (exact)			
°C	Celsius temperature	9/5 (then add 32)	Fahrenheit temperature	°F

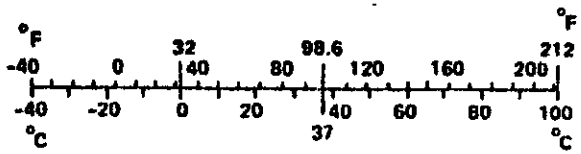

DISCLAIMER

The contents of this report reflect the views of the authors, who are responsible for the opinions, findings, and conclusions presented herein. The contents do not necessarily reflect the official views or policies of the Federal Highway Administration. This report does not constitute a standard, specification, or regulation.

KEY WORDS

Bridge Rail, Crash Test(s), Construction, Safety

ACKNOWLEDGMENTS

This research study was conducted under a cooperative program between the Texas Transportation Institute (TTI), the Texas State Department of Highways and Public Transportation (SDHPT), and the Federal Highway Administration (FHWA). Mr. John Panak of the SDHPT worked closely with the researchers, and his comments and suggestions were appreciated.

A LOW-MAINTENANCE, ENERGY-ABSORBING BRIDGE RAIL

ABSTRACT

A low-maintenance, energy-absorbing bridge rail has been developed for use in high traffic volume situations where the cost of repairing conventional bridge rails has become prohibitively expensive. The new bridge rail is designed to meet or exceed current bridge rail design guidelines. The new bridge rail incorporates structural steel tube railings and posts and high strength rubber energy absorbers. The new bridge rail is designed to be installed on new or existing standard bridge decks. Results of crash tests show that the bridge rail can smoothly redirect a 4500 lb (2043 kg) automobile impacting with a velocity of 60 mph (96.6 km/hr) and an angle of 25° and remain in service with no maintenance. If exposed to a more severe impact, the bridge rail may have to be repaired, but the bridge deck will remain undamaged. Finally, the new energy-absorbing rail occupies less bridge deck area than conventional bridge rails.

TABLE OF CONTENTS

LIST OF FIGURES

LIST OF FIGURES (continued)

LIST OF FIGURES (continued)

LIST OF TABLES

A LOW-MAINTENANCE, ENERGY-ABSORBING BRIDGE RAIL

INTRODUCTION

Bridge rails currently in use are capable of smoothly redirecting errant automobiles. However, virtually all types of bridge rails require some type of repair when they are subjected to moderate-to-severe impacts. The types of damage normally incurred include damage to the bridge rail, bridge rail posts, and bridge deck. The damage is more prevalent with metal bridge rails, but even concrete parapet bridge rails are susceptible to damage when exposed to severe impacts. In many cases, the costs associated with bridge rail repair can be greater than the original installation costs. The repair and maintenance costs can become overwhelming on high volume, multilane expressways where bridge rails are subjected to a greatly increased risk of impact. There is a need for an alternative bridge rail which can redirect errant automobiles without damage.

The research reported herein was directed toward development of a low-maintenance, energy-absorbing bridge rail which meets or exceeds current bridge rail design criteria. The bridge rail developed incorporates structural steel tube railing and post members, and rubber energy absorbers. Further, the bridge rail is designed to be installed on standard Texas State Department of Highways and Public Transportation (SDHPT) bridge decks. No special deck reinforcement is required. Therefore, the bridge rail can be installed on either new or existing bridge decks.

DEVELOPMENT OF THE ENERGY-ABSORBING BRIDGE RAIL

The objective of the research presented in this report was to develop an energy-absorbing bridge rail that conforms to current bridge rail design standards and that can withstand the impact of a 4500 lb (2043 kg) automobile traveling with a velocity of 60 mph (96.6 km/h) and impacting at an angle of 25° with no damage to the rail. Further, it was desired to develop a bridge rail that can be installed on either new or existing bridge decks. Development of the energy-absorbing bridge rail involved a study of related bridge rail test results, a conceptual design of the bridge rail, and static testing of critical components.

Previous Research

Results of crash tests on different types of conventional bridge rails show that current deck-to-post and deck-to-concrete parapet connections are not capable of transferring the loads associated with severe automobile impacts without significant damage to either the bridge rail or the bridge deck (7,8). This was found to be the case with both steel and concrete bridge rails. Further, it was found that the accelerations associated with vehicles impacting the conventional bridge rails often exceed the limits set forth in NCHRP Report 230 (2).

One way to improve the performance of bridge rails is to incorporate an energy-absorbing mechanism. Results of previous studies show that vehicular accelerations during impact can be reduced and that the magnitudes of the forces transferred to the bridge slab can be attenuated through the use of an energy-absorbing bridge rail (9,10,11,12). However, the initial costs associated with the different types of energy-absorbing bridge rails surveyed are much higher than the initial costs associated with conventional bridge rails. In addition, none of the energy-absorbing bridge rails surveyed were maintenance free following the large automobile crash test. Finally, none of the energy-absorbing rails surveyed can be attached to a standard bridge deck. Therefore, the previously developed energy-absorbing bridge rails have not gained widespread acceptance.

New Bridge Rail

The decision was made early in this project to develop an energy-absorbing bridge rail which employs a stiff rail that is supported at regular intervals by flexible energy-absorbing supports. Figure 1

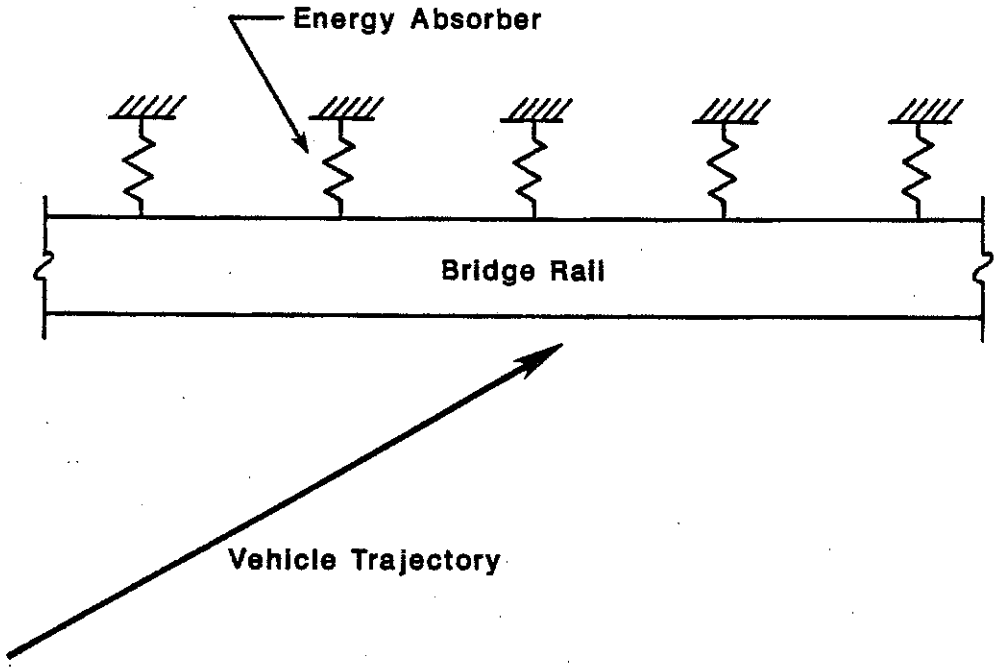

Figure 1. Idealized Energy-Absorbing Bridge Rail.

presents an idealized section of the proposed energy-absorbing bridge rail. This arrangement allows impact forces to be spread over a greater distance along the length of the bridge rail than conventional bridge rail systems which employ flexible rail sections and stiff posts. Therefore, more of the bridge deck is brought into action to resist impact forces.

Conceptually, the bridge rail could be made of either concrete or steel. The researchers opted to use a bridge rail which is made of two square structural steel tubes which are stacked one on top of the other and skip welded along their length. This type of bridge rail is very stable, and it is not susceptible to local crushing or buckling prior to development of its full plastic flexural capacity. Similar rails have been used in two other recent TTI projects (3,4).

In previously developed energy-absorbing bridge rails, the energy-absorbing element has been a steel member which absorbs energy by either crushing or deforming (9,10,11,12). The researchers chose to use rubber energy absorbers in development of the bridge rail presented herein. The rubber energy absorbers used are primarily manufactured to be dock fenders in marine applications. Rubber energy absorbers of this type are available from a wide variety of different manufacturers. The rubber is highly resilient, it remains elastic when subjected to large strains, and it is resistant to the elements of nature. Further, it is readily available in a wide range of different geometries. A cylindrical rubber energy absorber was chosen for the current application.

To complete the system, the energy absorbers have to be supported in a manner that allows the impact loads to be transferred into the bridge deck. There are several different ways in which this could be accomplished. One way would be to mount the energy absorbers to the face of a concrete parapet. This option would be acceptable if the rail were to be mounted on a new bridge, but this approach would be prohibitively expensive for a retrofit operation. Therefore, the researchers chose to support the rubber energy absorbers with steel posts.

Conventional steel bridge posts are welded to a base plate which is attached to the bridge deck with anchor bolts. Previous tests on

conventional bridge posts show that the bridge deck is severely cracked and spalled before the post reaches its full potential (17). As a result, severe damage is often done to the bridge deck in even moderate impacts. As stated earlier, one of the major objectives of this project was to prevent damage to the bridge deck. To accomplish this, a new bridge post design was developed.

Figure 2 represents a sketch of the new bridge post developed for this project. The bridge post is attached to the deck with three bolts which pass through the deck. The mounting holes in the bridge deck can be cast during construction or they can be drilled after construction. When the post is subjected to a lateral force, both a shear force and a moment must be transferred into the bridge deck. The post is designed so that the bolt furthest from the edge of the slab transfers the shear into the deck. This is accomplished by control of the mounting hole tolerances. The moment is transferred into the deck through a couple which develops between the inboard contact force and the tensile forces in the two bolts near the edge of the deck. The inboard force is transferred to the bottom of the deck through a neoprene bearing pad. The outboard force is transferred to the top of the deck through base plates which rest on neoprene bearing pads. In both cases the load experienced by the bridge deck is a compressive load as shown in Figure 3. The magnitudes of the contact stresses are controlled by the sizes of the bearing areas.

The weight of the rail is supported by a rectangular tube which passes through the center of the cylindrical energy absorber and through a sleeved opening in the post as shown in Figure 2. During installation of the bridge rail the energy absorber is compressed slightly and striker plates are attached to the back side of the support tube with bolts. The entire assembly is then held firmly in place by the compressive force locked into the energy absorber. The sleeved opening is larger than the support tube so that when the rail is subjected to an impact force with a lateral component, the force is transferred to the post through the energy absorber as the support tube passes freely through the post.

In selecting the final member sizes for the energy-absorbing bridge rail, the researchers relied on structural analysis techniques for beams on elastic foundations, results generated using the BARRIER VII crash

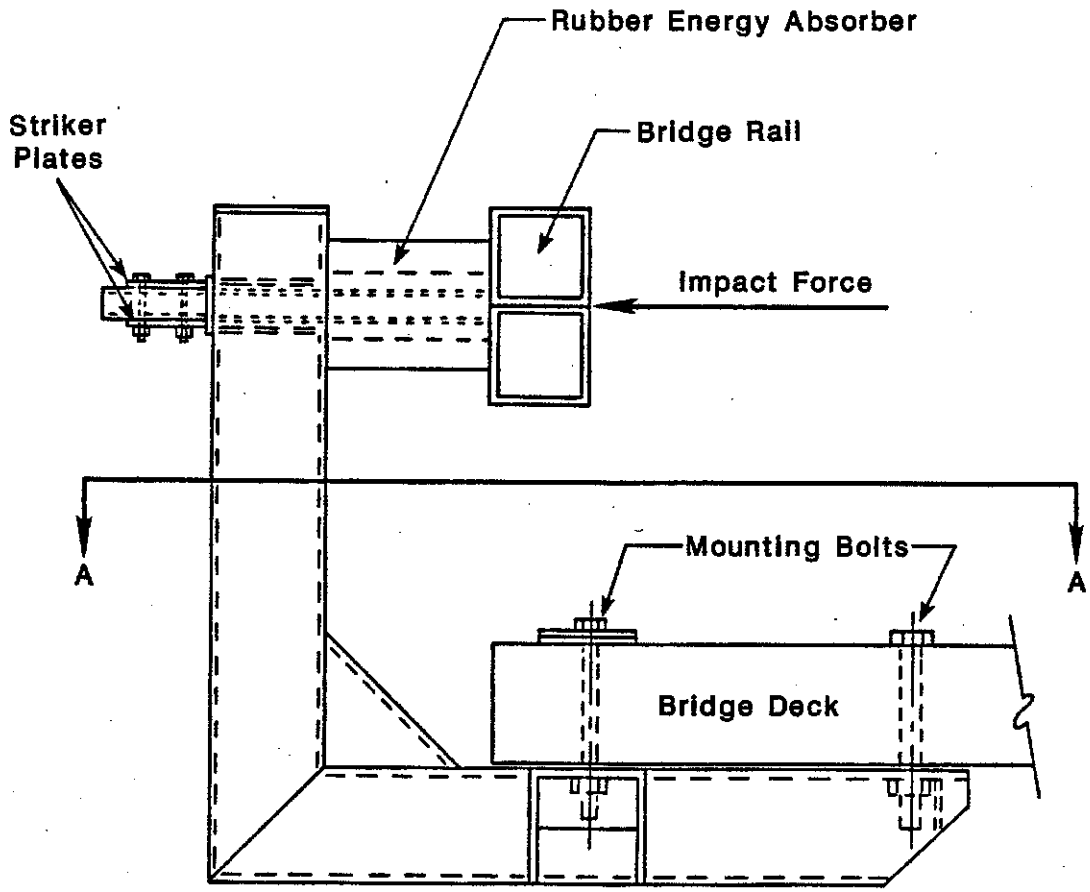

Figure 2. Energy-Absorbing Bridge Post.

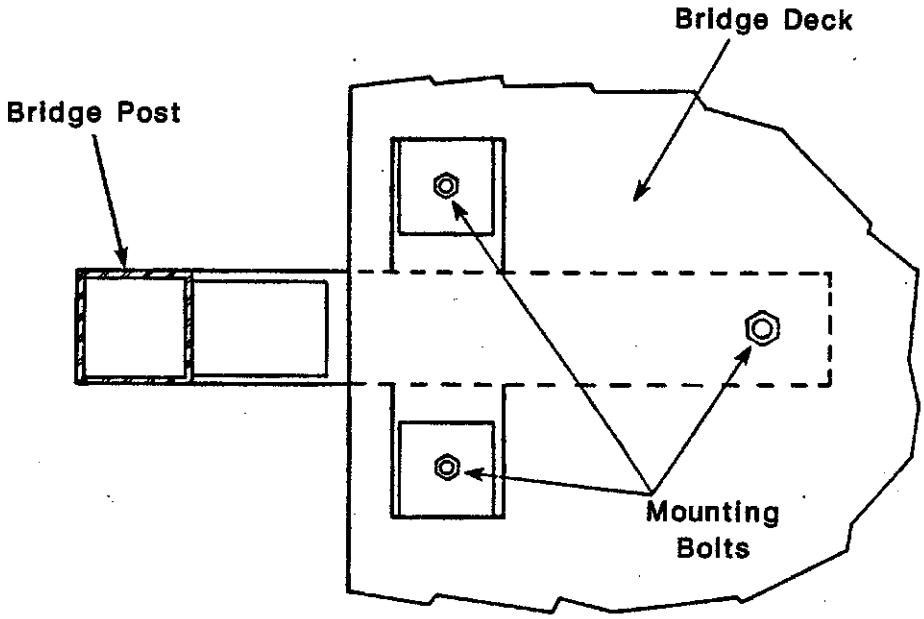

Figure 2. Energy-Absorbing Bridge Post. (continued)

simulation program (5), results of selected static tests, and engineering judgment. Based upon these considerations, the bridge rail was fabricated with 6 x 6 x 1/4 in. (152 x 152 x 6.4 mm) structural tubes, and the bridge posts were fabricated with 7 x 7 x 1/4 in. (178 x 178 x 6.4 mm) structural tubes. The cylindrical rubber energy absorbers chosen had 8 in. (203 mm) outer diameters, 4 in. (102 mm) inner diameters, and were 10-1/2 in. (267 mm) long. Figure 4 presents a view of the prototype energy-absorbing bridge rail. Complete fabrication details of the final energy-absorbing bridge rail are presented in Appendix A.

It is estimated that the energy absorbing bridge rail incorporates approximately 76 lb of steel per linear foot. This is about twice the amount of steel that is normally used in standard metal bridge rails. The cost associated with the steel fabrication will vary with the supplier, but it is reasonable to assume that the cost would be in proportion to the weight of the steel. The actual cost of the energy absorbers used in the prototype bridge rail was about $4.50 per linear foot of bridge rail. The energy absorbing bridge rail requires 16 to 20 in. less bridge deck width than standard metal rails. This could result in direct cost savings with new installations. Further, if the energy absorbing rail is installed on an existing bridge deck, 16 to 20 in. of usable bridge deck width will be returned to service. It is difficult to quantify the savings associated with using less bridge deck, but these savings should be taken into account when evaluating the overall cost of an energy absorbing bridge rail installation. Finally, discussions with SDHPT engineers suggest that the maintenance costs associated with standard metal bridge rails can be significantly more than the original installation costs. The energy absorbing bridge rail is designed to require no structural maintenance unless it is subjected to a very severe impact. Even in an extreme impact, the bridge deck will experience no damage. If the overall costs of construction and maintenance are taken into account, the energy absorbing bridge rail should be cost effective.

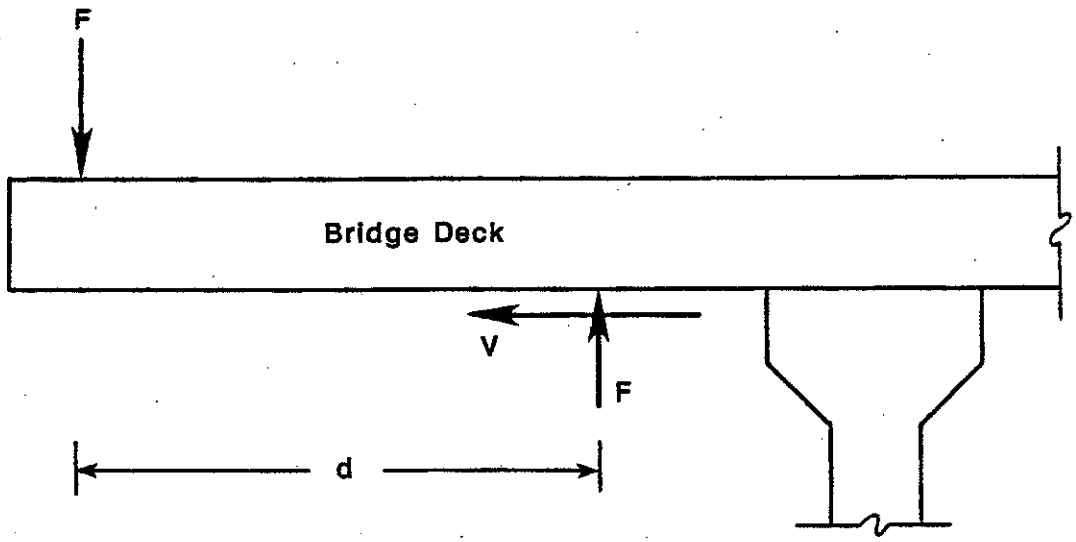

Figure 3. Forces Exerted on Bridge Deck.

Figure 4. Energy-Absorbing Bridge Rail

ENERGY-ABSORBING BRIDGE RAIL TESTS

Because the energy absorbing bridge rail presented in this report is such a departure from conventional bridge rails, a thorough series of tests was performed on the bridge rail and bridge rail components to fully document its performance. Three different types of tests were conducted:

1. static tests to determine the stiffness of the cylindrical rubber energy absorbers,
2. static tests to determine the performance of the energy-absorbing post, and
3. full-scale crash tests to determine the actual performance of a prototype energy-absorbing bridge rail.

The first series of tests was conducted in the structural laboratory of the Engineering Research Center on the Texas A&M University campus in College Station, Texas. The other two test series were conducted at the Texas Transportation Institute Proving Grounds in Bryan, Texas. Results of each group of tests are discussed below.

Static Rubber Energy Absorber Tests

The rubber dock fender material used as the energy absorber is usually oriented so that its cross section is loaded in flexure. However, in the energy absorbing bridge rail presented herein, the energy absorber is oriented so that it is loaded in uniaxial compression. This allows for a more efficient storage of strain energy within the energy absorber. However, most of the available design information is for the flexural mode. Therefore, it was necessary to conduct a series of tests to study the response of the rubber cylinders exposed to uniaxial compression.

Preliminary calculations using available information suggested that tests should be conducted on two different rubber cylinder geometries: 8 in. outside diameter by 4 in. inside diameter and 7 in. outside diameter by 3 in. inside diameter. The 8 x 4 in. cylinders were tested in lengths of 4, 8, and 17 in. The 7 x 3 in. cylinders were tested in lengths of 6 and 12 in.

The tests were conducted using a Materials Testing System 500,000 lb capacity load machine with Digital data processing equipment. In these tests, the specimens were placed in the load machine and slowly loaded in axial compression until the length of the specimen was a specified

fraction of the uncompressed length. The specimen was then slowly unloaded. Load deflection data was recorded at regular intervals throughout the test.

Typically, the load-deflection response of the rubber cylinders was linear until the strain in the cylinder exceeded 35%. At this point, the cylinders would begin to stiffen. Twenty three separate tests were conducted with strains of up to 50%. Load deflection curves for the different rubber cylinders tested are presented in Appendix B. The information presented in Appendix B is summarized in Table 1.

Energy Absorbing Post Tests

Most structural steel designs incorporate a safety factor with respect to yield at the design load. However, the energy absorbing post was designed to reach yield when subjected to the design load. This design philosophy increases the cost effectiveness of the energy absorbing rail. However, there is little margin for error with this design philosophy. Therefore, a series of static tests was conducted to insure that the energy absorbing post performs as designed. The primary objectives of the tests were:

1. to identify detail changes needed to assure that the posts are adequately stiffened so that full plastic hinges can develop at the design load,
2. to assure that the rubber energy-absorber/plunger mechanism works as designed and that the load deformation characteristics of the post are as designed,
3. to assure that the energy-absorbing post fails before the concrete bridge deck is damaged,

To accomplish these tests, a short section of a standard 7.5 in. thick bridge deck overhang was constructed as shown in Figure 5. The bridge deck section was constructed using standard SDHPT bridge deck reinforcement. This bridge deck section was similar to the bridge deck sections previously used in tests of conventional bridge rail posts (7). Mounting holes for the energy-absorbing posts and for a loading frame were cast into the bridge deck section. The load was then applied to the bridge post with a horizontally mounted hydraulic cylinder mounted so that the line of action of the load was 21 in. above the bridge deck (refer to

TABLE 1. SUMMARY OF RUBBER CYLINDER TESTS

No. of Tests	Outer Diameter (in.)	Inner Diameter (in.)	Length (in.)	Percent Strain (%)	Average Apparent Stiffness (K/in.)	Average Secant Modulus ($K/in.^2$)
4	8	4	8	50	4618	980
3	8	4	6	20	7511	1195
2	8	4	6	35	7560	1203
2	8	4	6	50	9725	1548
2	8	4	17	20	3028	1365
2	8	4	17	30	2888	1302
2	7	3	12	20	6095	2330
2	7	3	12	35	5513	2107
2	7	3	12	42	5389	2060
2	7	3	6	35	10813	2066

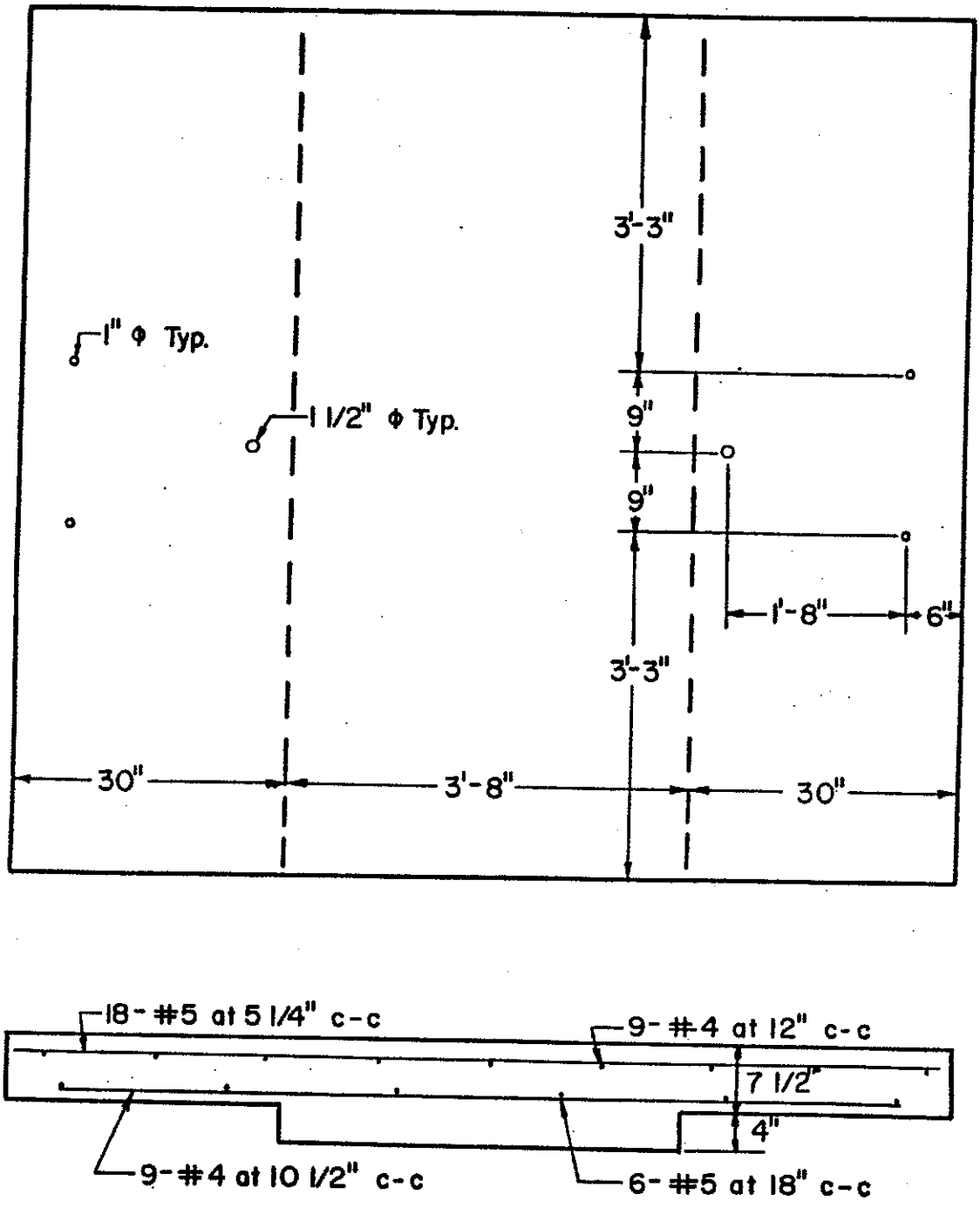

Figure 5. Concrete Deck Used for Static Load Tests

Figure 6). Further, as shown in Figure 6, a short section of bridge rail was attached to the post to hold the energy absorber in place. Displacement transducers were mounted to point B on the plunger and point A on the post as shown in Figure 6 so that the displacements of the post and the traffic face of the rail could be independently measured. With this information, the load deformation response of the rubber energy absorber can be deduced. A total of four bridge post tests were conducted with this arrangement. Results from these tests are reported below.

Static Test ST-1

The energy-absorbing post used in test ST-1 employed the same structural members used in the final post design with no stiffeners. This was done because a significant cost savings could be realized if the fabrication costs associated with the stiffeners could be eliminated. Figure 6 shows a schematic of the post used in this test. Figure 7 shows photographs taken during this test. The line of action of the load in this test was 90 degrees to the rail face. Continuous load deflection data was taken as the bridge post was slowly loaded to failure.

The ultimate load capacity of the post was 20,000 lb. The corresponding maximum deflection of the traffic face was 7.1 in. The permanent deflection of the post was 1.5 in. Failure of the post occurred when a crack formed at point C on the knee of the post member along the diagonal weld as shown in Figure 6. In addition, the wings on either side of the post member underneath the deck yielded (refer to Figure 6). Complete load deformation relationships for this test are presented in Appendix C. There was no visible cracking in the bridge deck.

Test ST-2

The second bridge post test involved a bridge post of the final design with stiffeners as shown in Figure 8 and in the final design drawings presented in Appendix A. These stiffeners were added to prevent crack initiation in the diagonal weld and premature yielding of the post wings. In this test the horizontal load was applied so that the angle between the line of action of the applied force and the traffic rail face was 77 degrees. This test was designed to simulate a load applied to the bridge post with both a lateral and longitudinal component as would occur in a real impact.

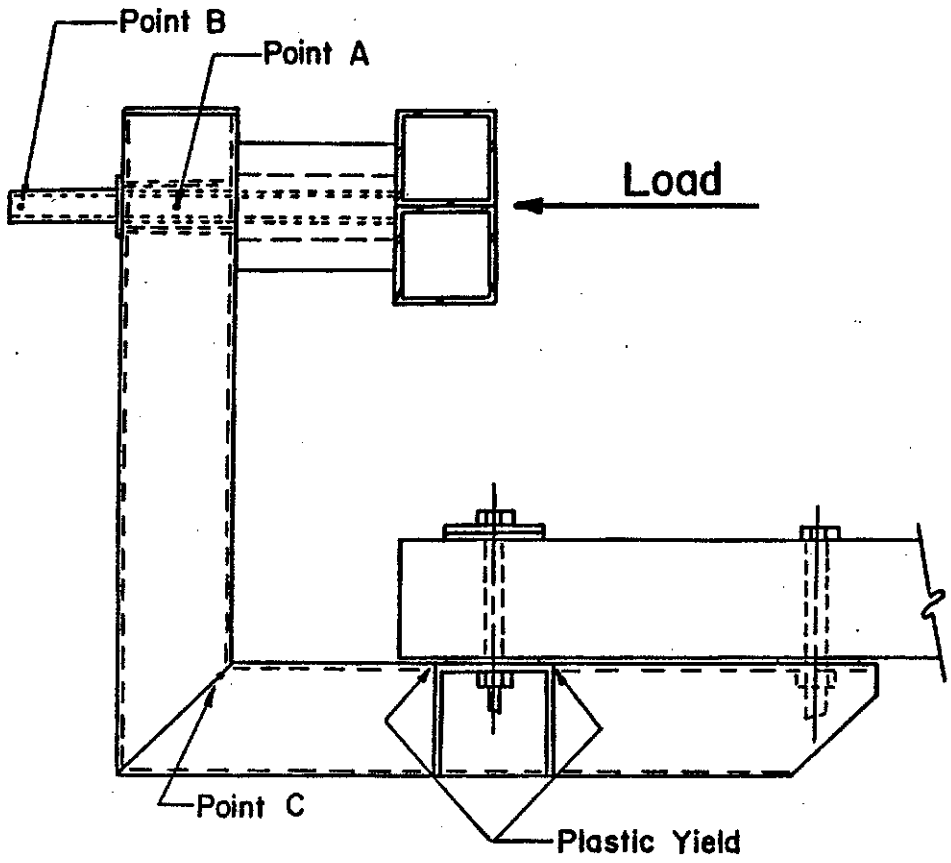

Figure 6. Static Load Test ST-1

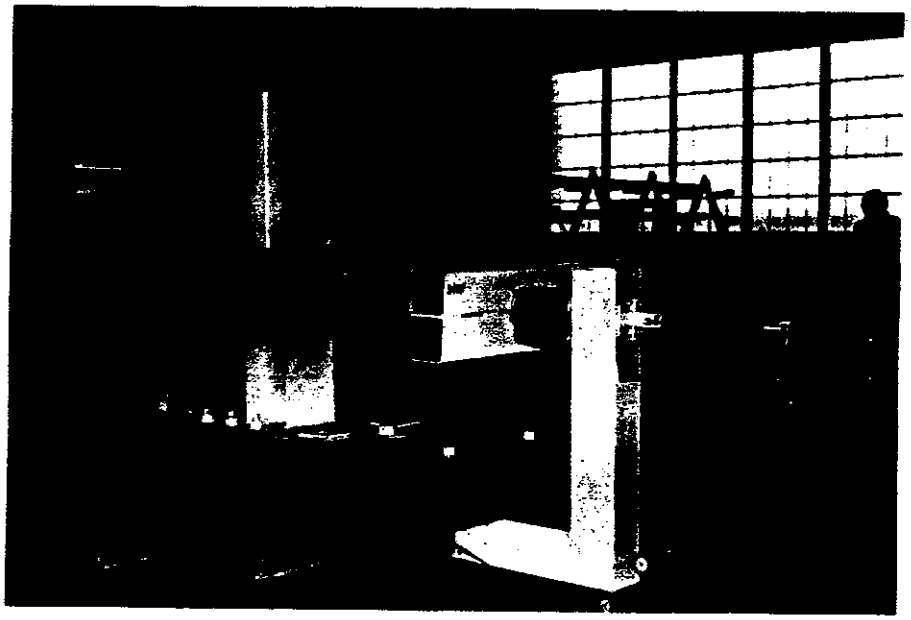

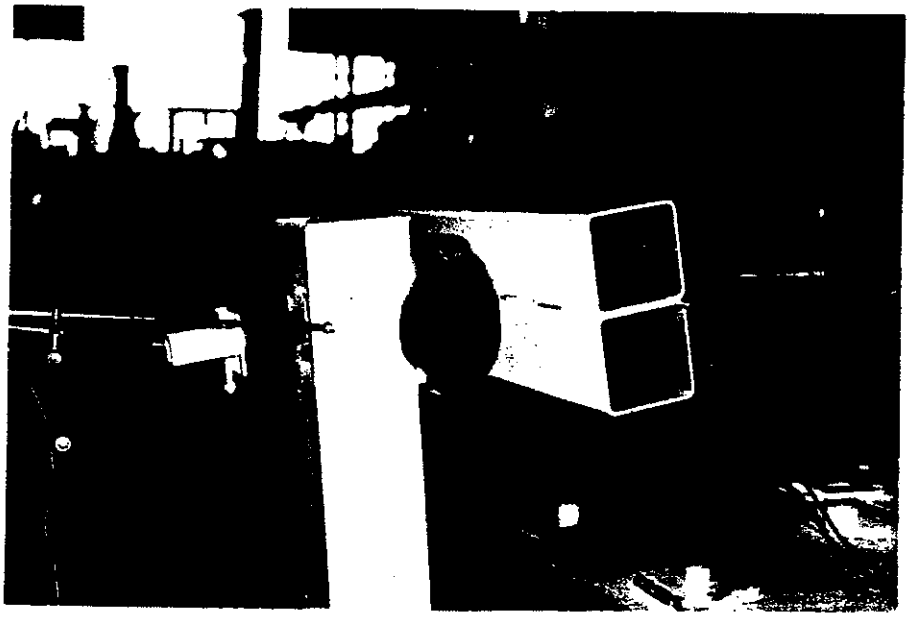

Figure 7. Photographs of Static Test ST-1

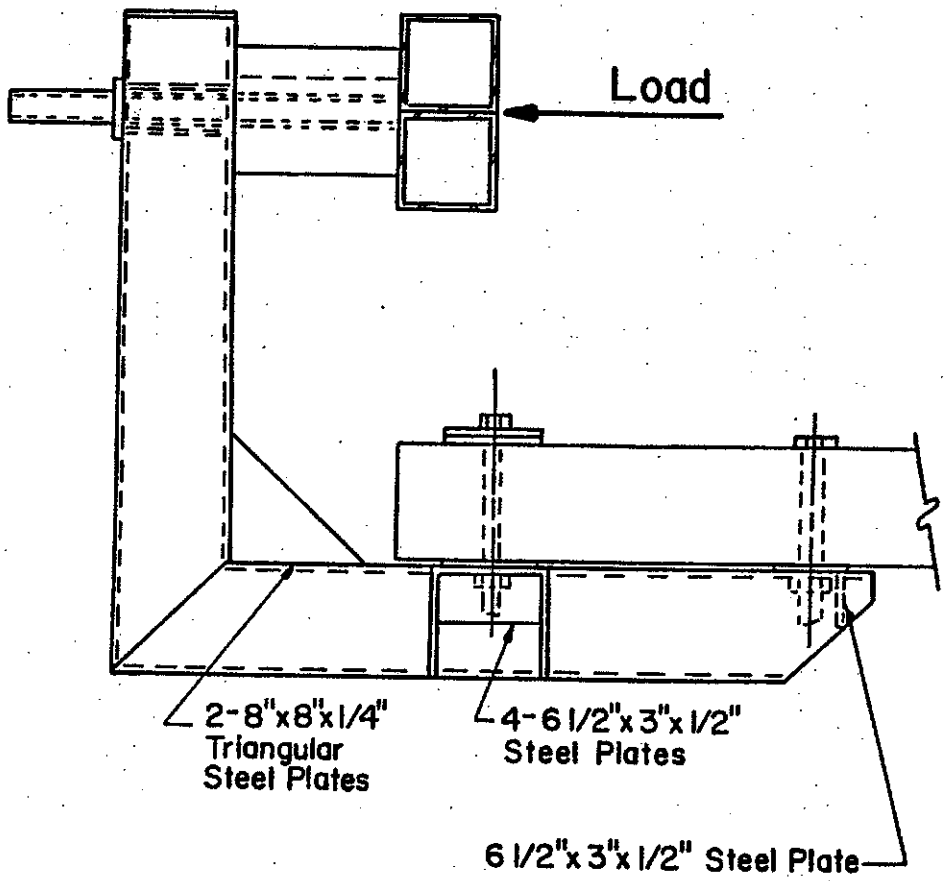

Figure 8. Static Load Test ST-2

The load was gradually increased to a load of 17,000 lb. Figure 9 presents photographs of this test. The 17,000 lb load is slightly less than the maximum load predicted by the BARRIER VII analysis. The maximum horizontal deflection of the traffic face of the rail was 4.5 in. The plunger slid smoothly through the sleeved opening in the post with no snagging. The permanent deflection of the rail face was measured to be .3 in., most of which was judged to be the result of slack in the mounting holes. The measure load deformation relationships for this test are presented in Appendix C. There was no visible cracking in the concrete bridge deck or yielding of the post.

Static Tests ST-3 and ST-4

The same post used in test ST2 was used in tests ST-3 and ST-4. In both of these tests the horizontal load was applied so that the angle between the bridge rail face and the line of action of the load was 90 degrees. The purpose of these tests was to determine the ultimate strength of the energy-absorbing bridge posts.

The maximum load applied to the post in test ST3 was 25,000 lb. Examination of the load-deformation relationships for this test (refer to Appendix C) show that yielding of the post began at about 20,000 lb. The maximum post deflection was 1.5 in. and the maximum deflection of the traffic face was 7 in. When the load of 25,000 lb was reached, the hydraulic cylinder was fully extended. As a result, the test had to be stopped before the ultimate strength was reached. Figure 10 presents photographs taken during this test. The permanent deflection of the post after the load was removed was 0.7 in.

In test ST-4, a steel pipe was substituted for the rubber energy absorber so that the post could be loaded to failure without making significant modifications to the test rig. In this test the load applied to the post was gradually increased until the ultimate strength of the post was reached. The post began to experience extensive yielding at a load of 26,000 lb as shown in the load deformation relationships presented in Appendix C. Plastic hinges formed at point C above the knee brace and at point B below the knee brace as shown in Figure 11. At the same time the weld attaching the post wings to the horizontal post member developed a crack. Figure 12 presents photographs taken during this test. No cracking or other visible damage to the bridge deck was apparent.

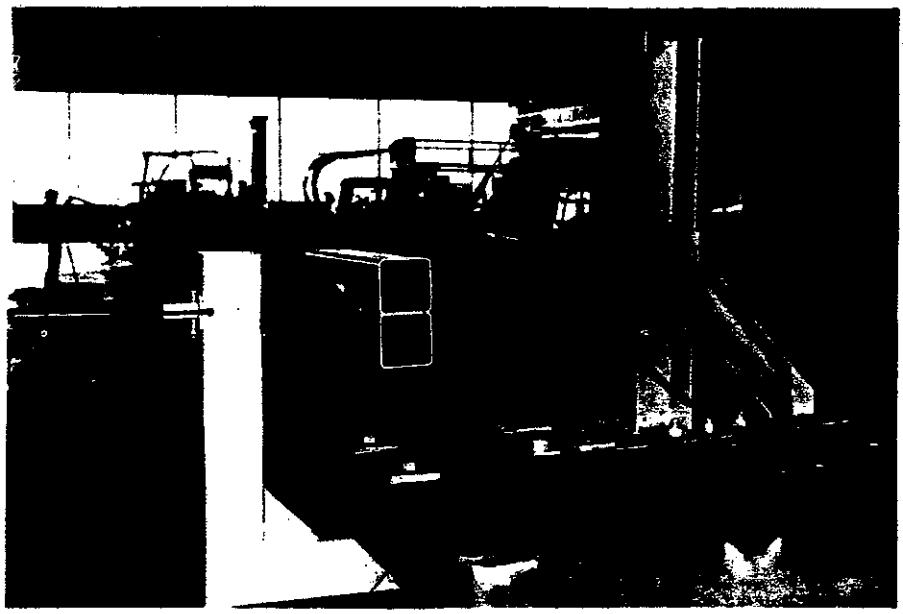

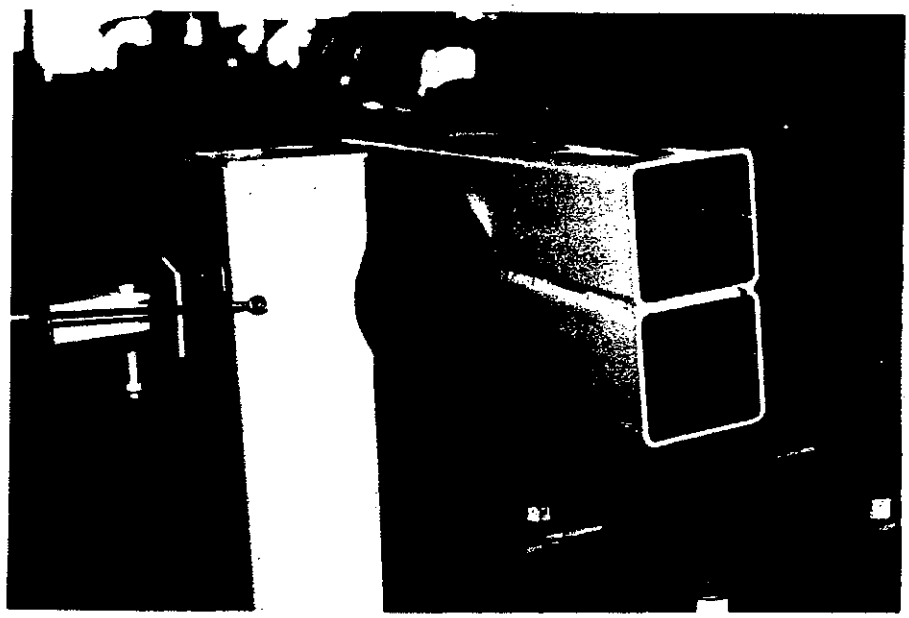

Figure 9. Photographs of Static Test ST-2

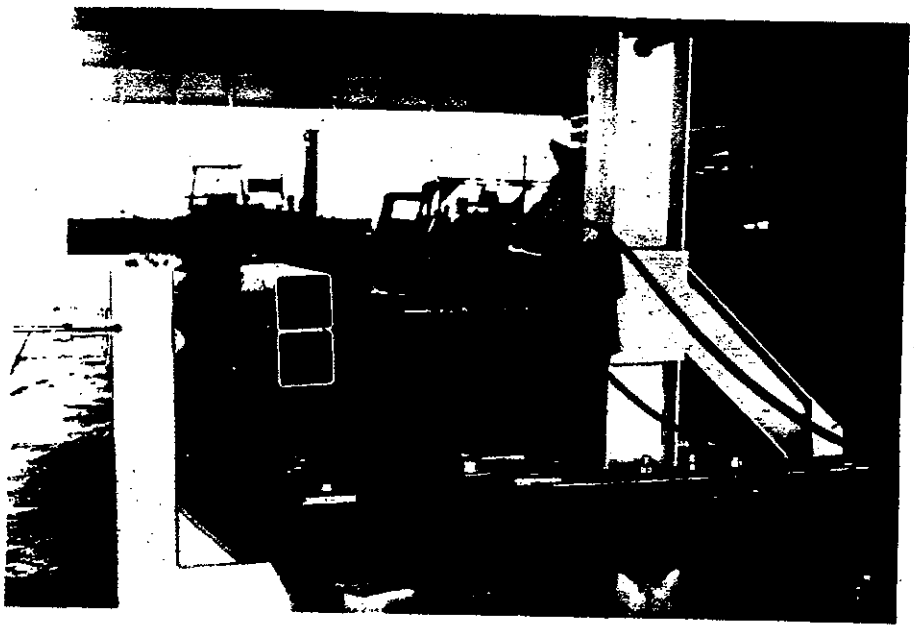

Figure 10. Photographs of Static Test ST-3

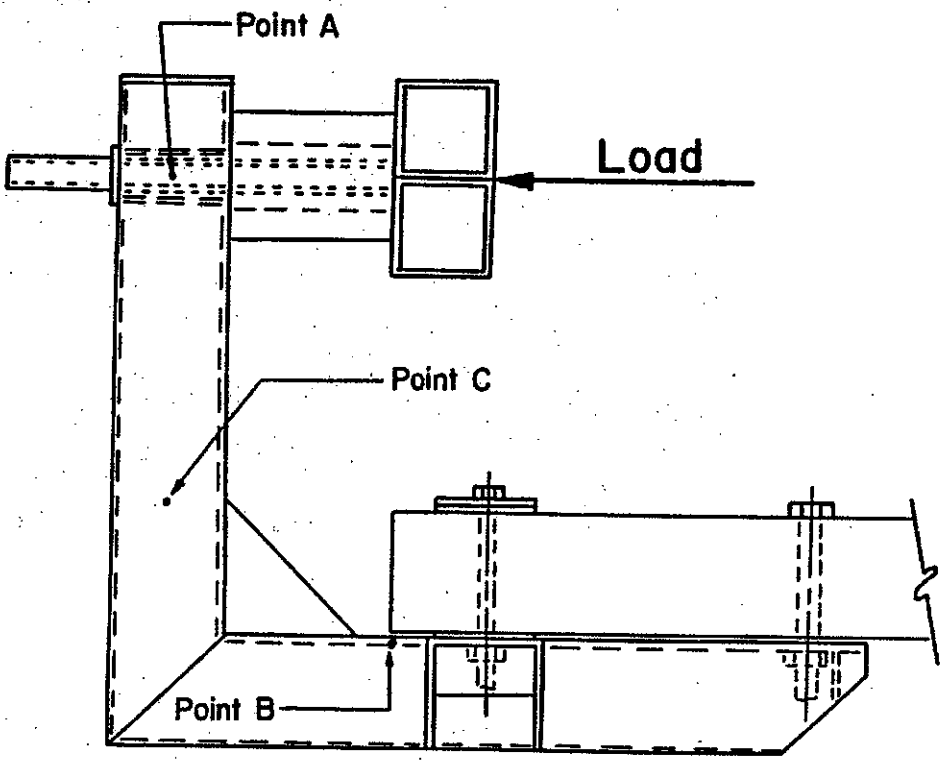

Figure 11. Static Load Tests ST-3 and ST-4

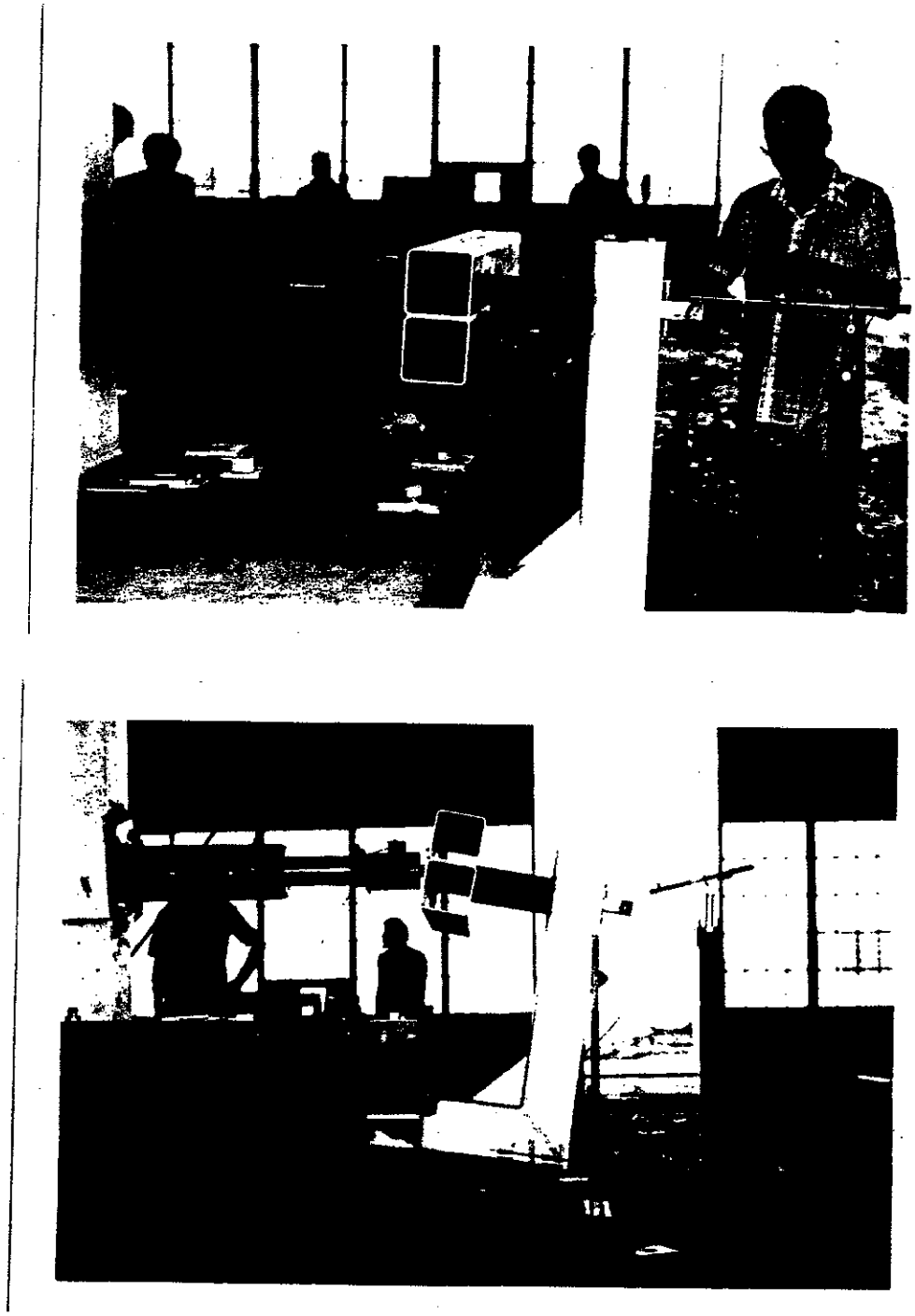

Figure 12. Photographs of Static Test ST-4

Full-Scale Crash Tests

Two full-scale crash tests were conducted on a prototype bridge rail to evaluate the performance of the energy-absorbing bridge rail in terms of structural adequacy, occupant risk, and vehicle exit trajectory. These tests were conducted in accordance with NCHRP Report 230 (2). The first test involved the impact of an 1800 lb subcompact automobile. The second test involved a 4500 lb full-size automobile.

The tests were conducted using a 59 ft (18 m) section of the energy-absorbing bridge rail. NCHRP Report 230 specifies that a 75 ft (22.9 m) section of the bridge rail should be tested (2); however, it was the opinion of the researchers that the performance of the bridge rail is not affected by this deviation. Further, the acceptance of the shorter section allowed the use of an existing standard SDHPT bridge deck.

The bridge deck used is approximately 15 years old and has been used in at least three other TTI bridge rail tests. As a result, the bridge deck has accumulated a significant amount of cracking and spalling, which is typical of actual bridge deck damage. Figure 13 shows examples of the bridge deck damage prior to testing. The energy-absorbing bridge rail was mounted on the existing deck so that this worst area of spalling was located between two posts. No attempt was made to repair any of the cracked or spalled areas in the bridge deck. The necessary mounting holes were drilled in the deck using a coring machine without regard for the placement of internal reinforcement. This procedure would be typical of a retrofit operation.

The two tests were conducted in order of increasing severity on the same section of bridge rail. The impact point for the subcompact test was selected to coincide with a rail splice. This location was chosen to provide the greatest opportunity for snagging and destabilizing the small car. The impact point for the full-size automobile impact was centered in the area of maximum bridge deck damage shown in Figure 13. This was done to provide the bridge deck with the best opportunity to be damaged, thus demonstrating the performance of the system in a retrofit operation. Test statistics for the two crash tests are presented in Table 2. Sequential photographs of the tests are presented in Appendix D. Accelerometer traces and plots of roll, pitch and yaw are presented in Appendix E.

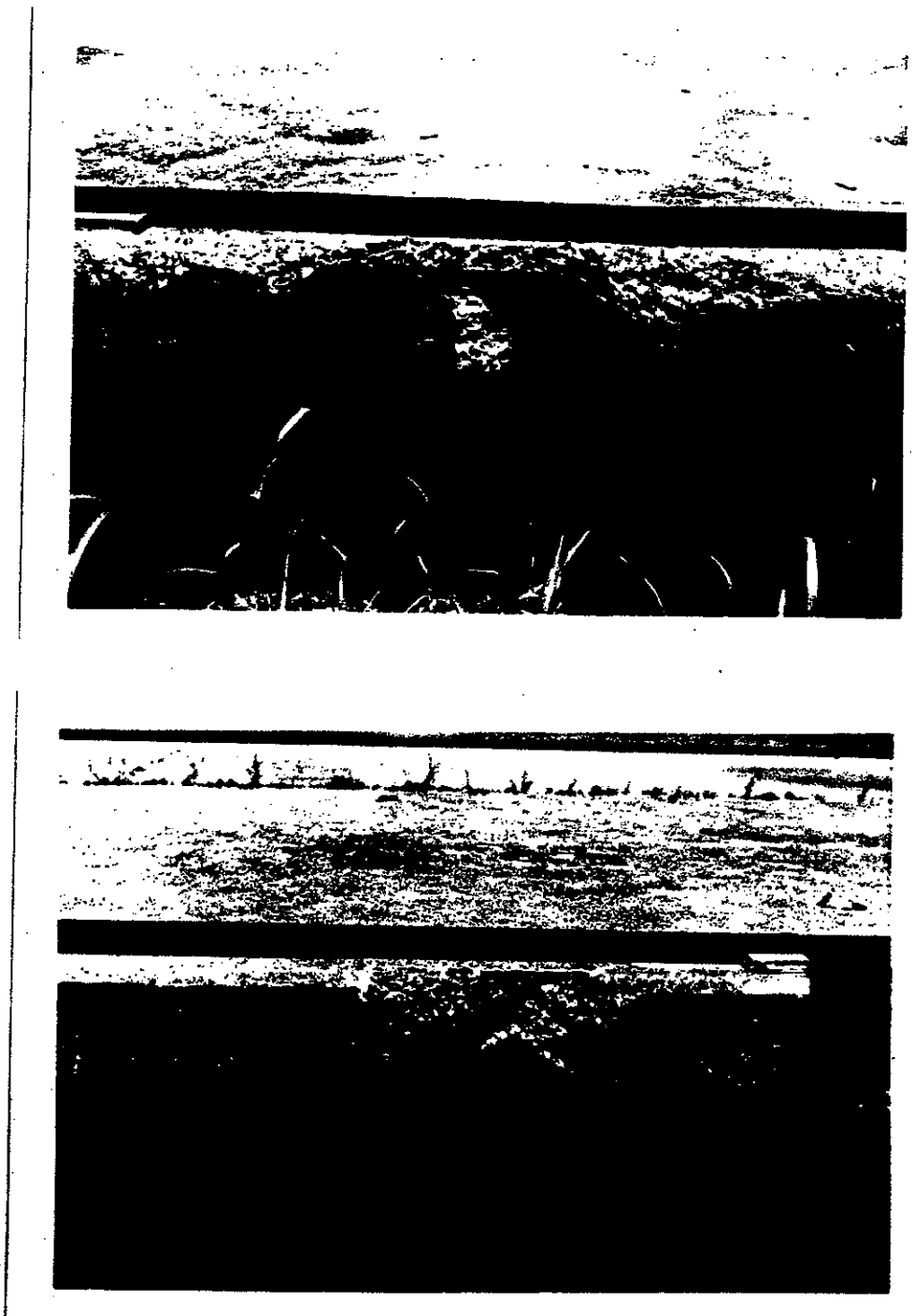

Figure 13. Photographs of Bridge Deck Prior to Tests

TABLE 2. SUMMARY OF CRASH TEST RESULTS

Test No.	2417-1	2417-2
Vehicle Weight, lb (kg)	1800 (816.5)	4500 (2041.2)
Impact Speed, mph (km/hr)	62.56 (100.72)	61.0 (98.2)
Impact Angle, degrees	16	25.5
Exit Angle, degrees	0.5	2.0
Dynamic Displacement, in. (mm)	4.56 (116)	7.2 (183)
Permanent Displ., in. (mm)	0.60 (15)	0.96 (24)
Occupant Impact Velocity fps (m/sec)		
Longitudinal	11.7 (3.57)	18.9 (5.76)
Lateral	20.4 (6.22)	28.5 (8.69)
Occupant Ridedown Acceleration g's		
Longitudinal	-0.6	-2.5
Lateral	8.7	10.0
Vehicle Damage Classification		
TAD	11LD4	10LD7
VDI	11LDES2	10LDES3

Test 2417-1

In this test, an 1802 lb (818 kg) Honda Civic impacted the energy-absorbing bridge rail with a velocity of 62.6 mph (101 km/hr) with an angle of 16°. Figures 14 shows the test vehicle and rail before the test. Figure 15 shows the vehicle and bridge rail after the test. Figure 16 presents a summary of the test results. The test vehicle was smoothly redirected with an exit angle of only 0.5 degrees. The damage to the impacting automobile was considered to be moderate given the severity of the impact. The maximum dynamic deflection of the bridge rail was 4.6 in. (117 mm) and the permanent deflection of the face of the rail was 0.6 in. (15.2 mm). This permanent deflection was the result of slack in the post-to-deck connections. The bridge deck experienced no cracking or spalling as a result of this test.

Test 2417-2

In this test, a 4500 lb (2043 kg) Oldsmobile Delta 98 impacted the bridge rail with a velocity of 61.0 mph (98.1 km/hr) with an impact angle of 25.5°. The same bridge rail used in test 2417-1 was used in test 2417-2. Figure 17 shows the test vehicle and bridge rail before the tests. Figure 18 shows the bridge rail after the test. Results of this test are summarized in Figure 19. In this test the automobile was smoothly redirected with an exit angle of only 2.0 degrees. In the opinion of the researchers, the damage done to the vehicle was significantly less than would be expected if the automobile impacted a rigid bridge rail such as a concrete parapet. The maximum dynamic deflection of the energy-absorbing bridge rail was 7.2 in. (183 mm) and the permanent deflection relative to the original face of the rail was 0.96 in. (24 mm). This permanent deflection was the result of connection slack coupled with a slight amount of yielding in the bridge rail and post. The bridge deck sustained no damage or cracking during the second test. No maintenance would have been required to keep the bridge rail in service following this impact.

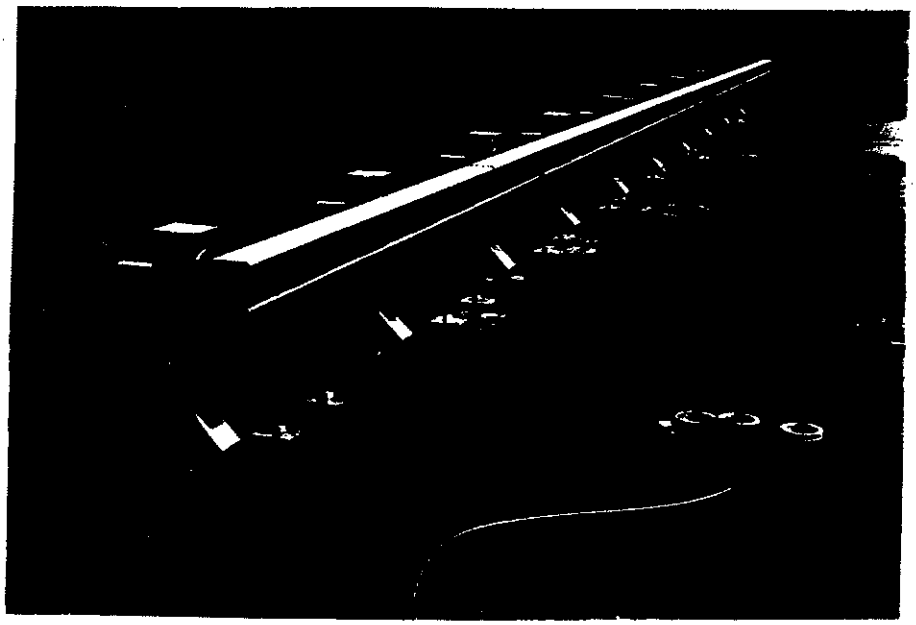

Figure 14. Bridge Rail and Vehicle Prior to Test 2417-1

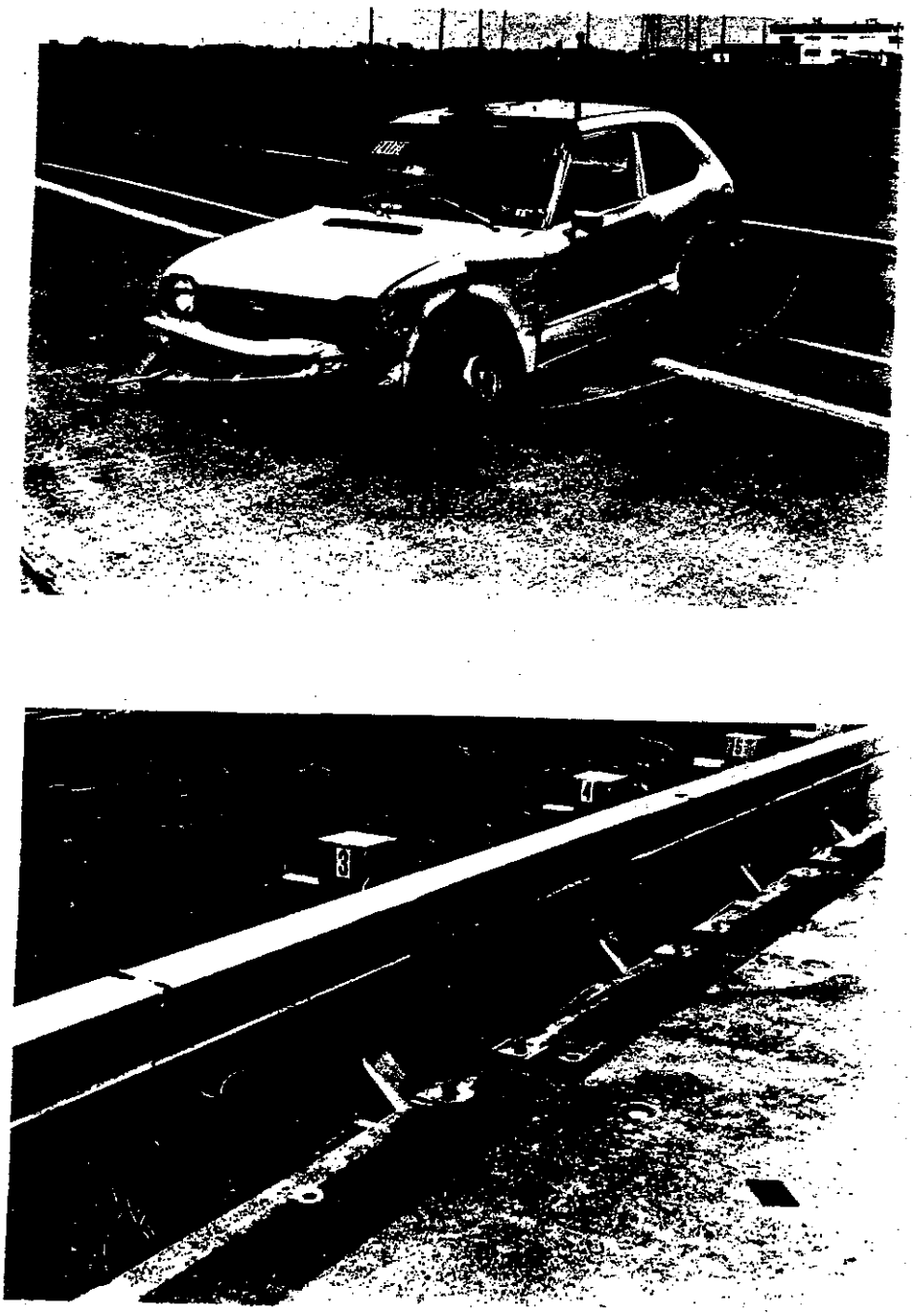

Figure 15. Bridge Rail and Vehicle After Test 2417-1

0.000 s 0.055 s 0.138 s 0.193 s

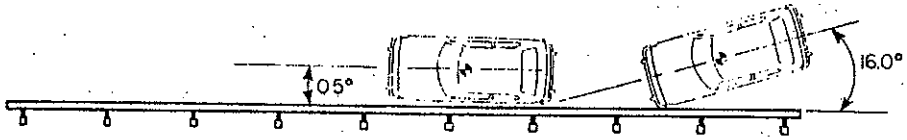

Test No. 2417-1
Date 5/21/85
Rail . . . . . Low-maintenance, energy-absorbing bridge rail
Post . . . . . 7x7x¼ in Structural Steel Tube
Post Spacing . . . . . 6.25 ft (1.91 m)
Length of Installation . 59 ft (18 m)
Rail Deflection
  Maximum . . . . . 0.38 ft (0.12 m)
  Permanent. . . . . 0.05 ft (0.02 m)
Vehicle. . . . . 1979 Honda Civic
Vehicle Weight
  Test inertia . . . . 1,802 lb (818 kg)
  Gross static . . . . 1,972 lb (895 kg)

Impact Speed. . . . . 62.56 mi/h (100.7 km/h)
Impact Angle. . . . . 16.0 degrees
Exit Angle. . . . . 0.5 degrees
Change in Velocity. . . . 7.79 mi/h (12.5 km/h)
Change in Momentum. . . . 639 lb-s
Occupant Impact Velocity
  Longitudinal. . . . . 11.7 fps (3.6 m/s)
  Lateral . . . . . 20.4 fps (6.2 m/s)
Occupant Ridedown Acceleration
  Longitudinal. . . . . -0.6 g
  Lateral . . . . . 8.7 g
Vehicle Damage Classification
  TAD 11LD4
  VDI 11LDES2

Figure 16. Summary of results for test 2417-1.

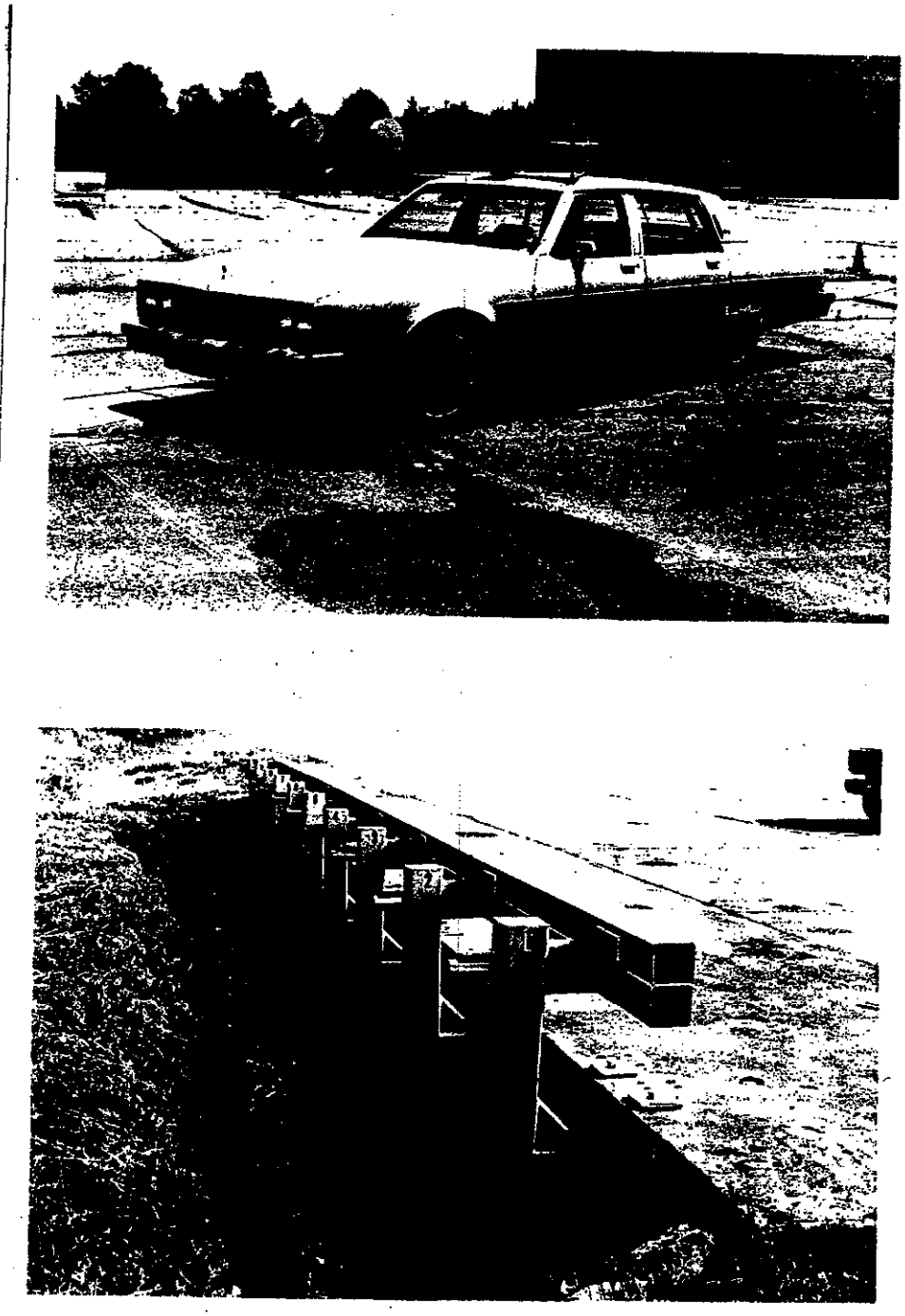

Figure 17. Bridge Rail and Vehicle Prior to Test 2417-2

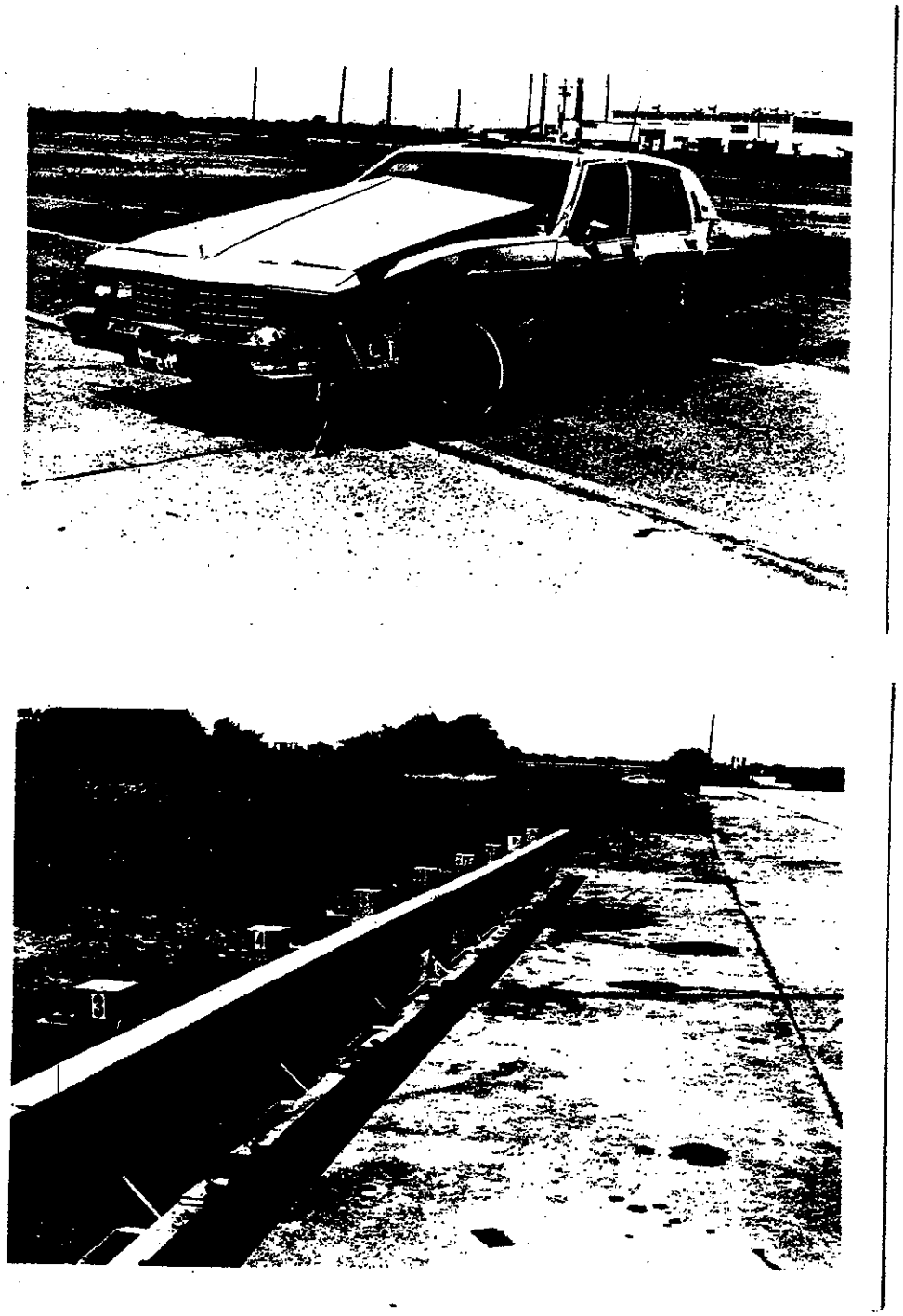

Figure 18. Bridge Rail and Vehicle After Test 2417-2

0.000 s 0.080 s 0.160 s 0.245 s

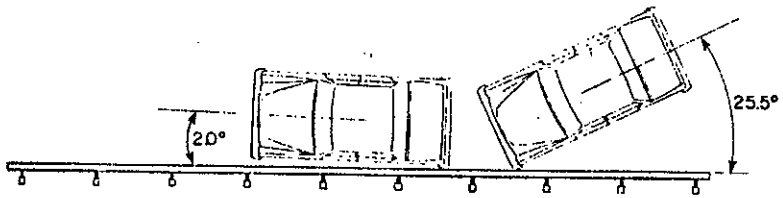

Test No.	2417-2
Date	5/24/85
Rail	Low-maintenance, energy-absorbing bridge rail
Post	7x7x¼ in Structural Steel Tube
Post Spacing	6.25 ft (1.91 m)
Length of Installation	59 ft (18 m)
Rail Deflection	
Maximum	0.60 ft (0.18 m)
Permanent	0.08 ft (0.02 m)
Vehicle	1980 Oldsmobile Ninety-eight
Vehicle Weight	4,500 lb (2,043 kg)

Impact Speed	61.0 mi/h (98.1 km/h)
Impact Angle	25.5 degrees
Exit Angle	2.0 degrees
Change in Velocity	14.36 mi/h (23.1 km/h)
Change in Momentum	2,943 lb-s
Occupant Impact Velocity	
Longitudinal	18.9 fps (5.8 m/s)
Lateral	28.5 fps (8.7 m/s)
Occupant Ridedown Acceleration	
Longitudinal	-2.5 g
Lateral	10.0 g
Vehicle Damage Classification	
TAD	10LD7
VDI	10LDES3

Figure 19. Summary of results for test 2417-2.

CONCLUSIONS

A low-maintenance, energy-absorbing bridge rail has been developed for use in high traffic volume situations where the cost of repairing conventional bridge rails has become prohibitively expensive. The new bridge rail is designed to meet or exceed all current bridge rail design guidelines for safety and structural capacity. The bridge rail is designed to smoothly redirect a 4500 lb (2043 kg) automobile traveling at 60 mph (96.6 km/hr) with an impact angle of 25° with no damage done to either the bridge rail or the bridge deck. If the bridge rail is subjected to a more severe impact it is anticipated that it would perform at least as well as a conventional bridge rail. Under extreme impact conditions, the bridge rail and posts would have to be repaired or replaced; however, the system is designed to inflict no damage to the bridge deck under any level of impact as demonstrated by the results of the bridge post tests.

A prototype bridge rail has been subjected to two full-scale crash tests involving an 1800 lb (817 kg) automobile and a 4500 lb (2043 kg) automobile as prescribed in NCHRP Report 230 (2). Results from both of these tests were within the acceptable limits for roll, pitch, yaw, acceleration, and velocity changes. The vehicles were smoothly redirected throughout the collisions with extremely shallow exit angles. The final vehicle trajectory after impact was parallel to the barrier face. Following the large automobile impact the bridge rail had less than 1 in. (25.4 mm) of permanent lateral deformation, the bridge deck was undamaged, and no maintenance would have been required to keep the bridge rail in service.

APPENDIX A.

FABRICATION DETAILS FOR ENERGY-ABSORBING BRIDGE RAIL

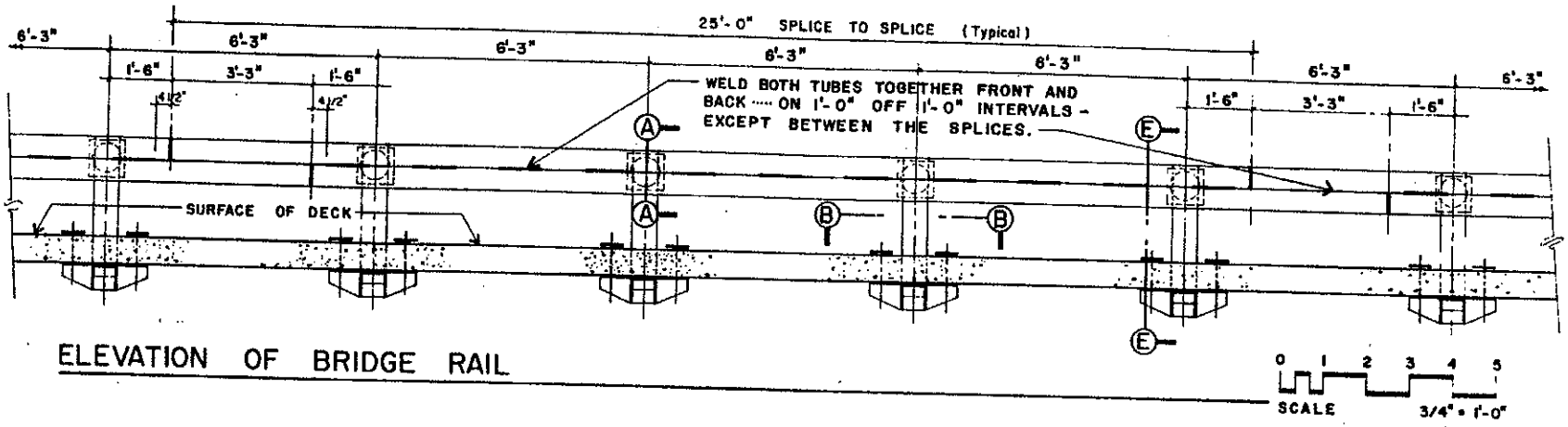

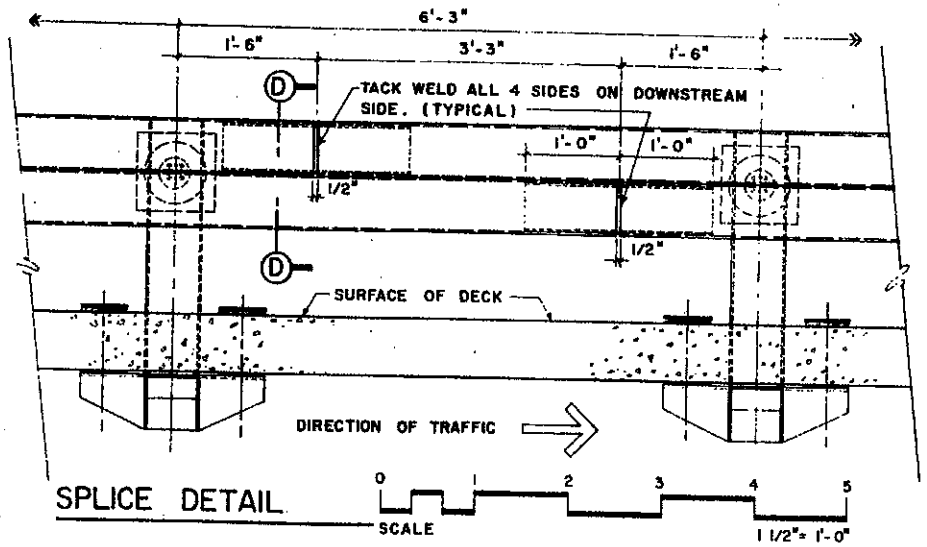

Figure 20. Fabrication Drawings of Energy-Absorbing Bridge Rail

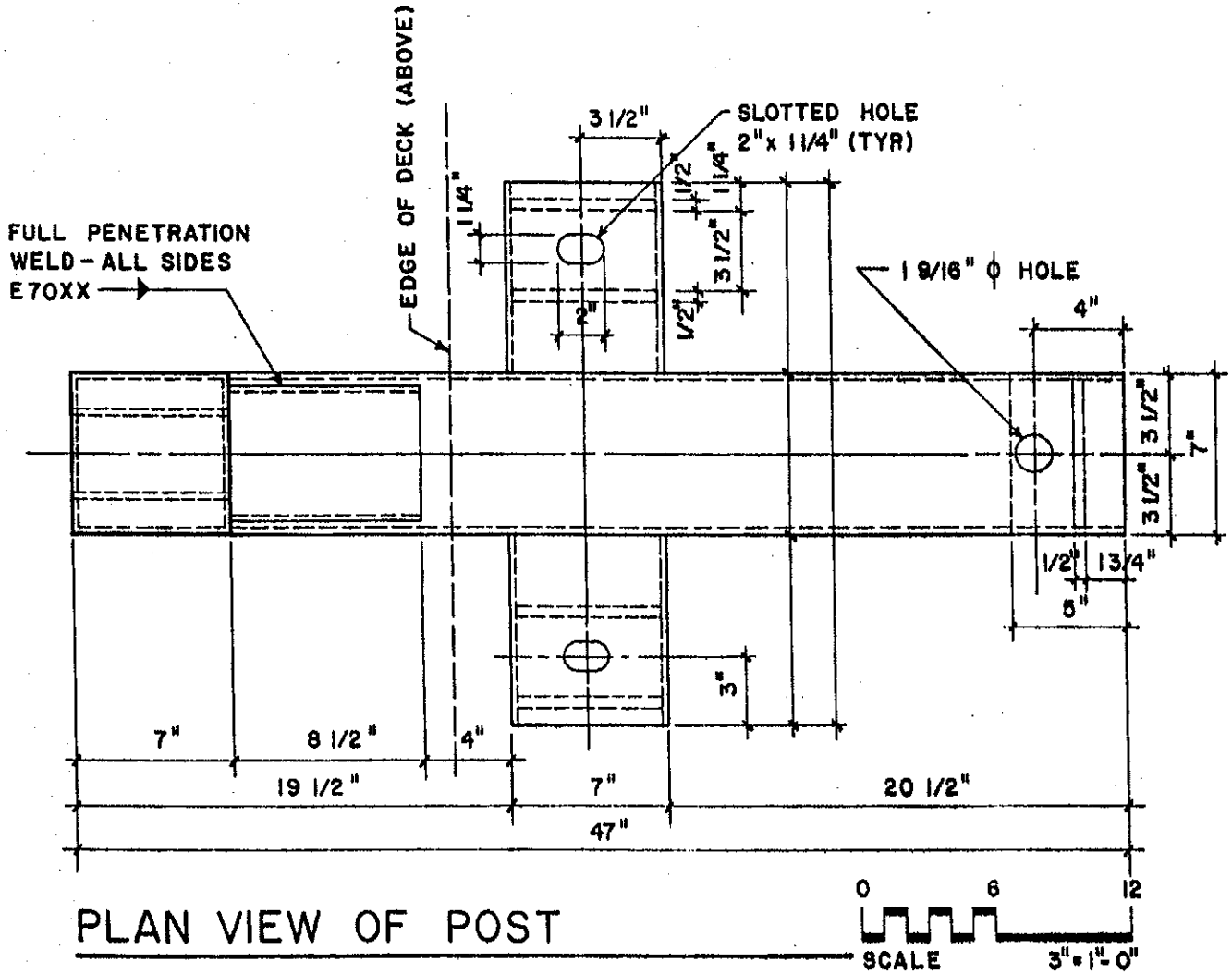

Figure 20. Fabrication Drawings of Energy-Absorbing Bridge Rail (continued)

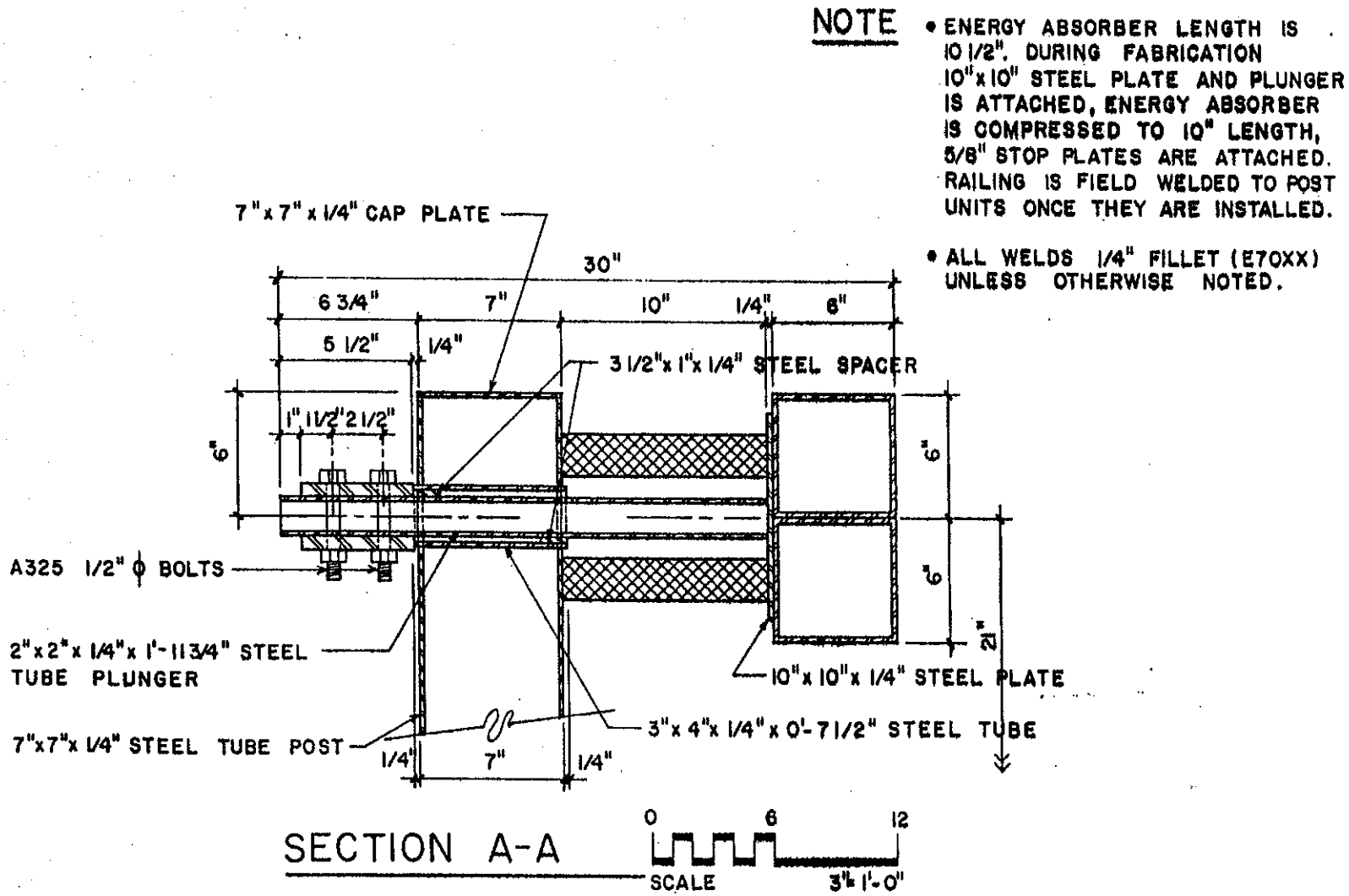

Figure 20. Fabrication Drawings of Energy-Absorbing Bridge Rail (continued)

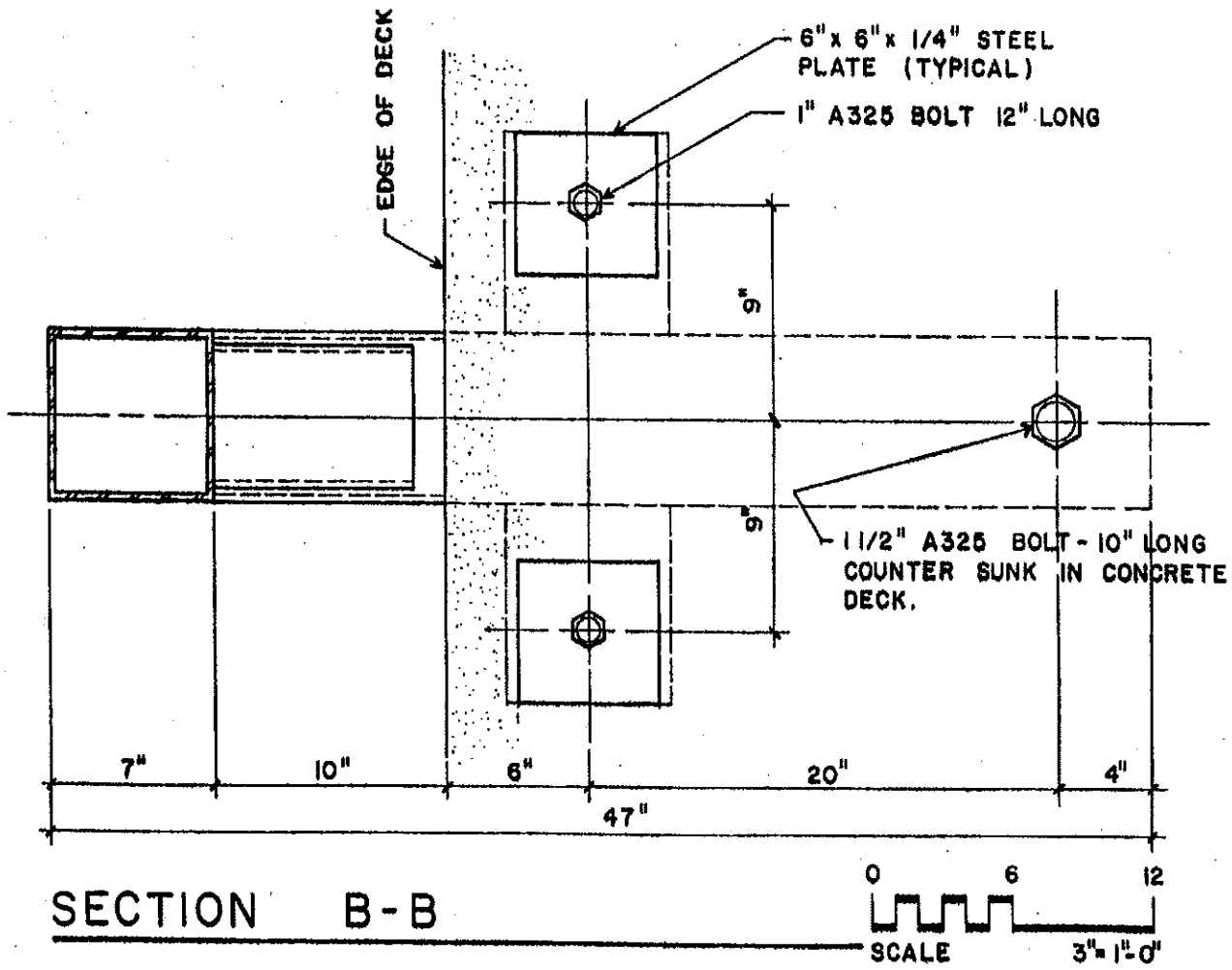

Figure 20. Fabrication Drawings of Energy-Absorbing Bridge Rail (continued)

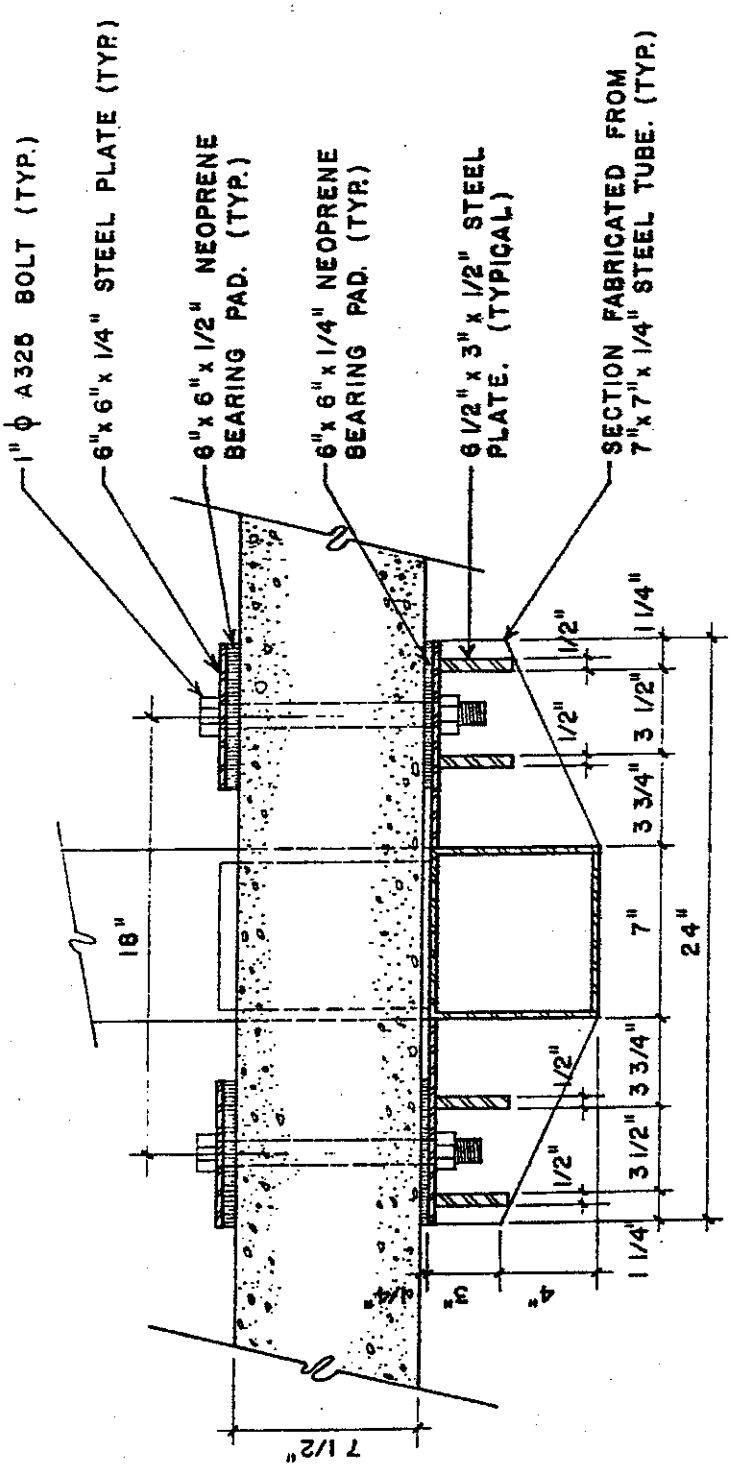

Figure 20. Fabrication Drawings of Energy-Absorbing Bridge Rail (continued)

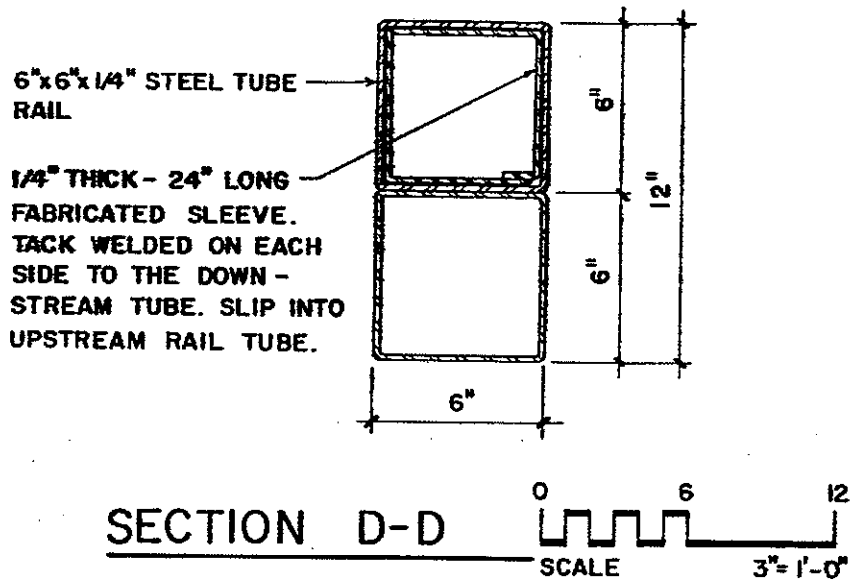

Figure 20. Fabrication Drawings of Energy-Absorbing Bridge Rail (continued)

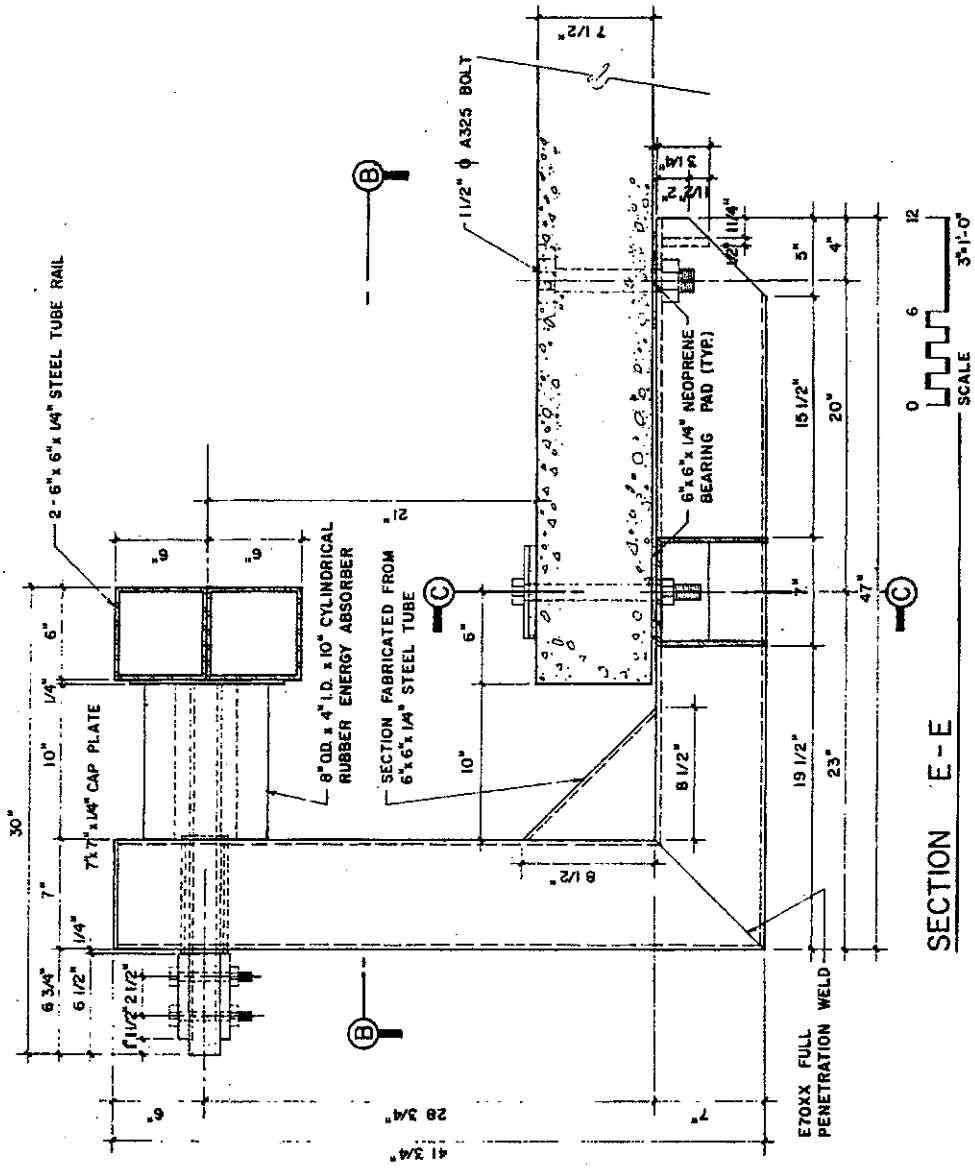

Figure 20. Fabrication Drawings of Energy-Absorbing Bridge Rail (continued)

APPENDIX B.

LOAD-DEFLECTION RESULTS

FOR RUBBER CYLINDER TESTS

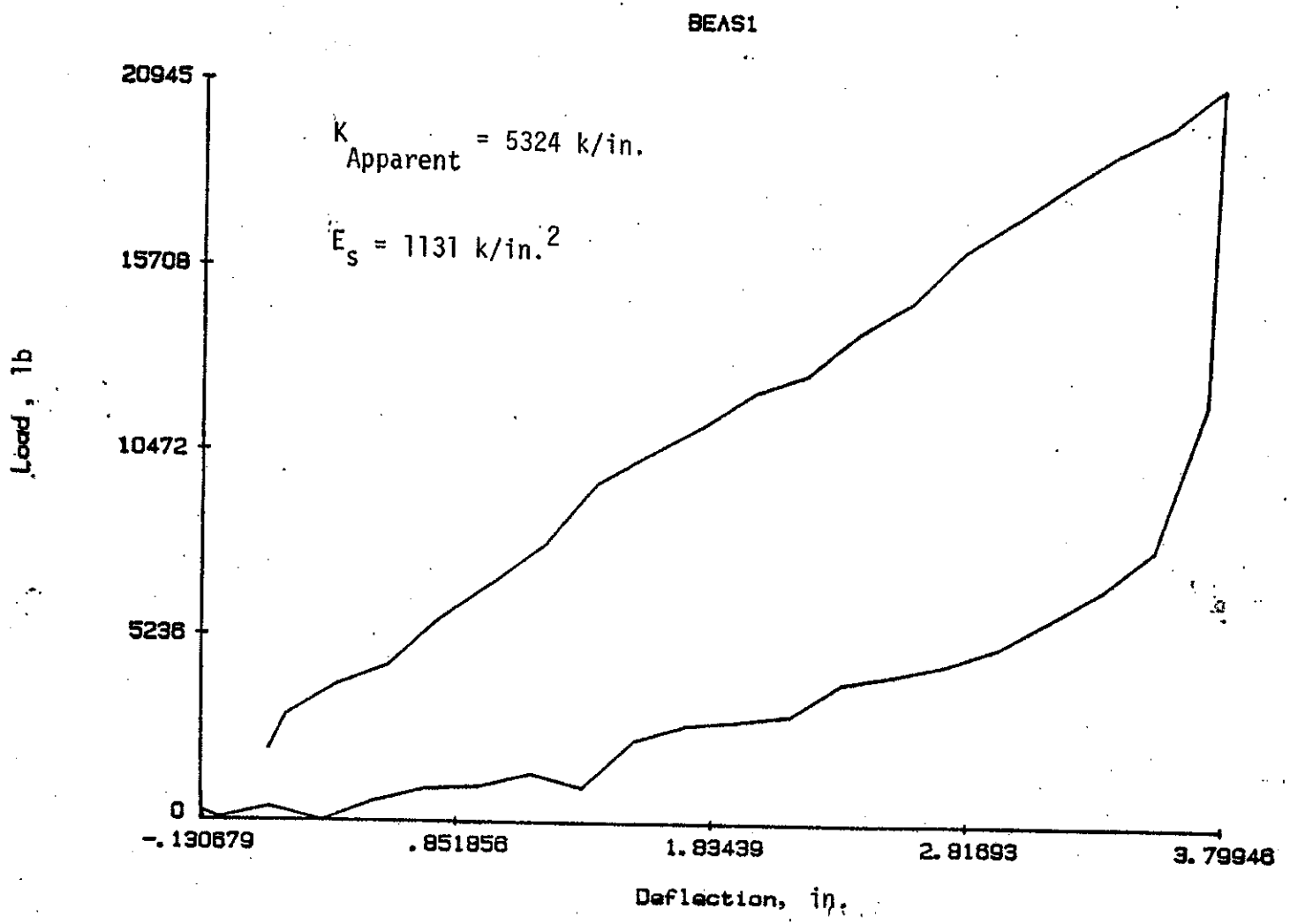

Figure 21. Test 1: 8 x 4 x 8 in. Rubber Cylinder, 50% Strain

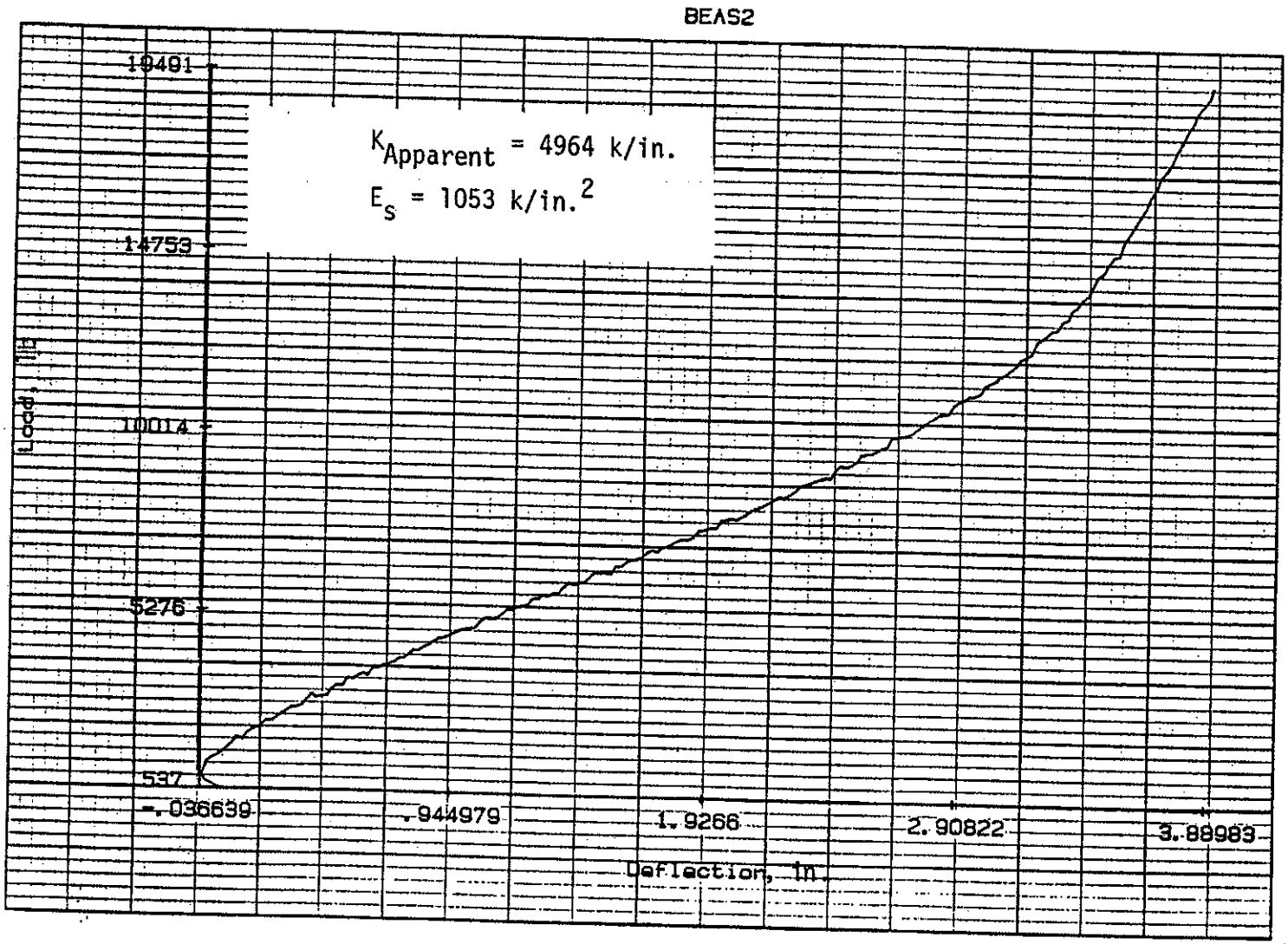

Figure 22. Test 2: 8 x 4 x 8 in. Rubber Cylinder, 50% Strain

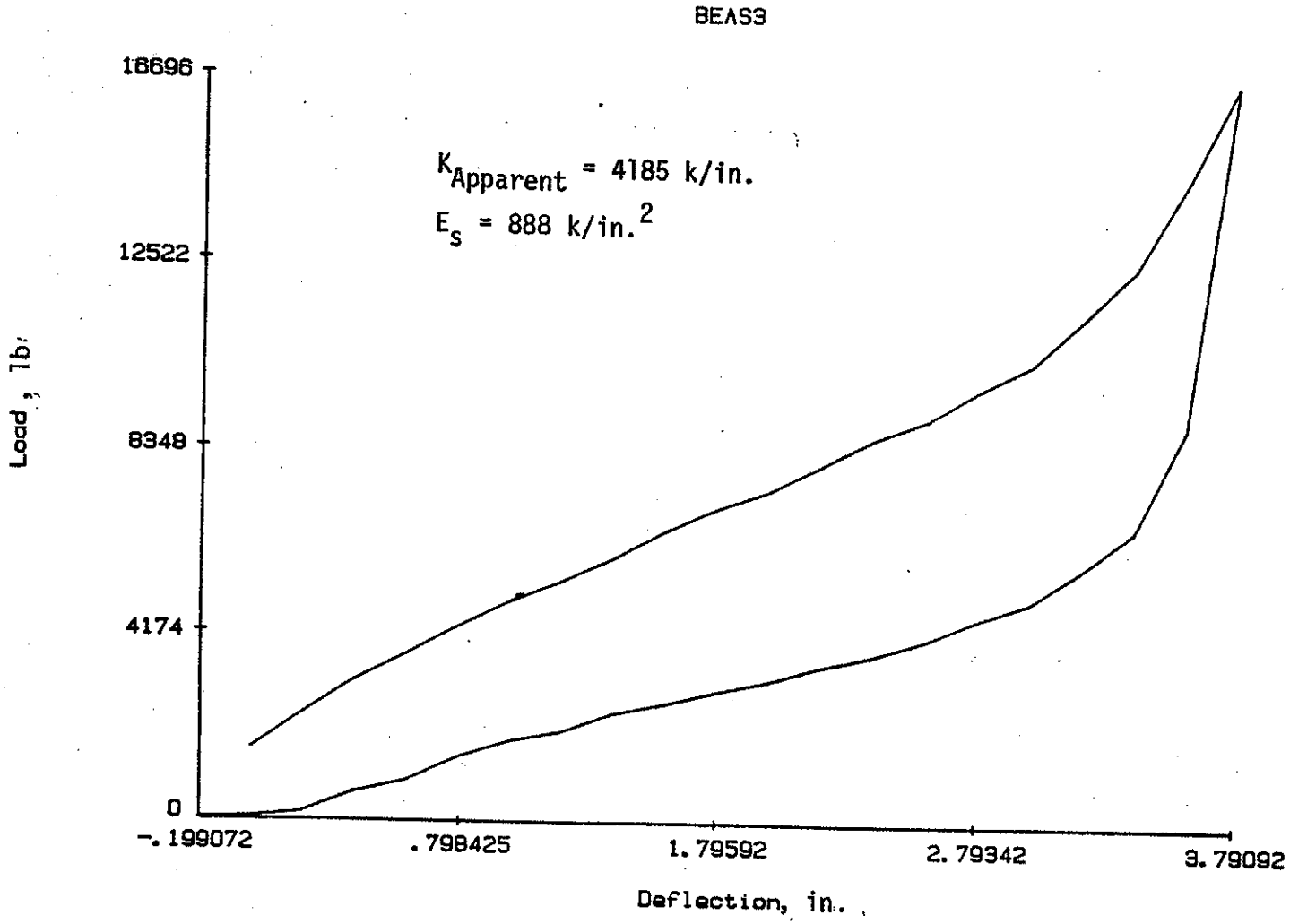

Figure 23. Test 3: 8 x 4 x 8 in. Rubber Cylinder, 50% Strain

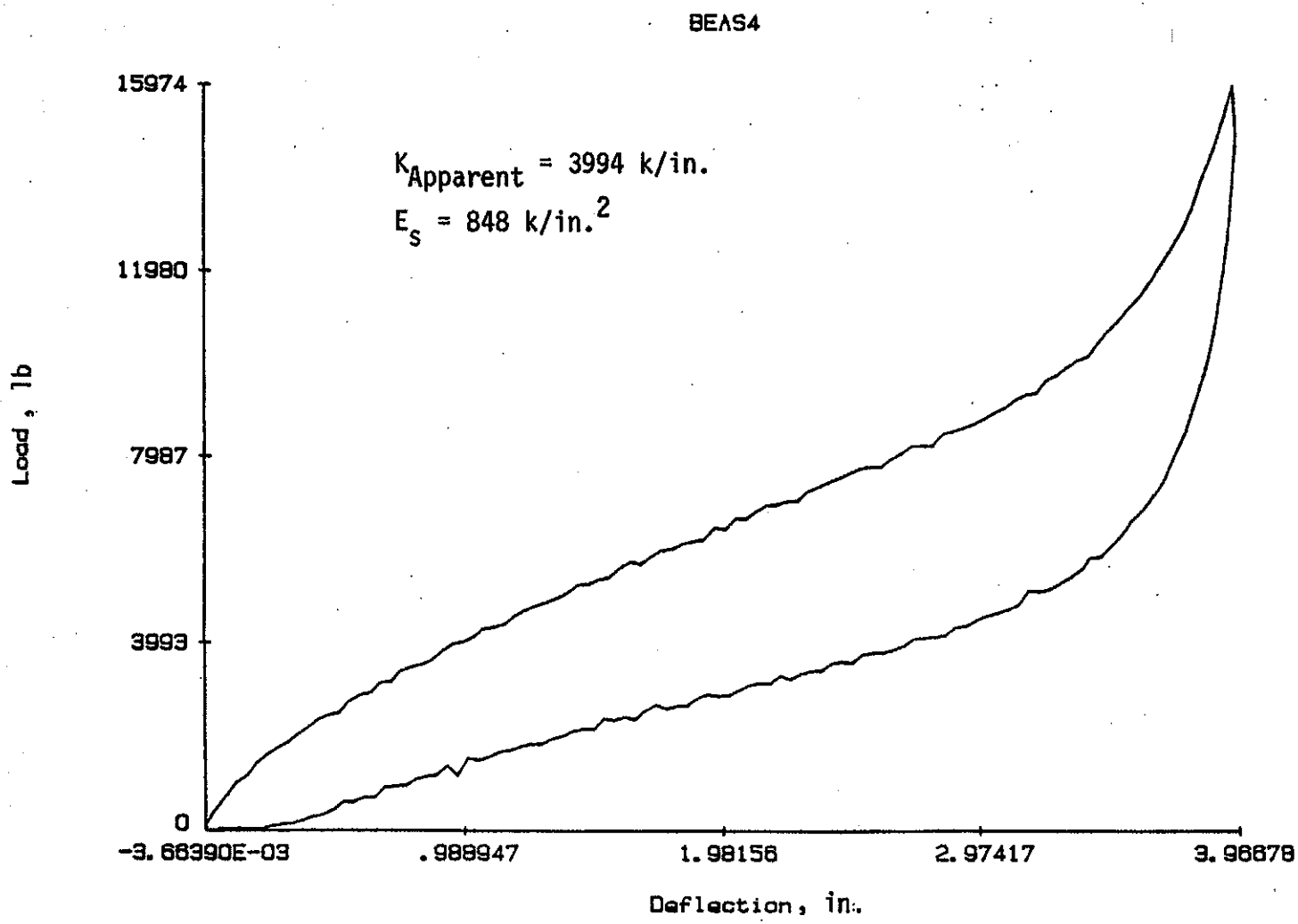

Figure 24. Test 4: 8 x 4 x 8 in. Rubber Cylinder, 50% Strain

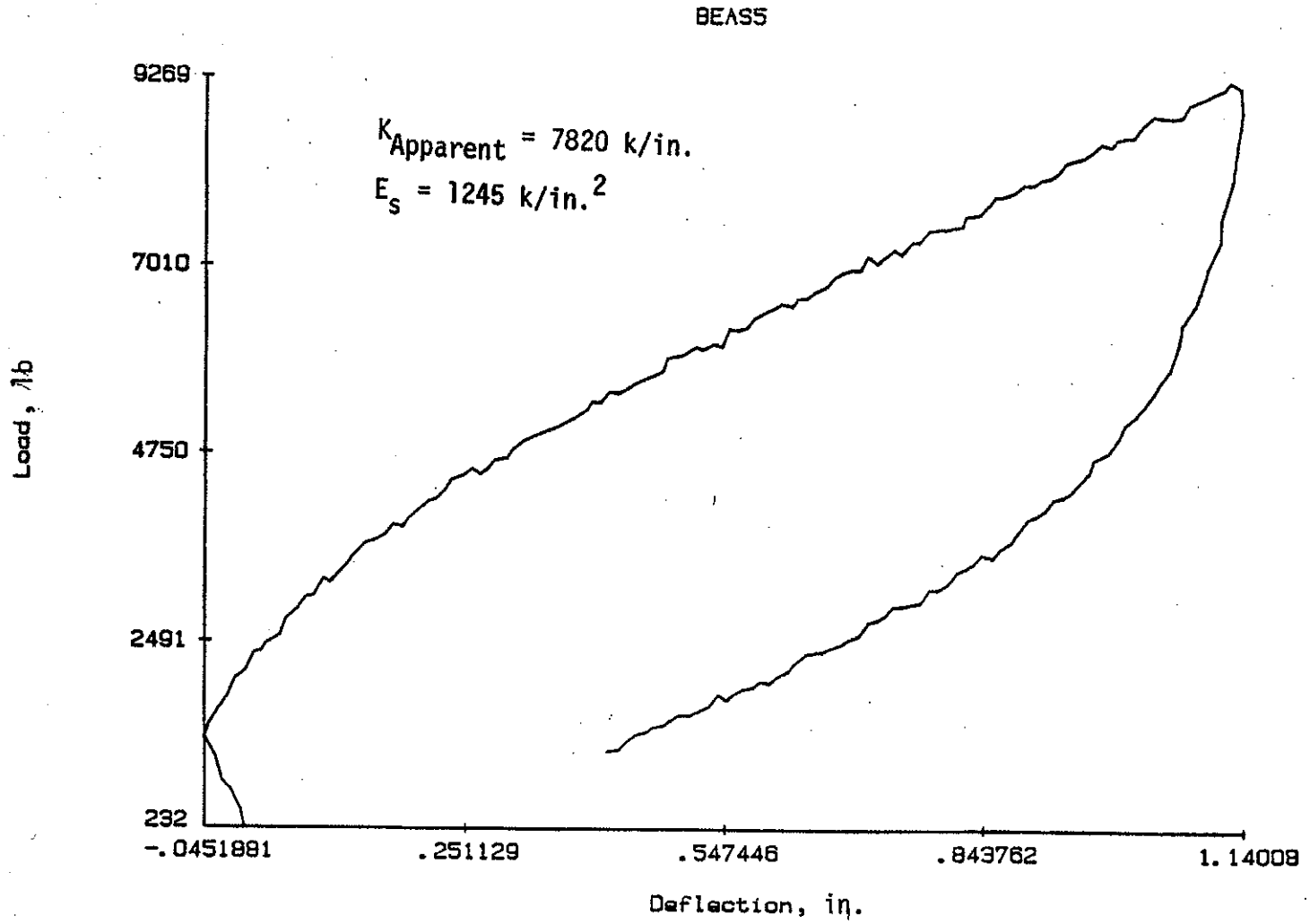

Figure 25. Test 5: 8 x 4 x 6 in. Rubber Cylinder, 20% Strain

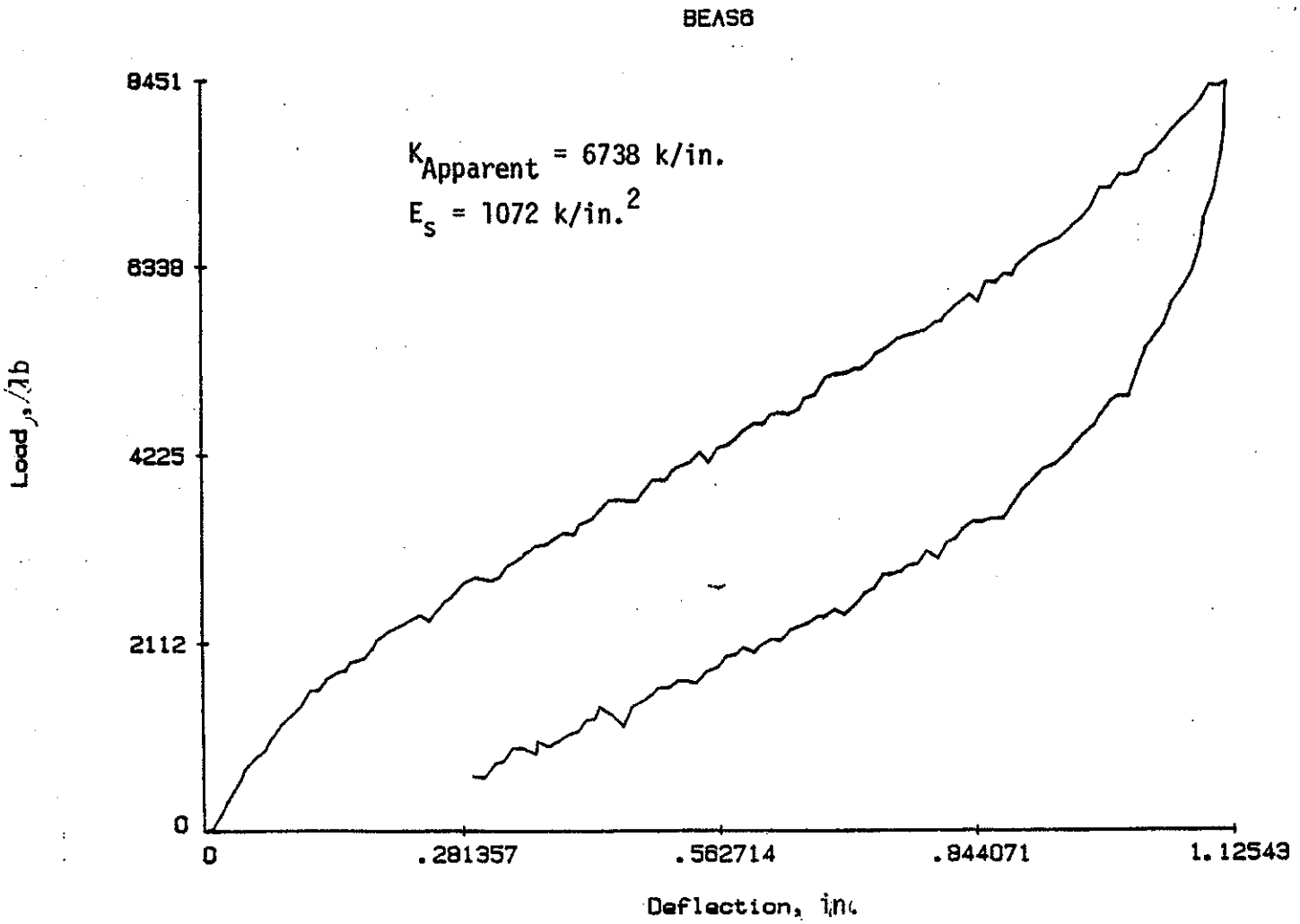

Figure 26. Test 6: 8 x 4 x 6 in. Rubber Cylinder, 20% Strain

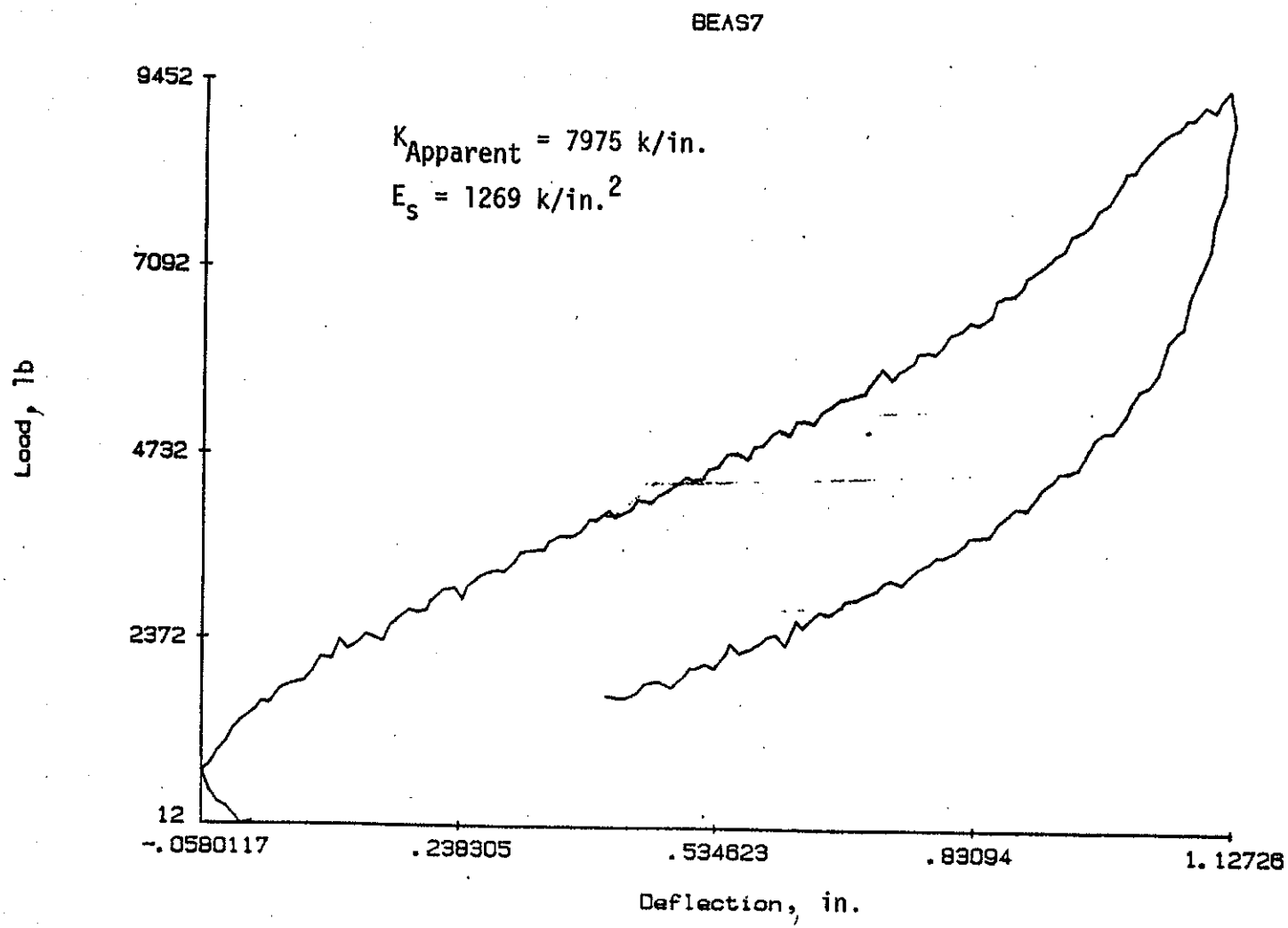

Figure 27. Test 7: 8 x 4 x 6 in. Rubber Cylinder, 20% Strain

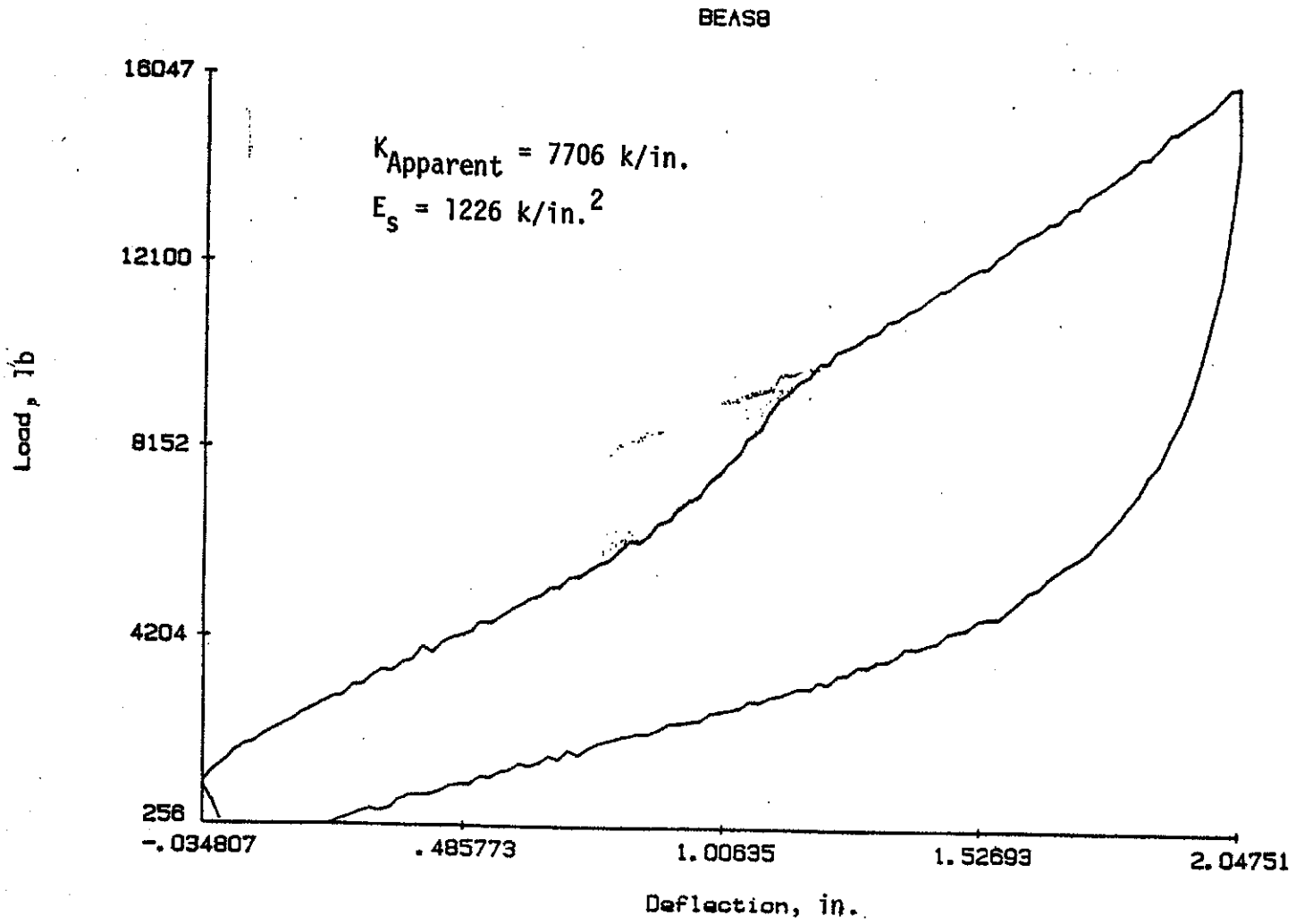

Figure 28. Test 8: 8 x 4 x 6 in. Rubber Cylinder, 35% Strain

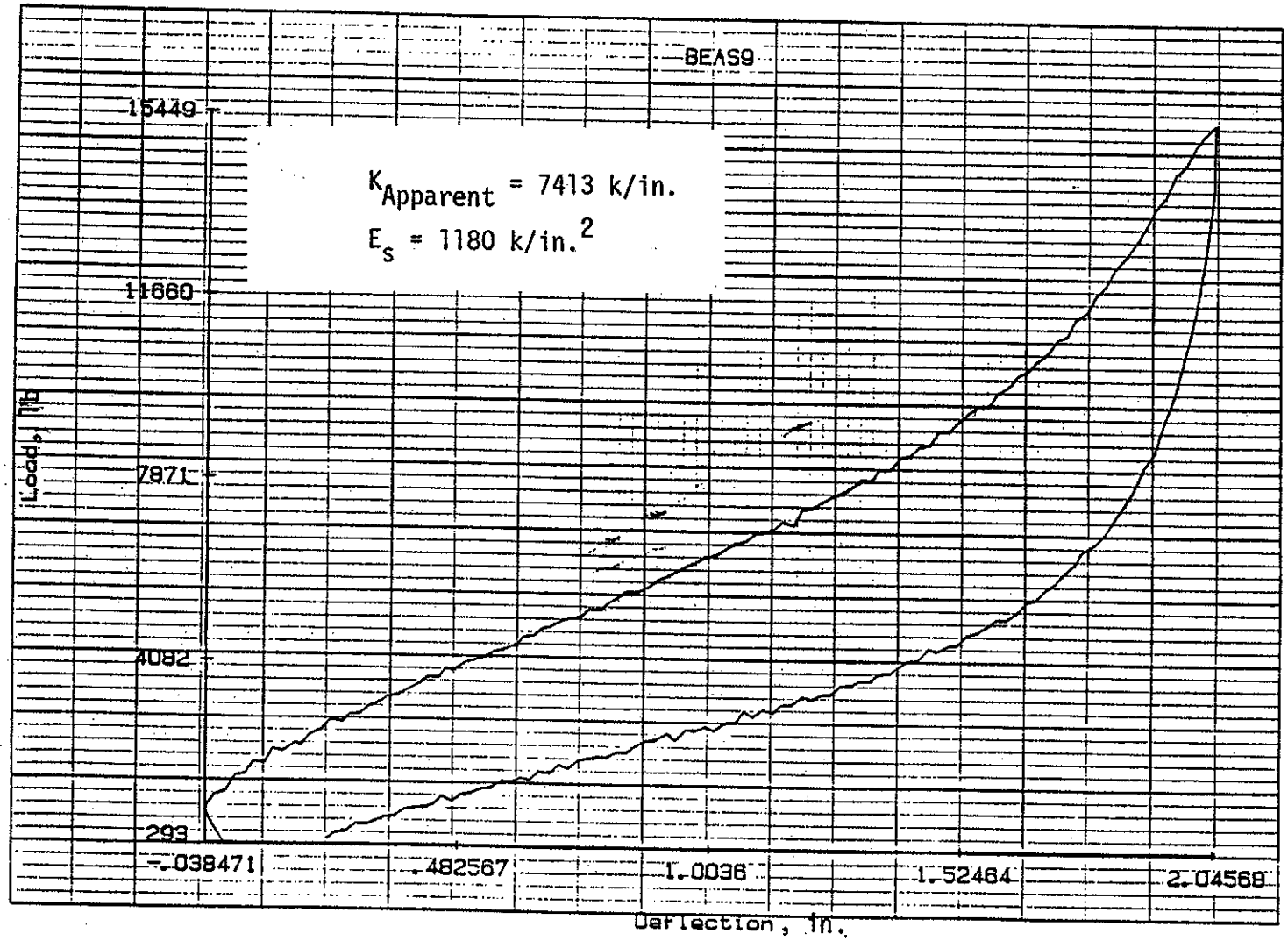

Figure 29. Test 9: 8 x 4 x 6 in. Rubber Cylinder, 35% Strain

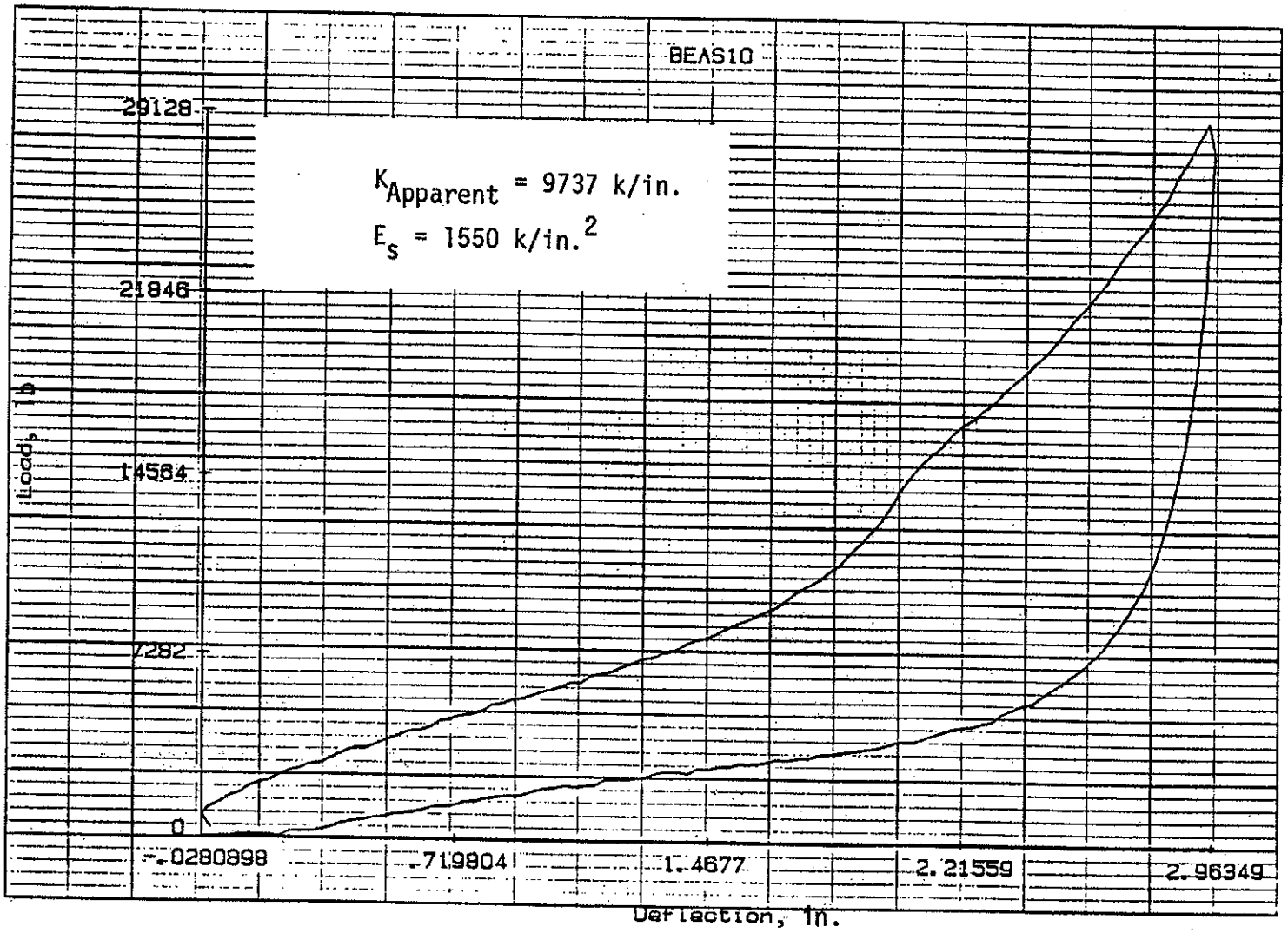

Figure 30. Test 10: 8 x 4 x 6 in. Rubber Cylinder, 50% Strain

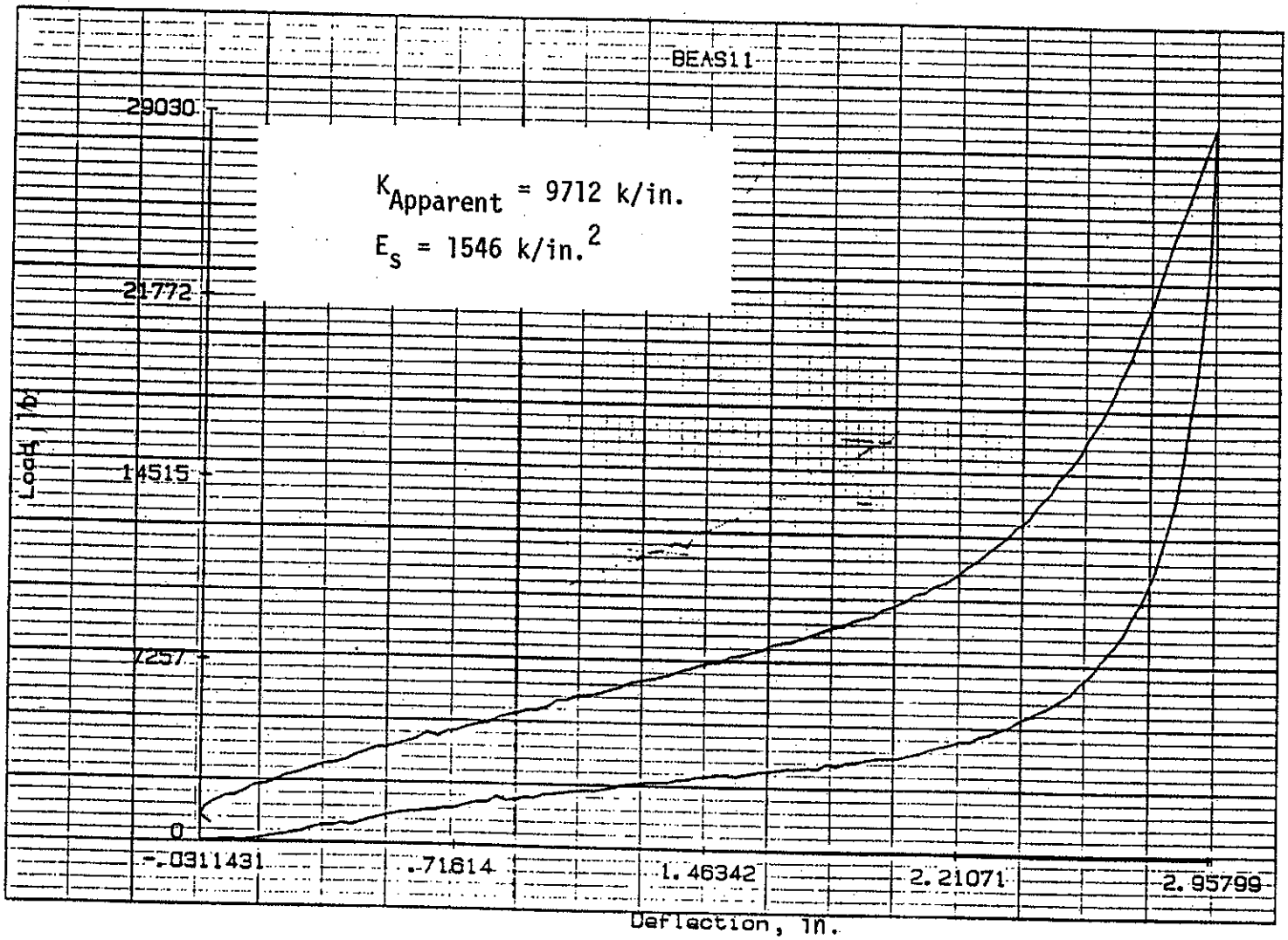

Figure 31. Test 11: 8 x 4 x 6 in. Rubber Cylinder, 50% Strain

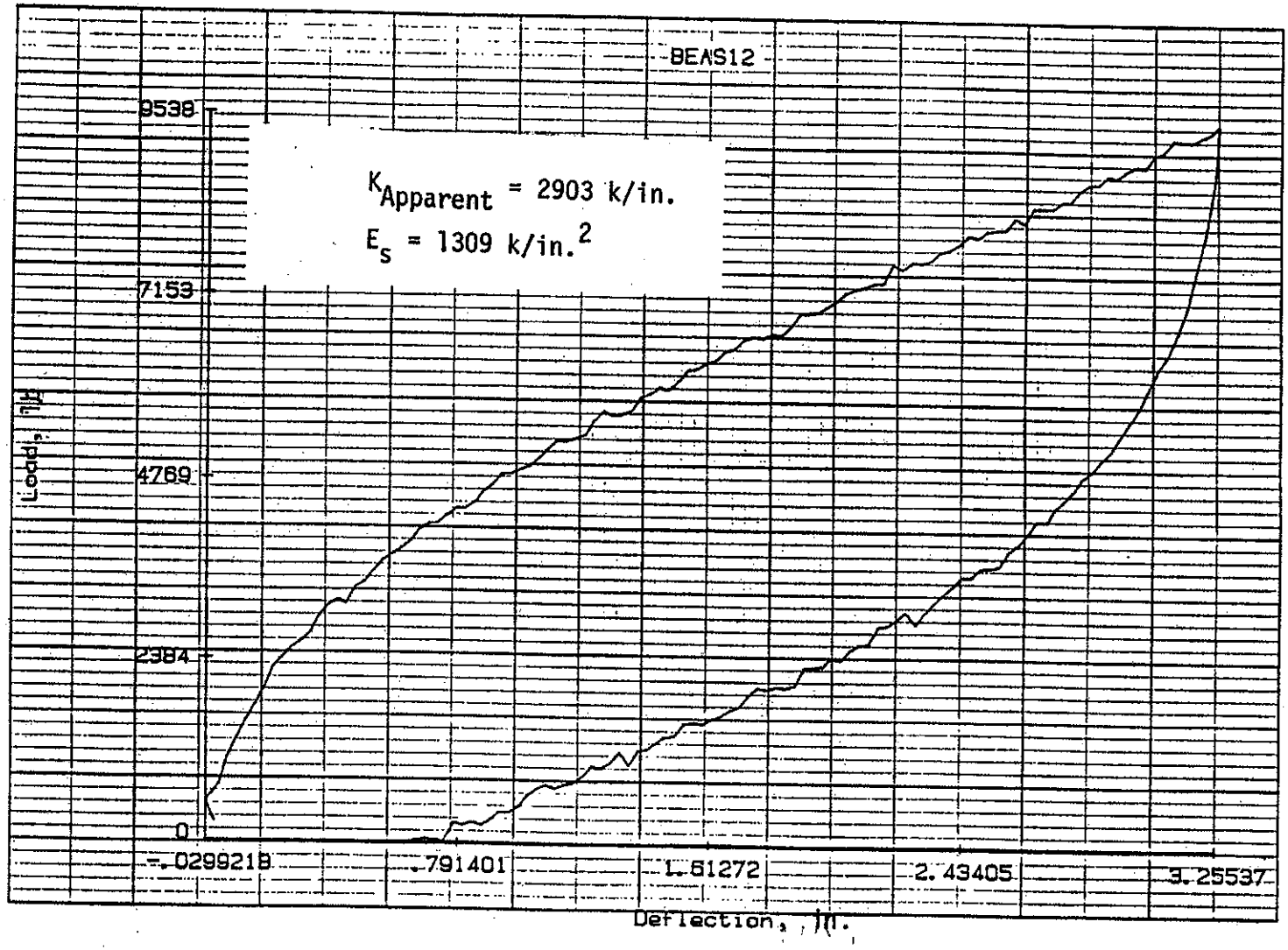

Figure 32. Test 12: 8 x 4 x 17 in. Rubber Cylinder, 20% Strain

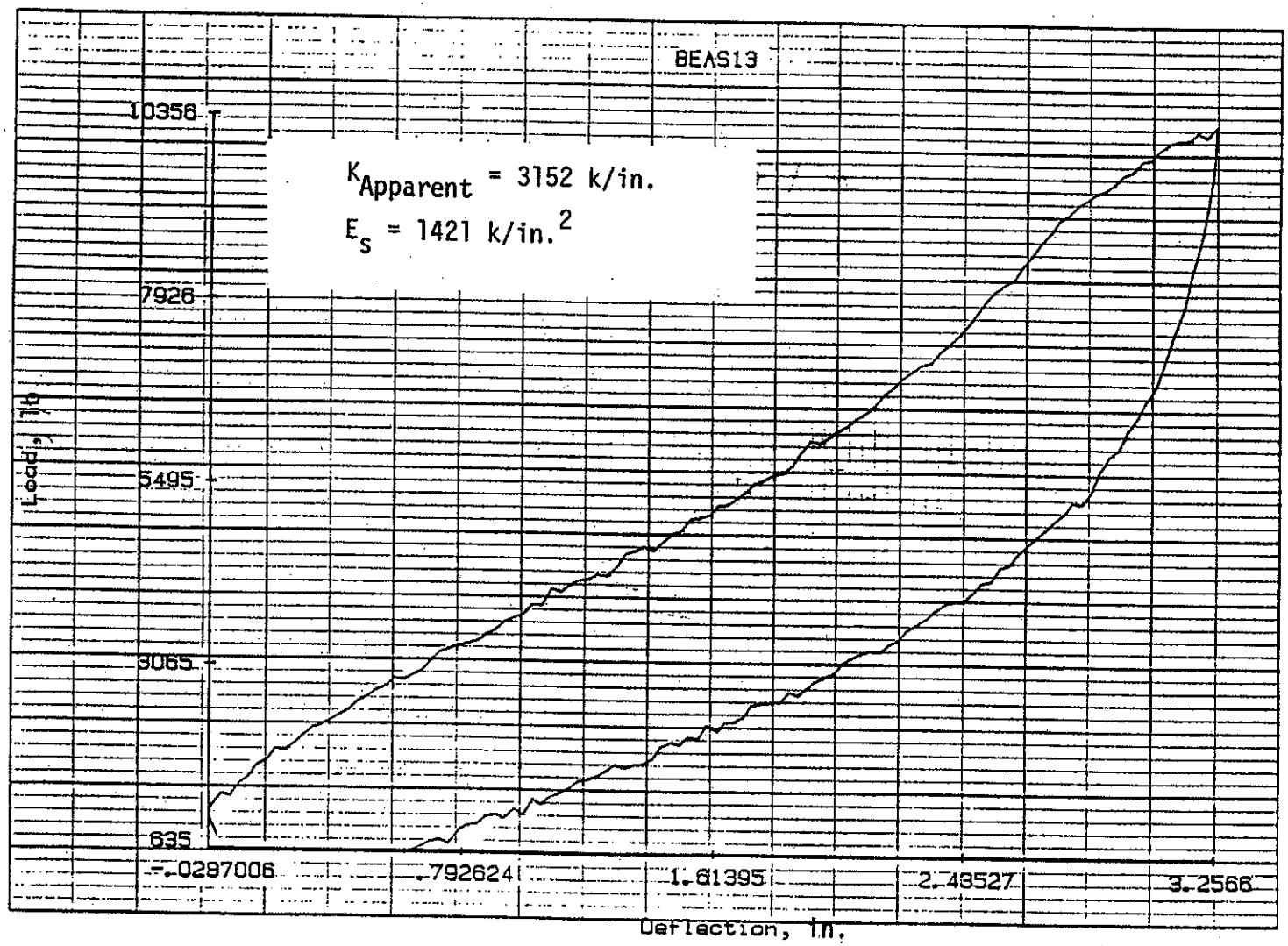

Figure 33. Test 13: 8 x 4 x 17 in. Rubber Cylinder, 20% Strain

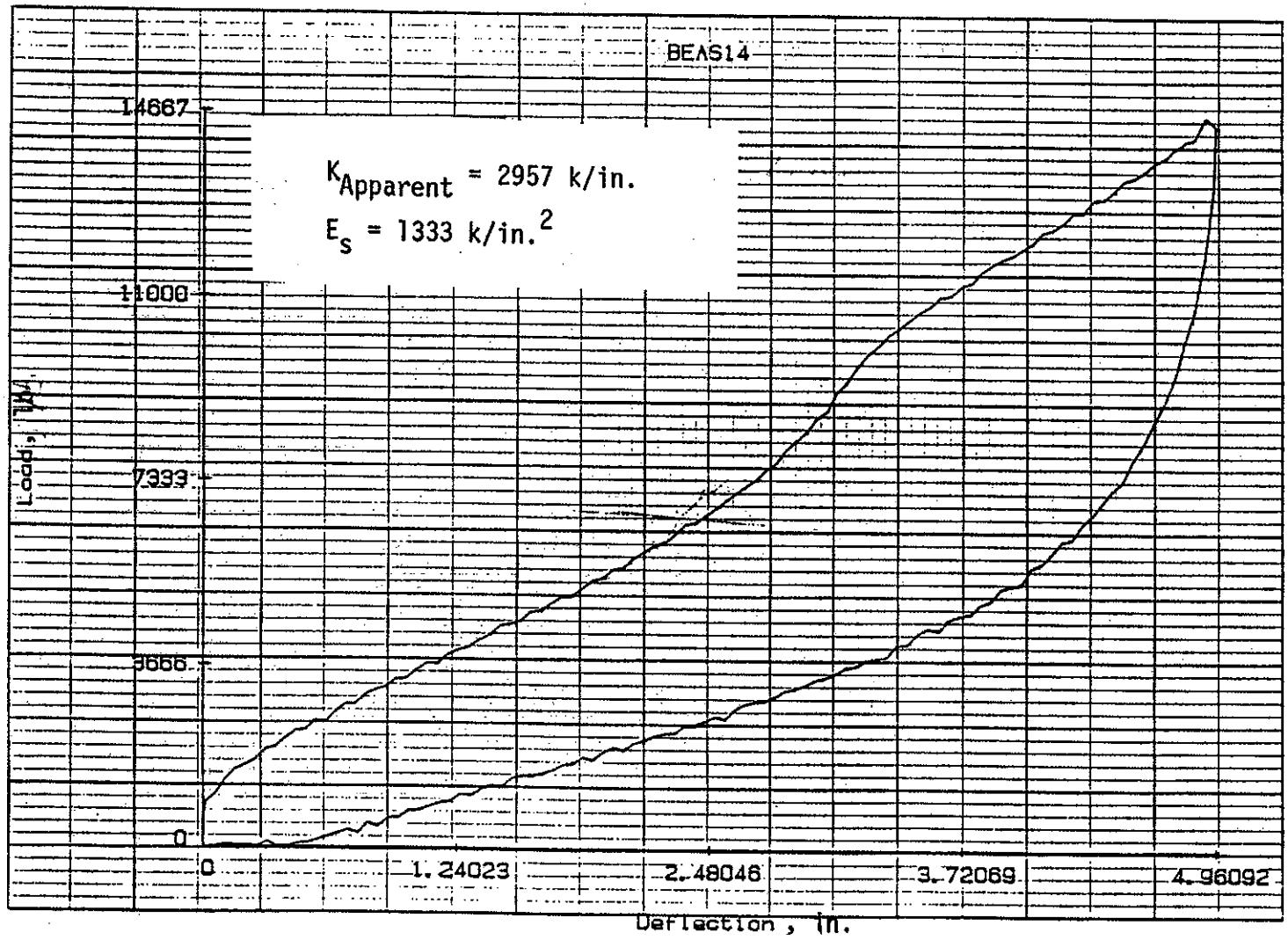

Figure 34. Test 14: 8 x 4 x 17 in. Rubber Cylinder, 30% Strain

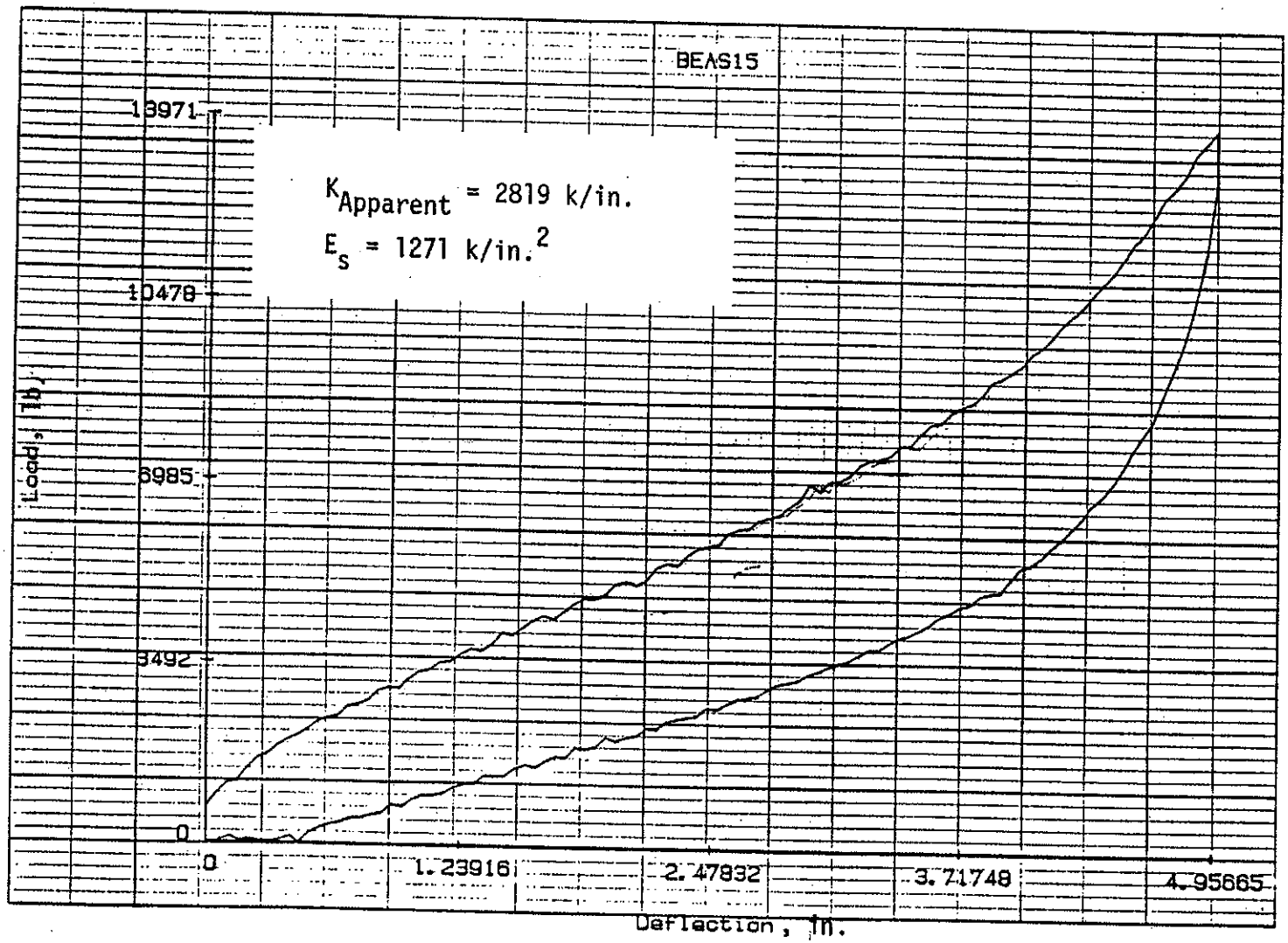

Figure 35. Test 15: 8 x 4 x 17 in. Rubber Cylinder, 30% Strain

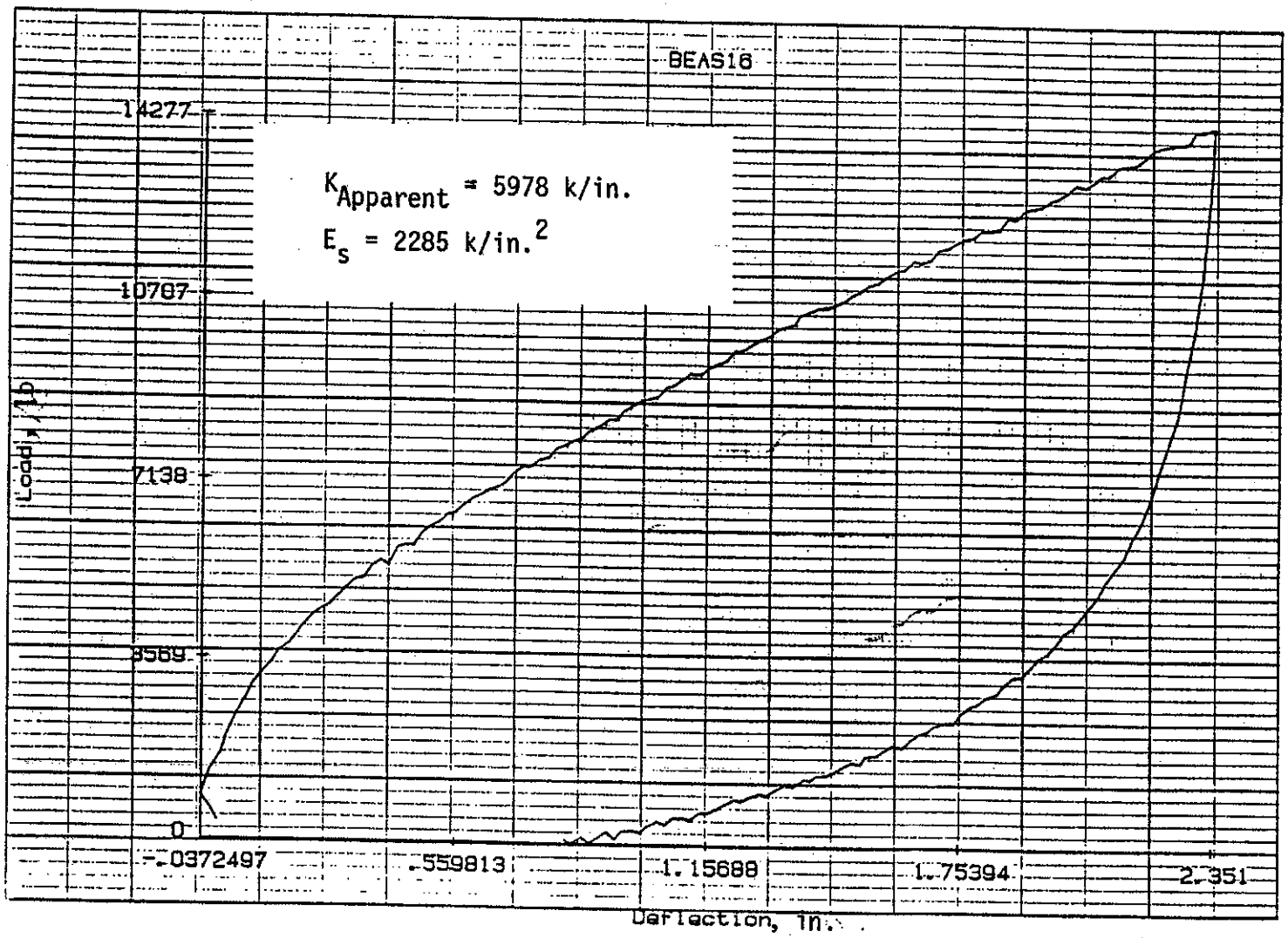

Figure 36. Test 16: 7 x 3 x 12 in. Rubber Cylinder, 20% Strain

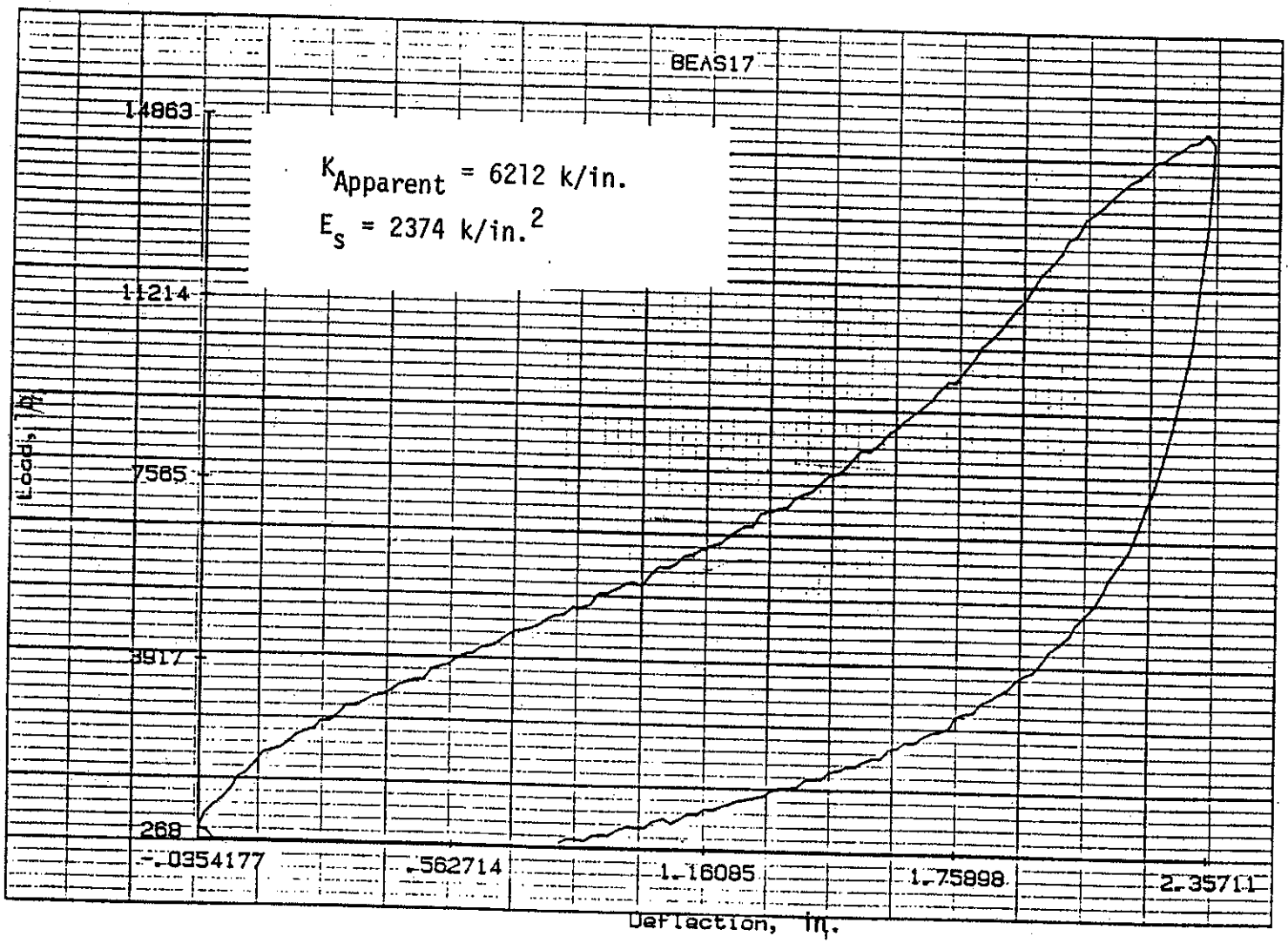

Figure 37. Test 17: 7 x 3 x 12 in. Rubber Cylinder, 20% Strain

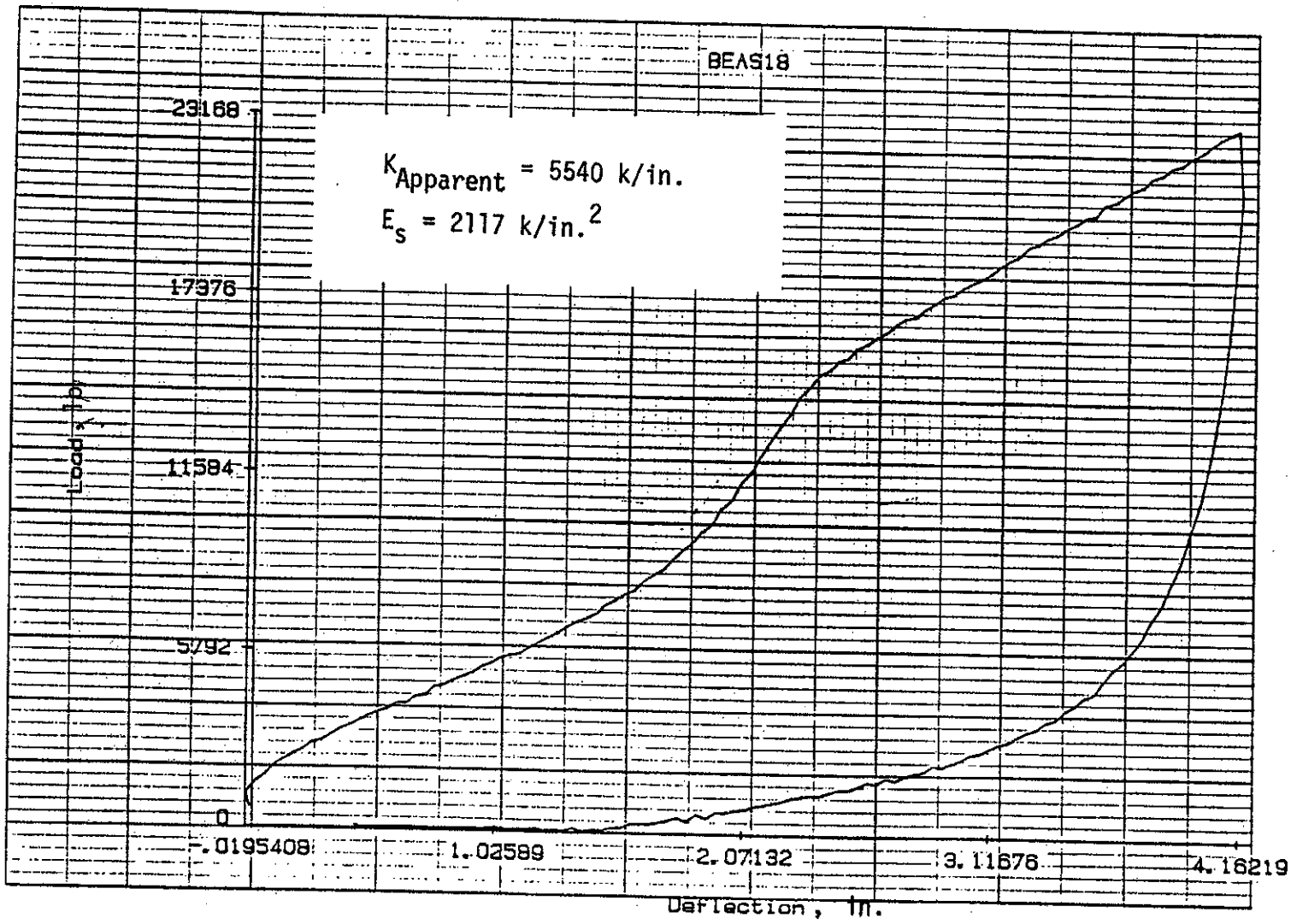

Figure 38. Test 18: 7 x 3 x 12 in. Rubber Cylinder, 35% Strain

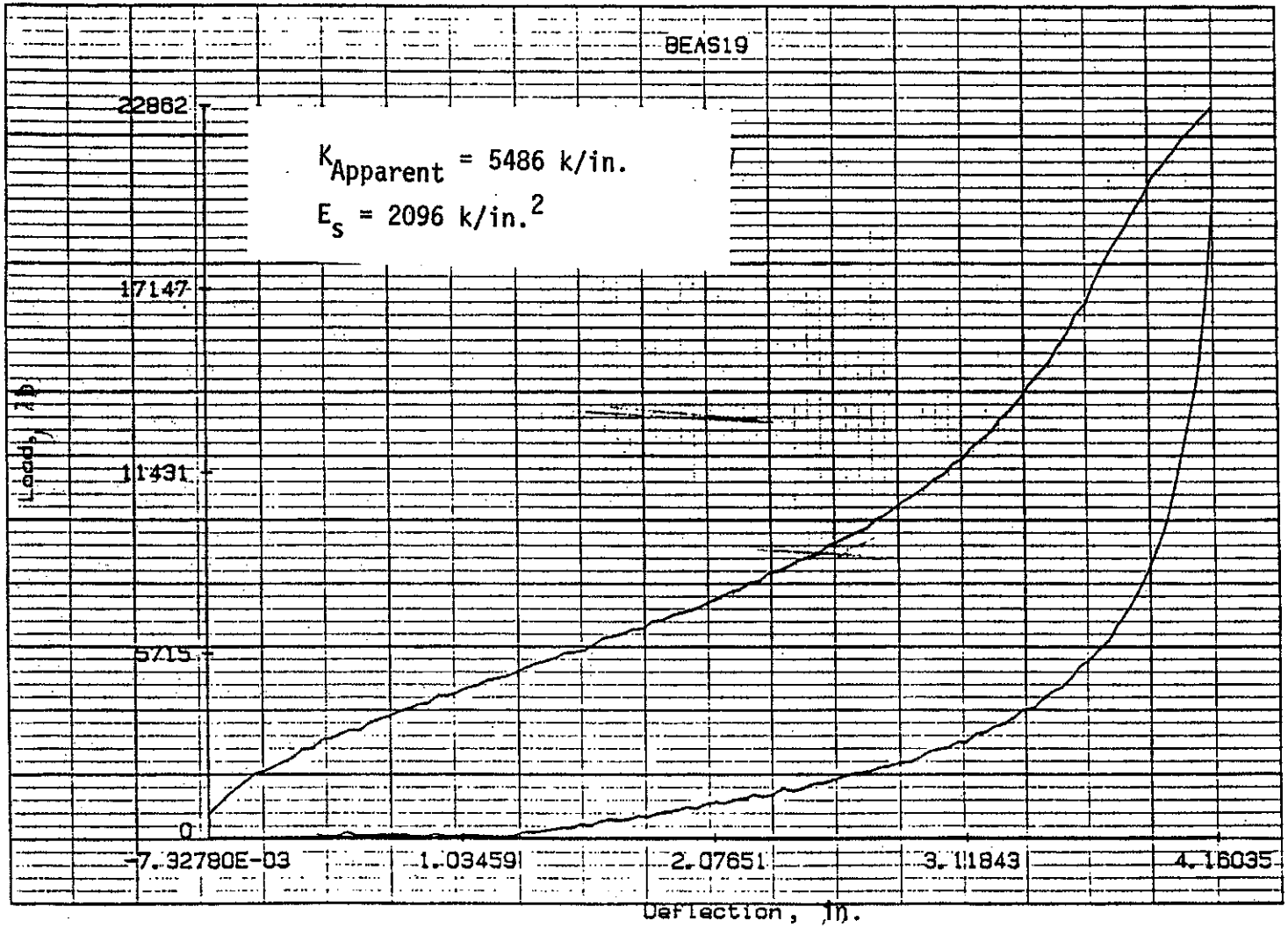

Figure 39. Test 19: 7 x 3 x 12 in. Rubber Cylinder, 35% Strain

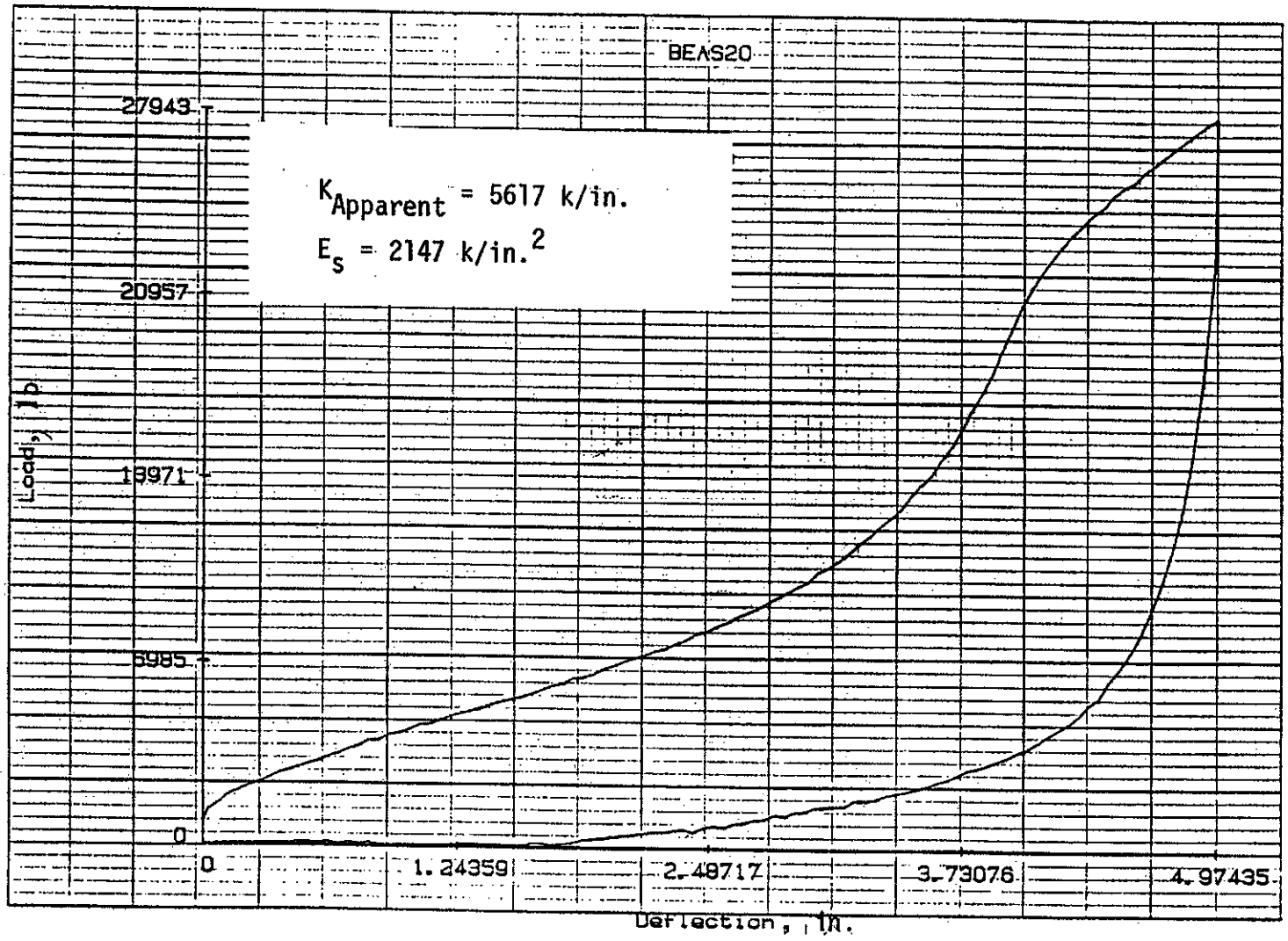

Figure 40. Test 20: 7 x 3 x 12 in. Rubber Cylinder, 42% Strain

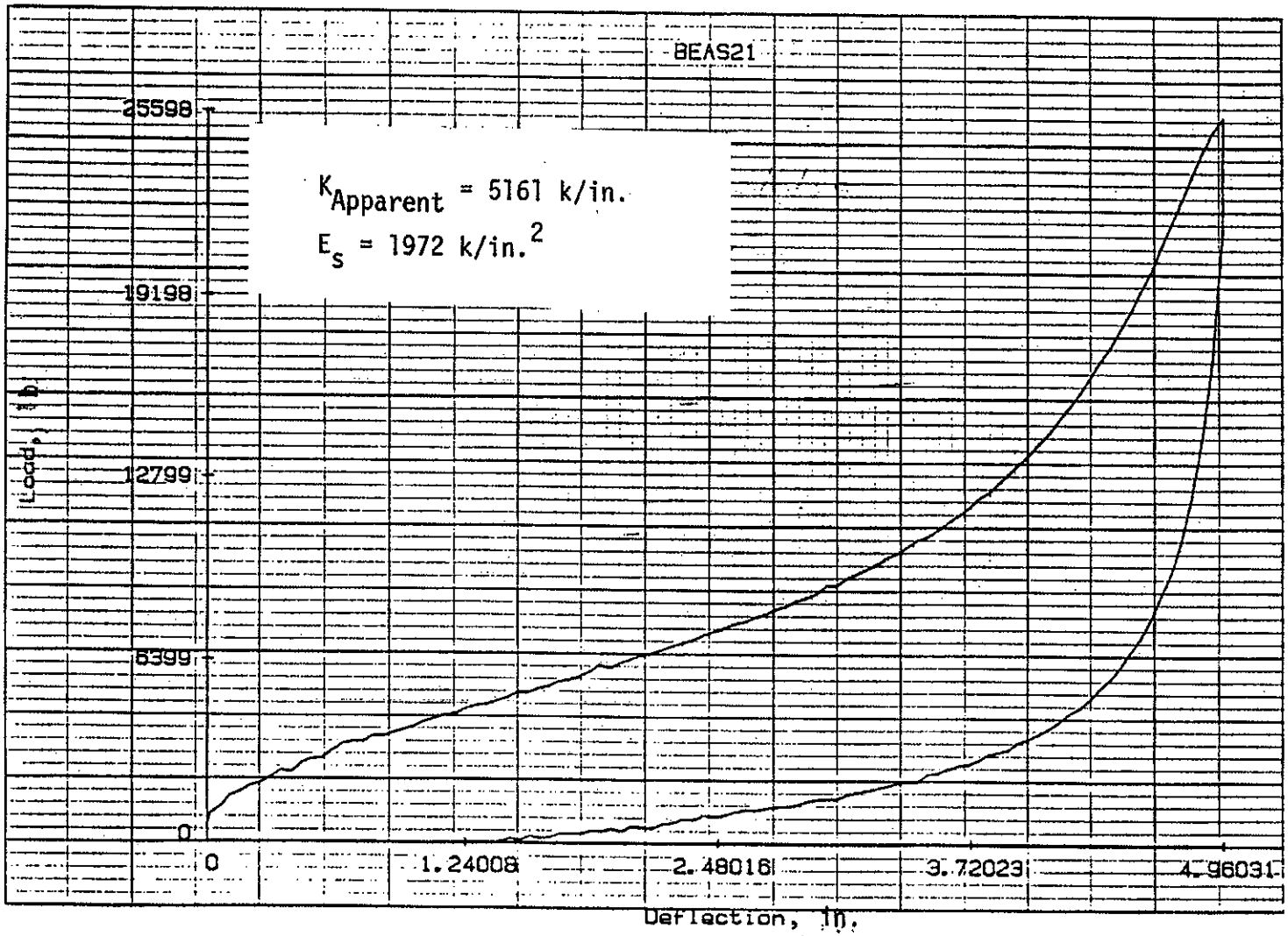

Figure 41. Test 21: 7 x 3 x 12 in. Rubber Cylinder, 42% Strain

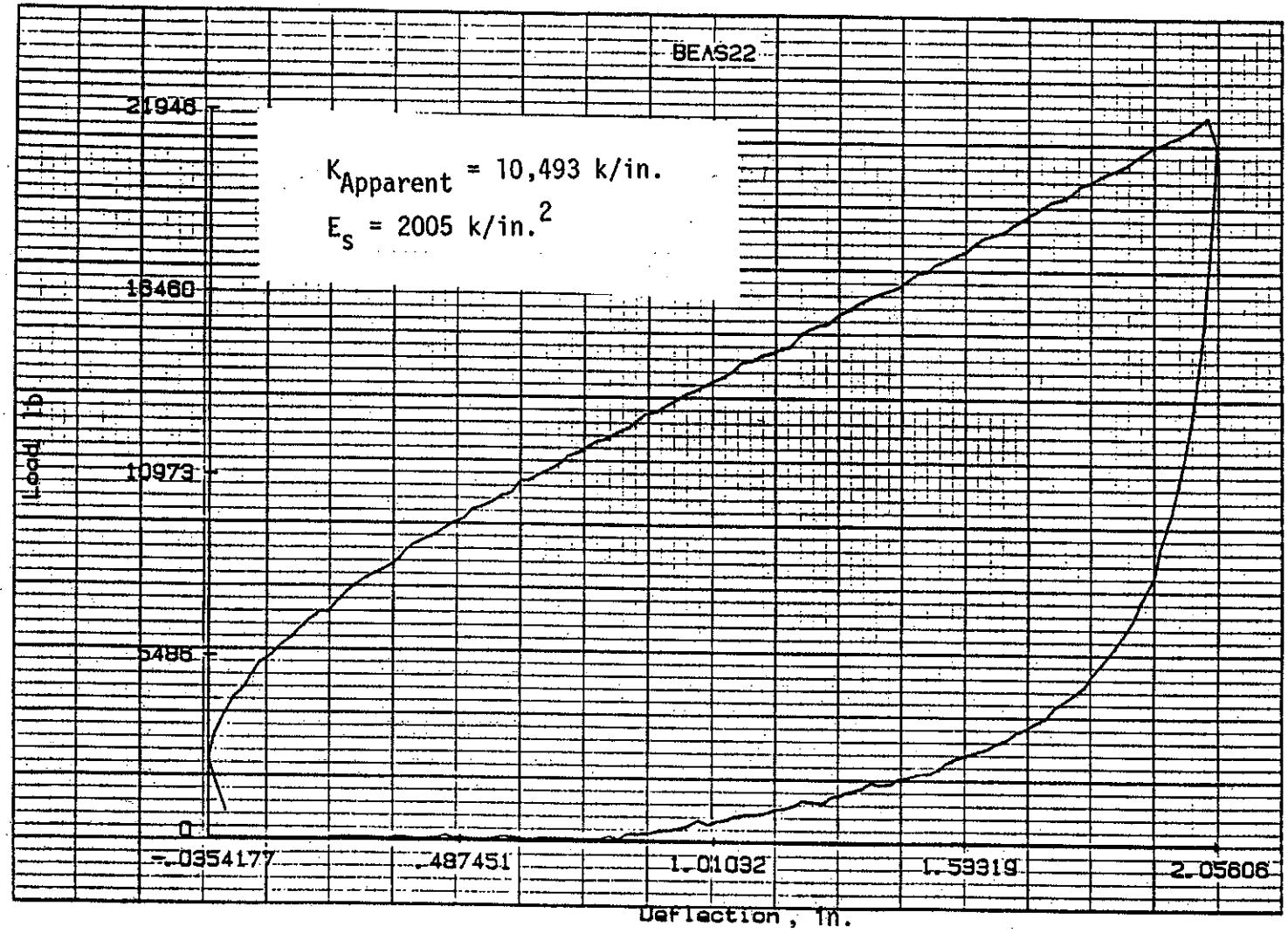

Figure 42. Test 22: 7 x 3 x 6 in. Rubber Cylinder, 35% Strain

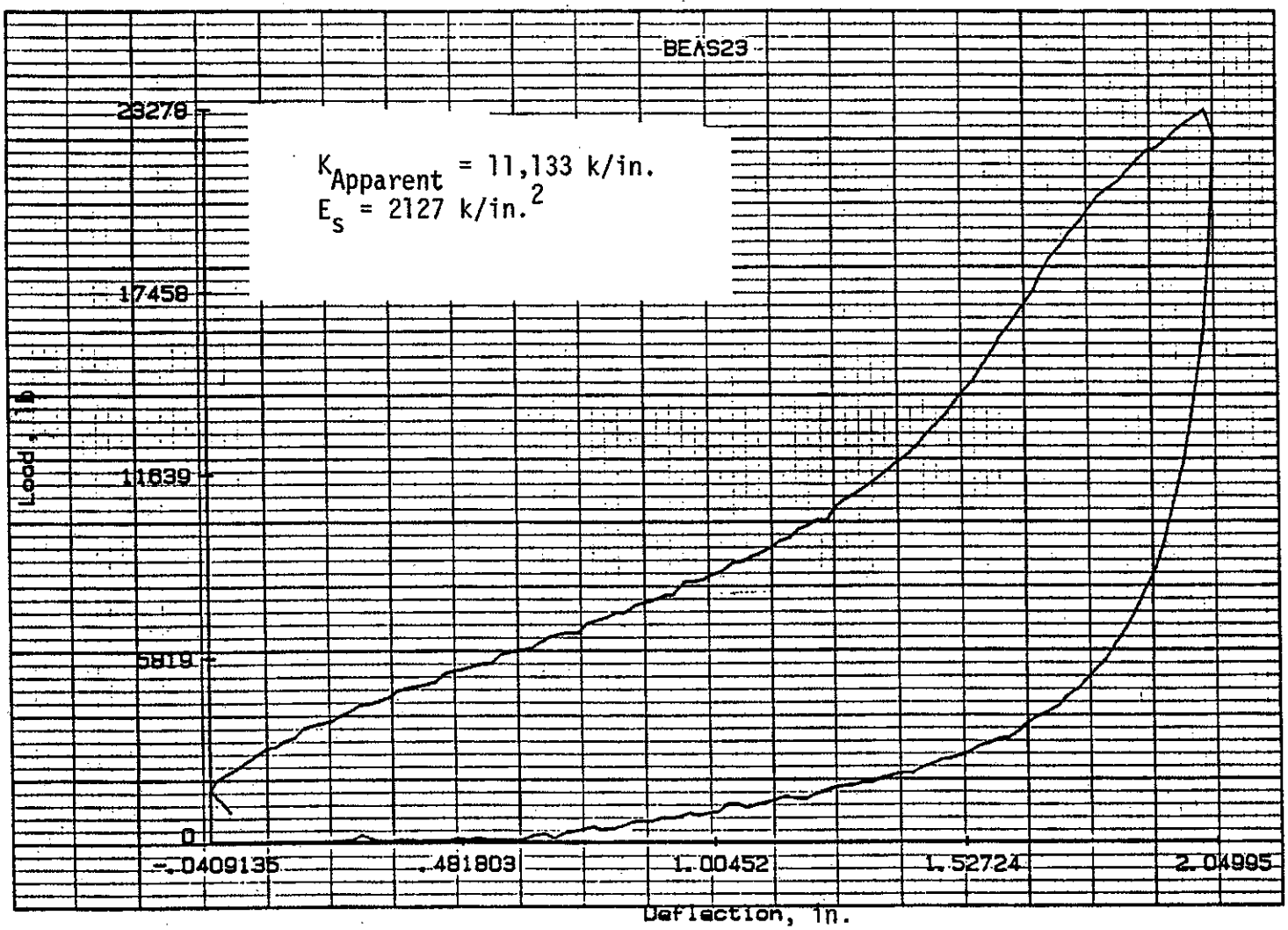

Figure 43. Test 23: 7 x 3 x 6 in. Rubber Cylinder, 35% Strain

APPENDIX C.

LOAD-DEFLECTION RESULTS

FOR ENERGY-ABSORBING POSTS

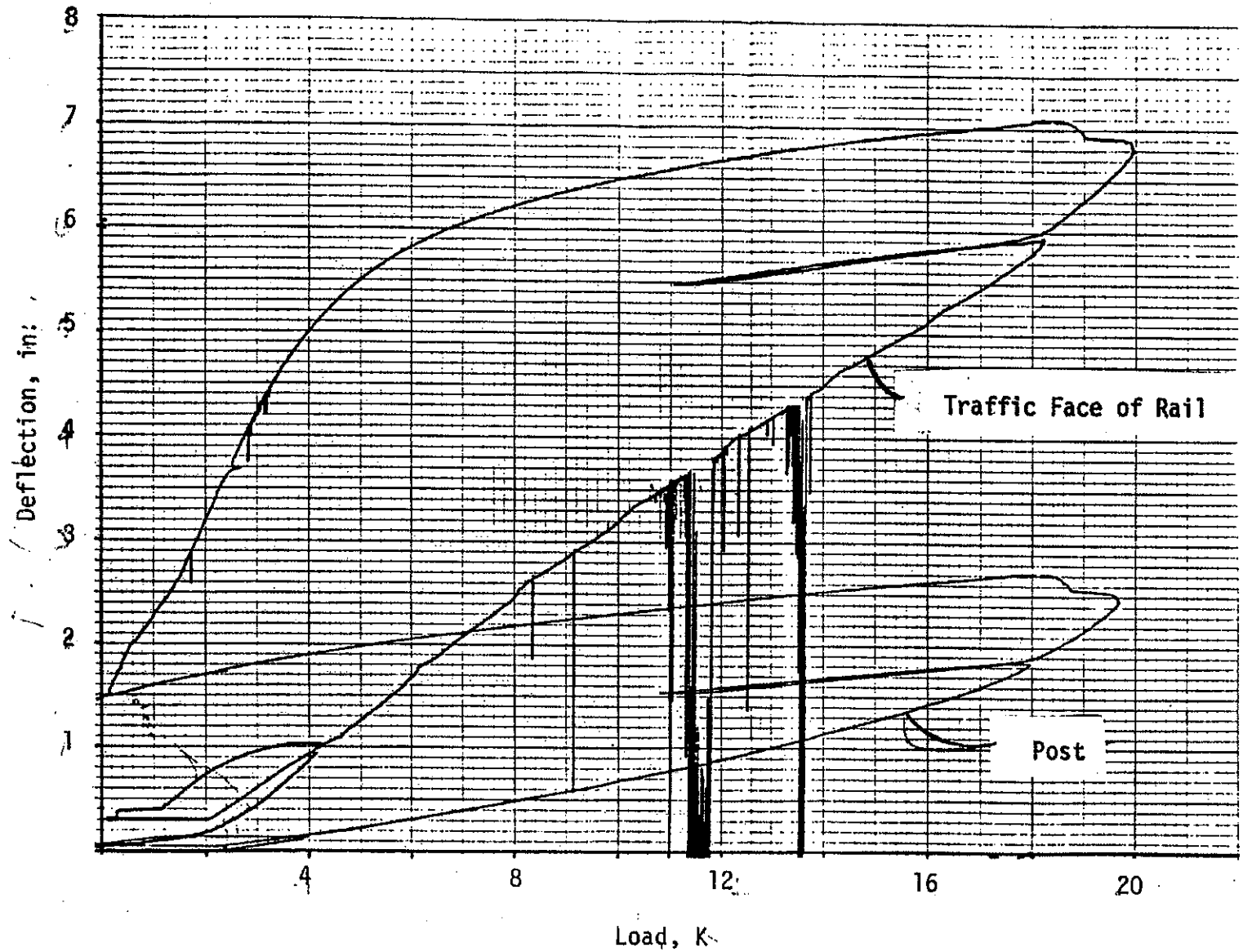

Figure 44. Static Post Test ST-1

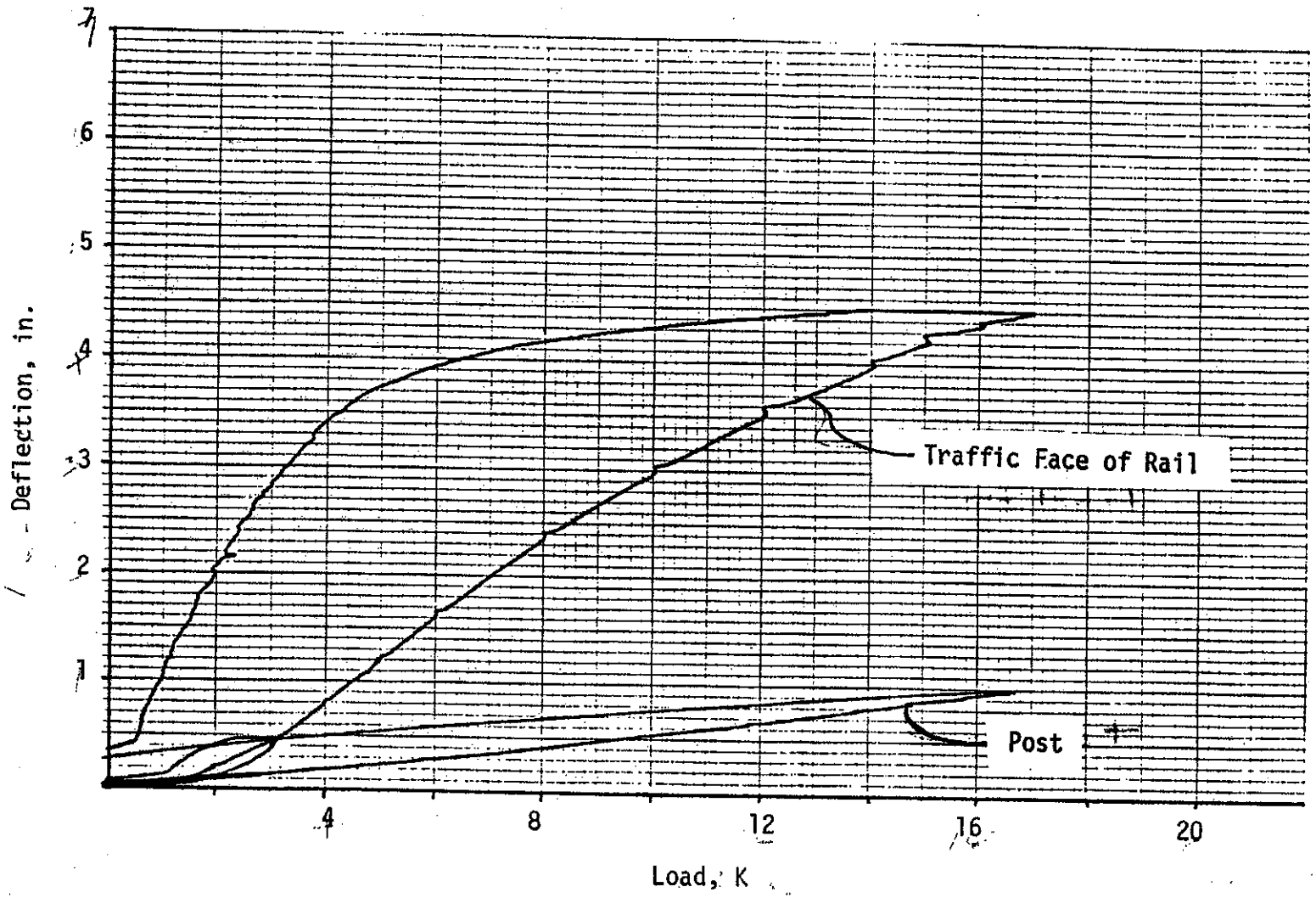

Figure 45. Static Post Test ST-2

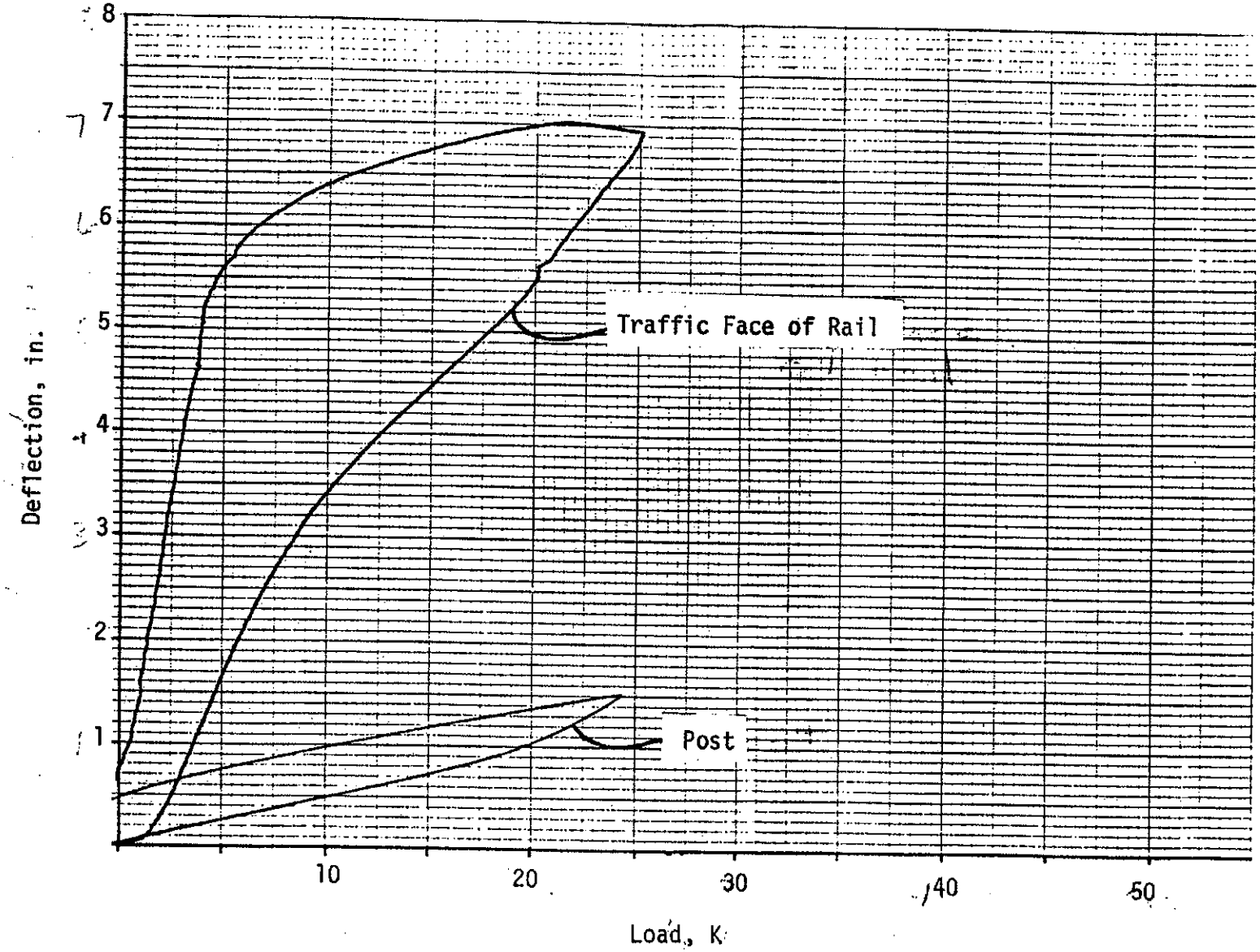

Figure 46. Static Post Test ST-3

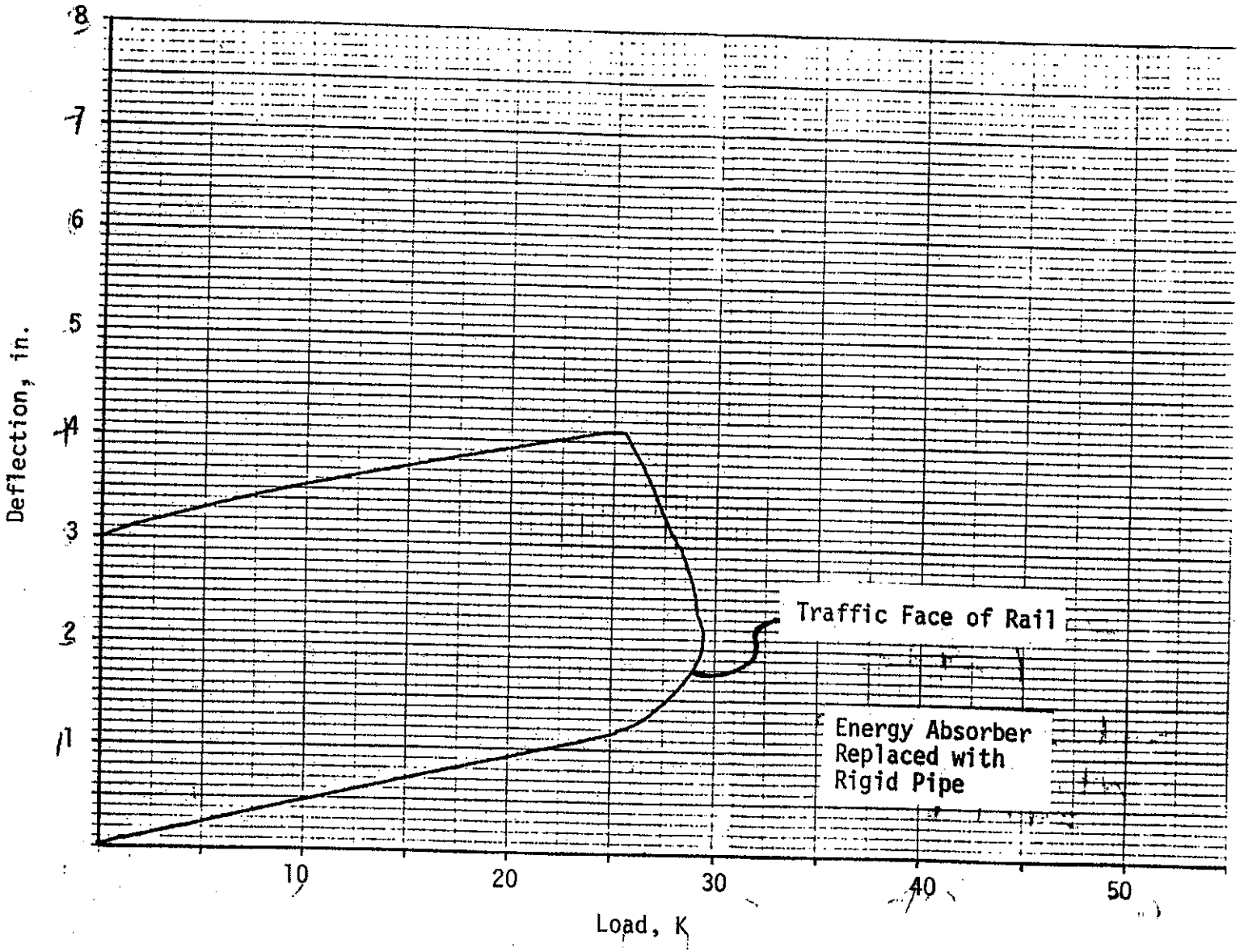

Figure 47. Static Post Test ST-4

APPENDIX D.

SEQUENTIAL PHOTOGRAPHS OF CRASH TESTS

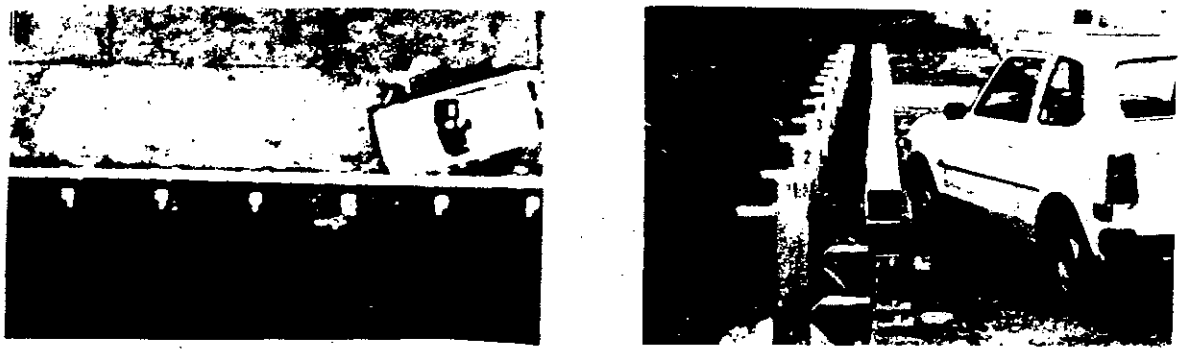

0.000 s

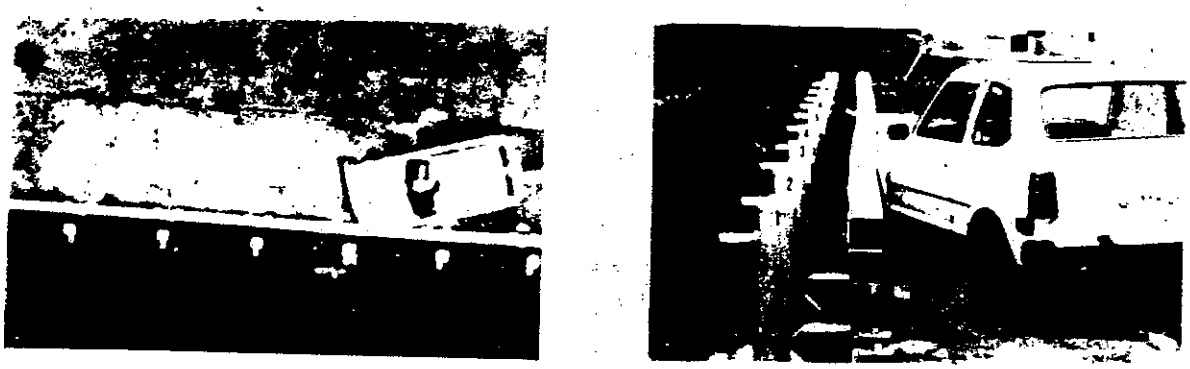

0.027 s

0.056 s

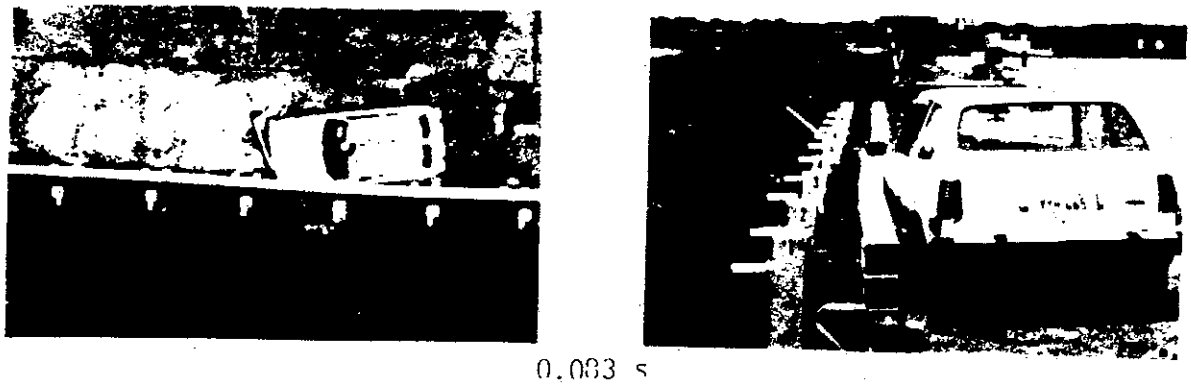

0.083 s

Figure 43. Sequential photographs for test 2417-1.

0.109 s

0.138 s

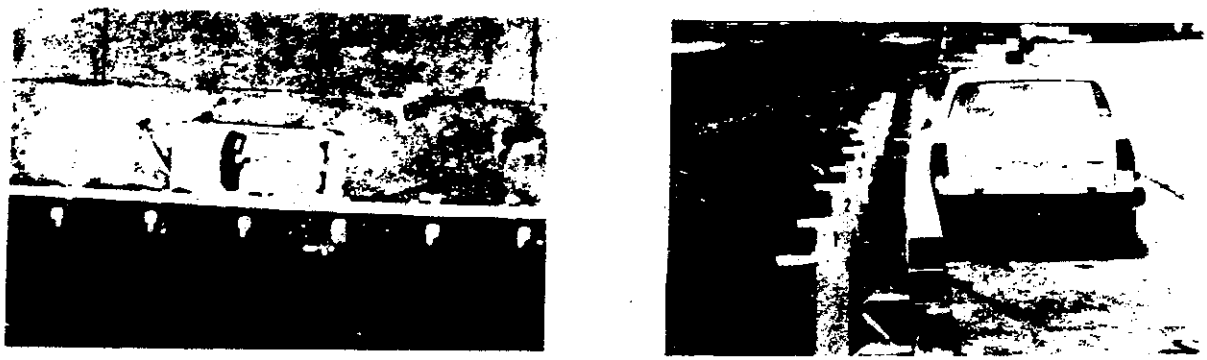

0.165 s

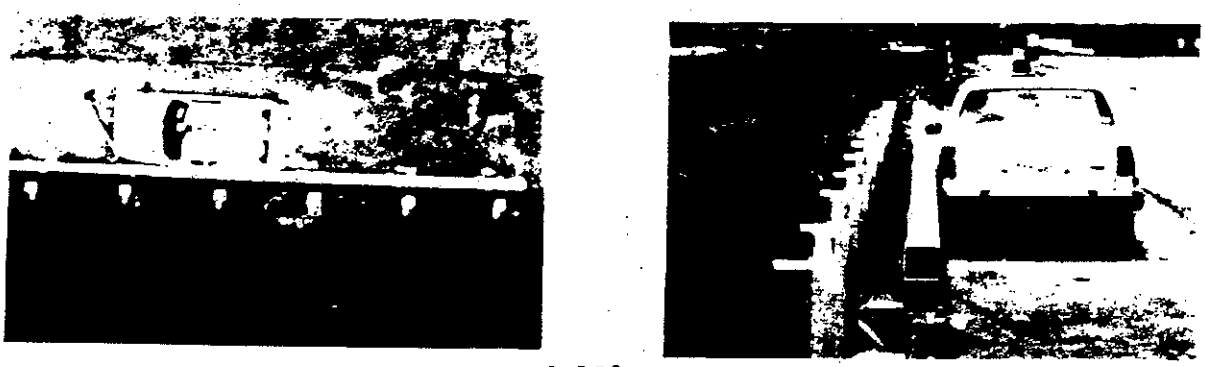

0.192 s

Figure 49. Sequential photographs for test 2417-1 (continued).

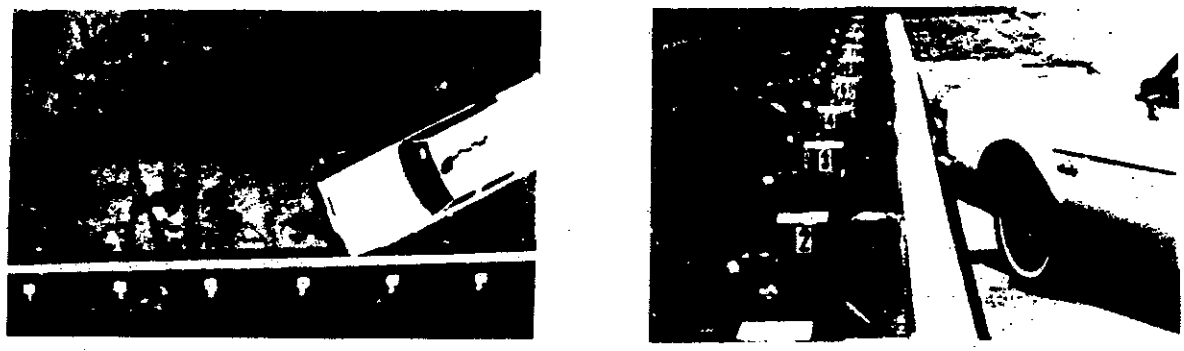

0.000 s

0.039 s

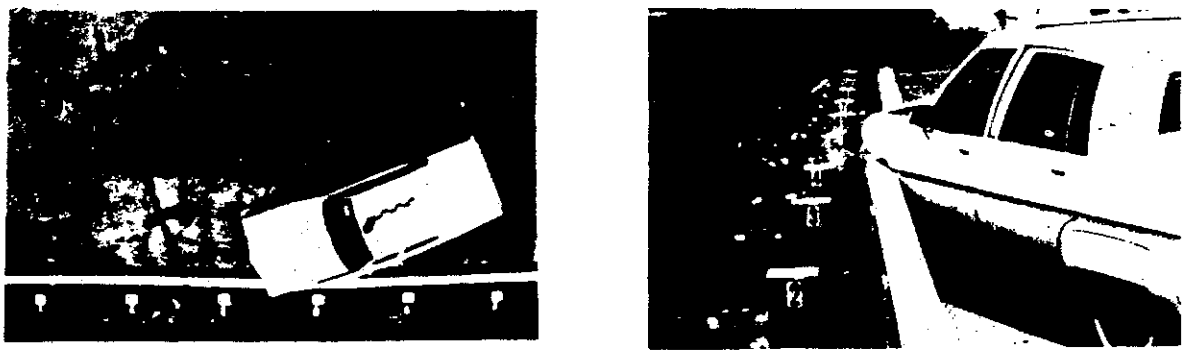

0.081 s

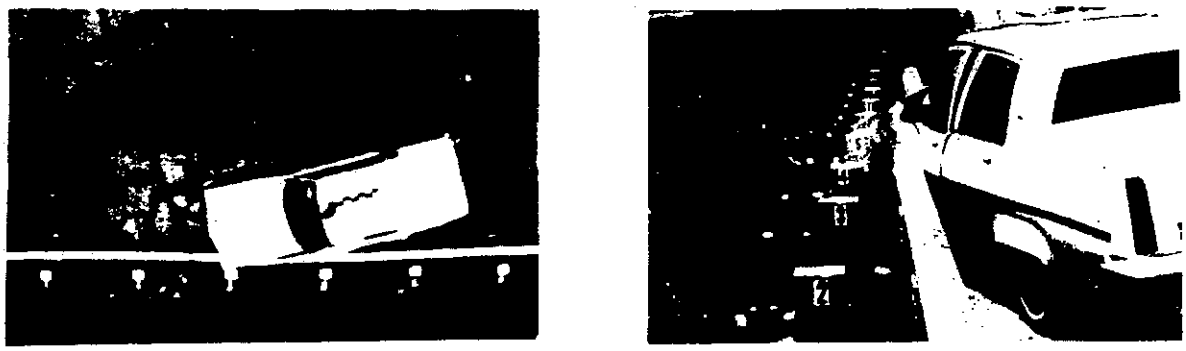

0.121 s

Figure 50. Sequential photographs for test 2417-2.

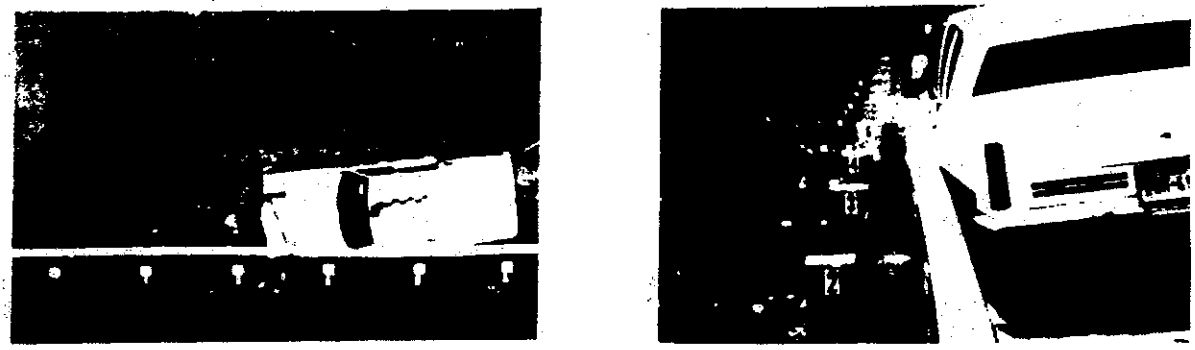

0.160 s

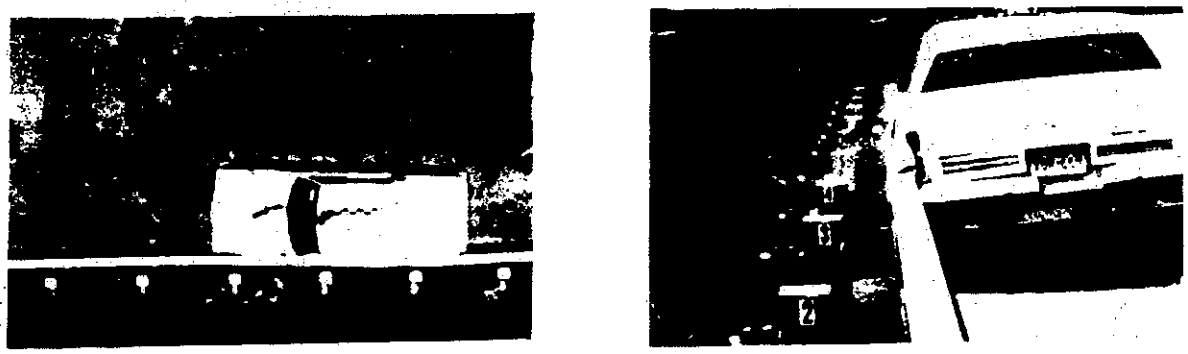

0.202 s

0.246 s

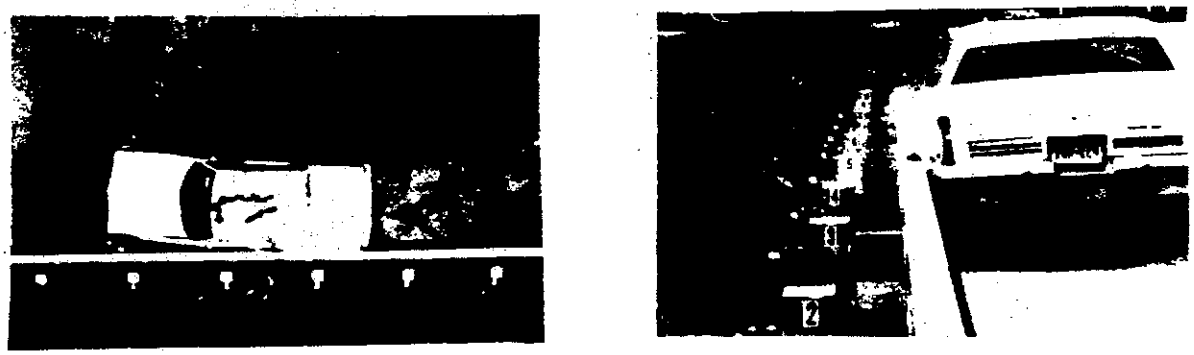

0.288 s

Figure 51. Sequential photographs for test 2417-2 (continued).

APPENDIX E.

ACCELEROMETER TRACES AND PLOTS OF ROLL, PITCH, AND YAW RATES

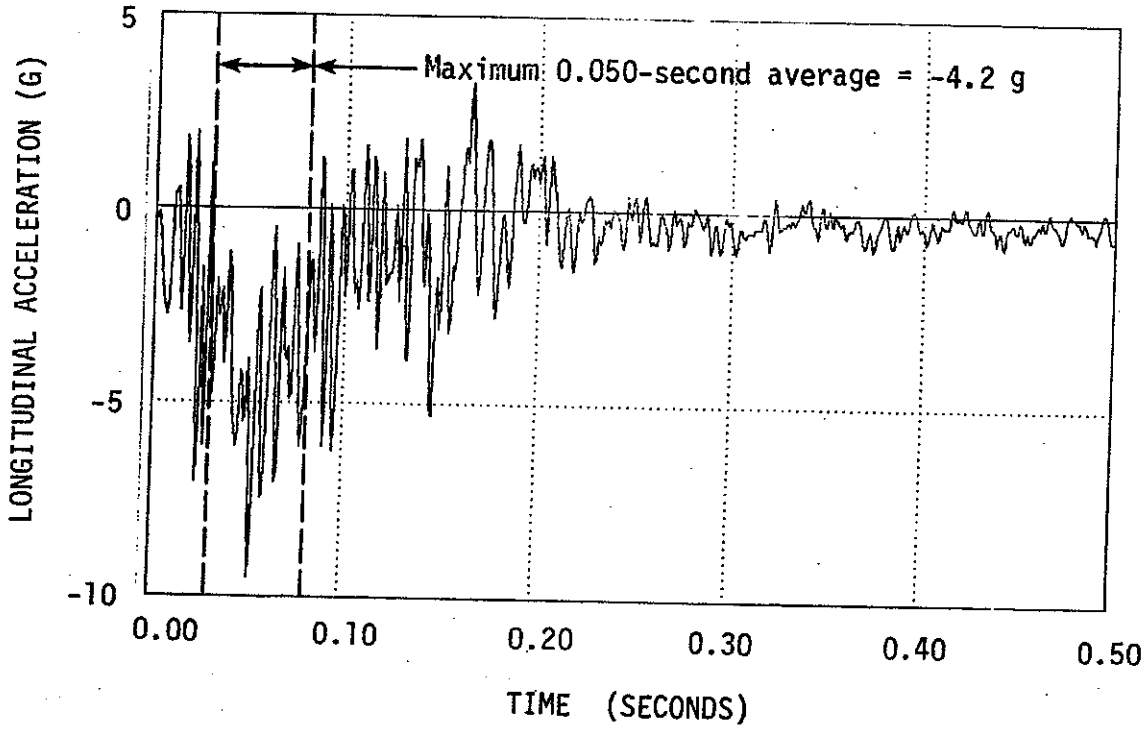

Figure 52. Vehicle longitudinal accelerometer trace for test 2417-1.

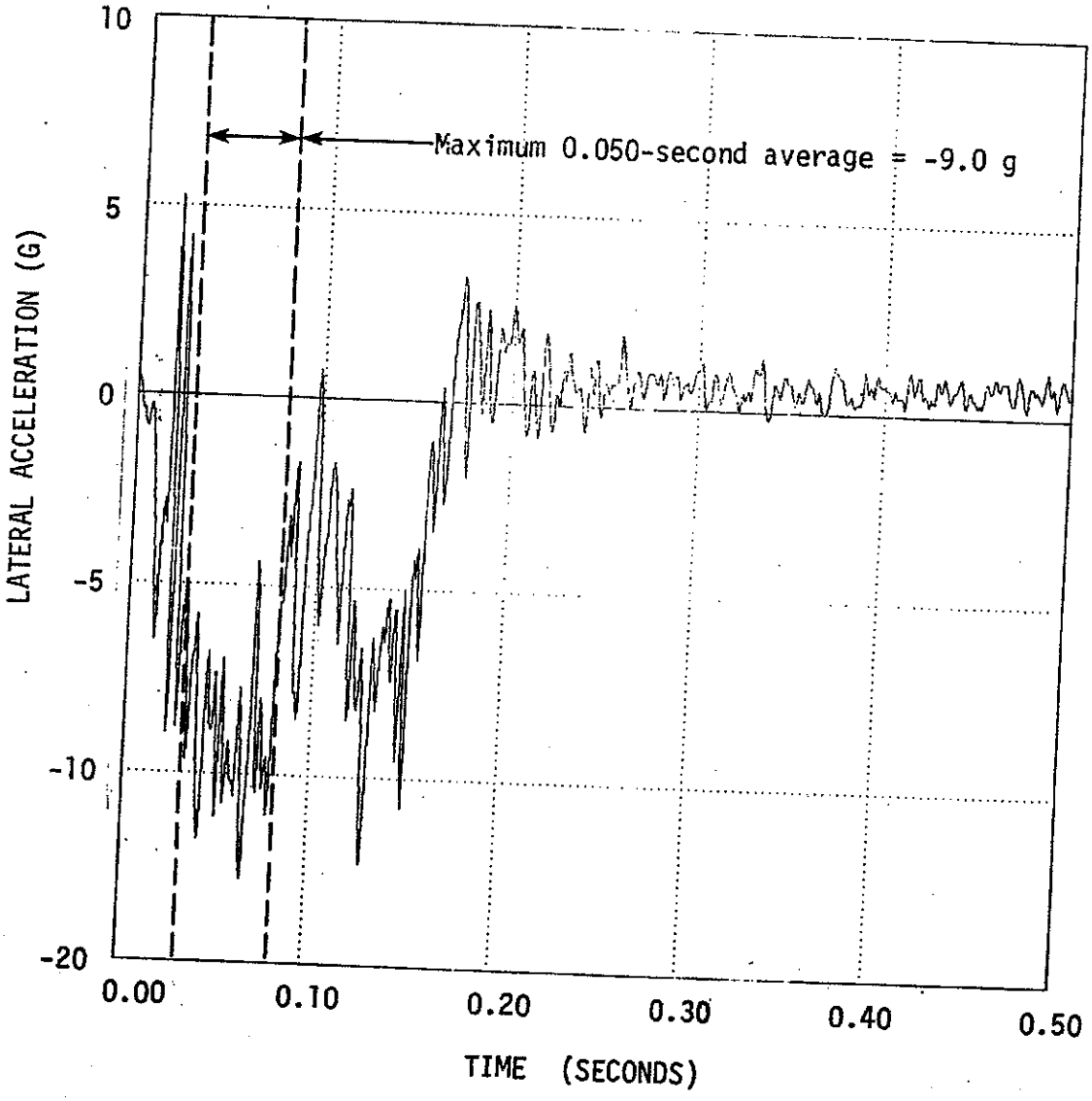

Figure 53. Vehicle lateral accelerometer trace for test 2417-1.

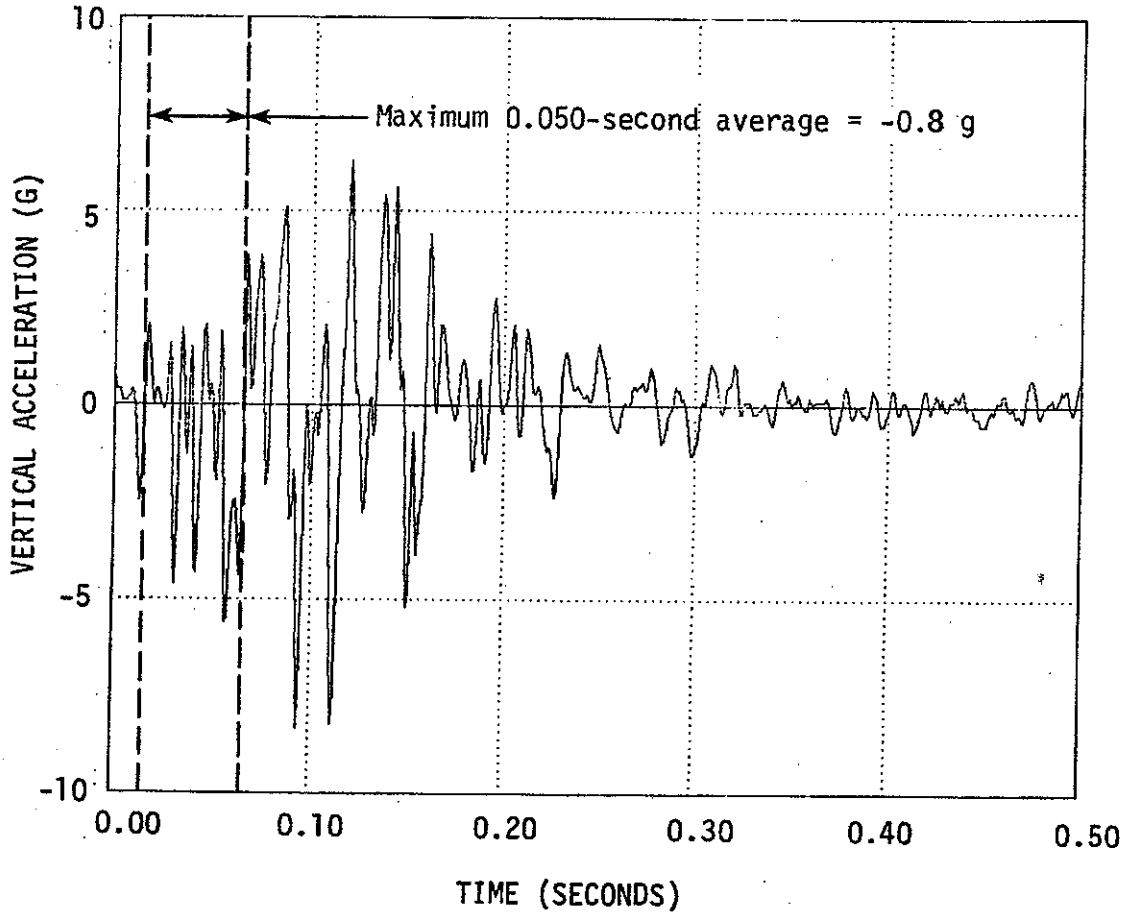

Figure 54. Vehicle vertical accelerometer trace for test 2417-1.

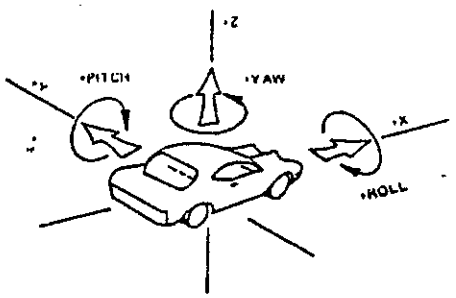

Axes are vehicle fixed.
Sequence for determining orientation is:

1. Yaw
2. Pitch
3. Roll

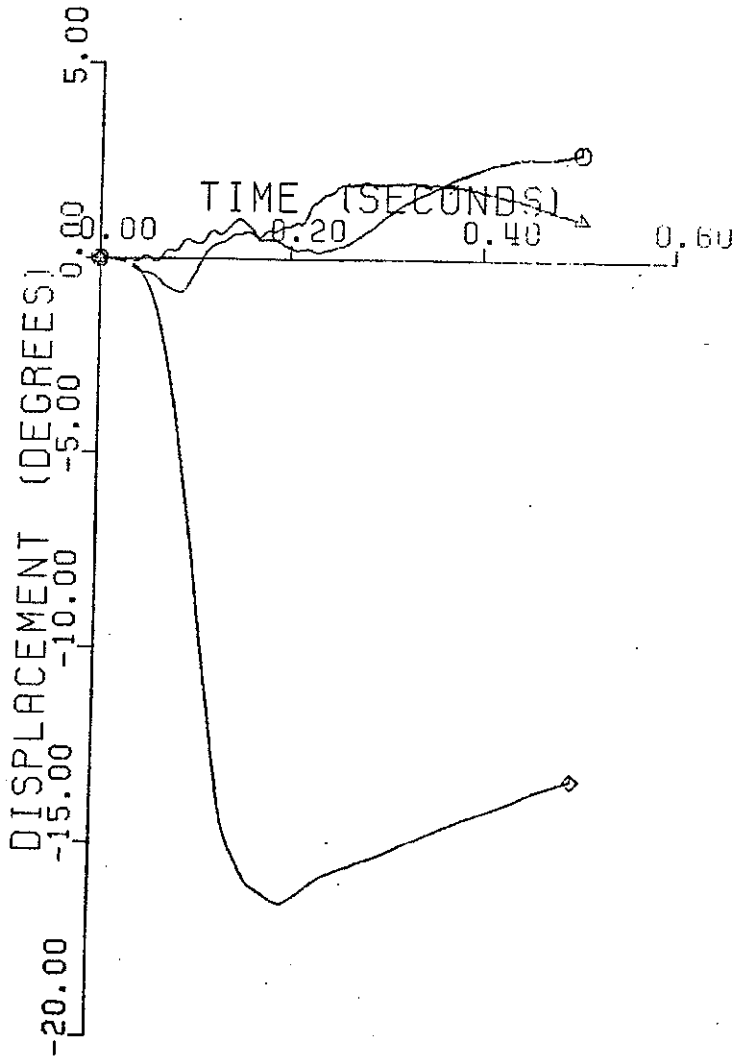

Figure 55. Vehicle angular displacements for test 2417-1.

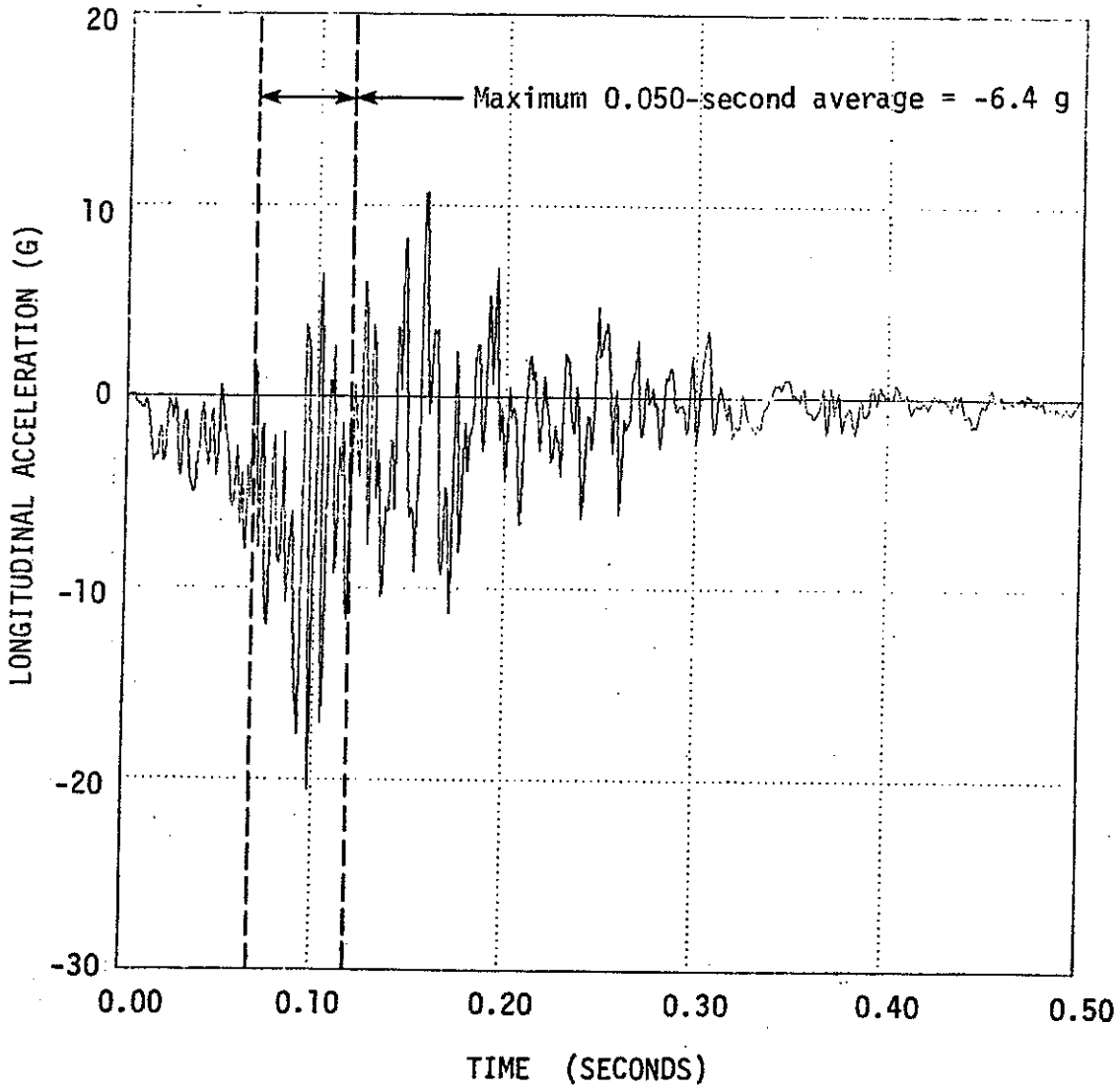

Figure 56. Vehicle longitudinal accelerometer trace for test 2417-2.

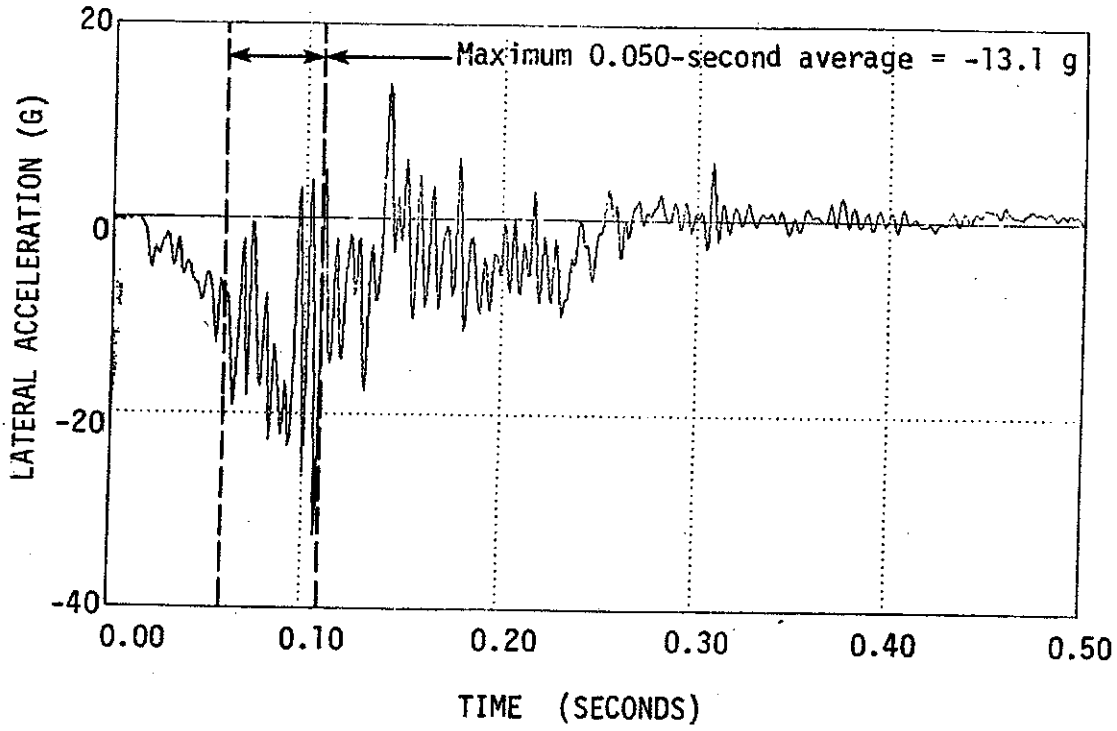

Figure 57. Vehicle lateral accelerometer trace for test 2417-2.

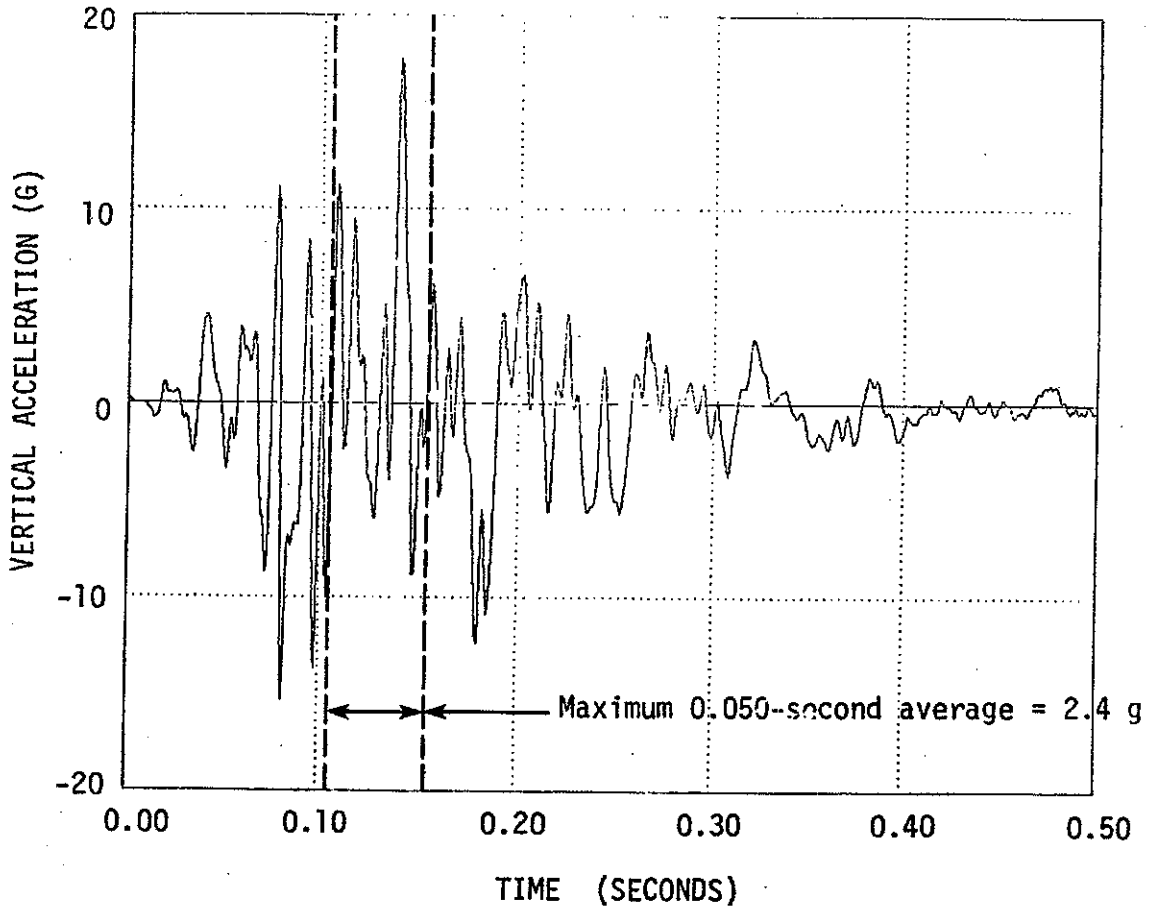

Figure 58. Vehicle vertical accelerometer trace for test 2417-2.

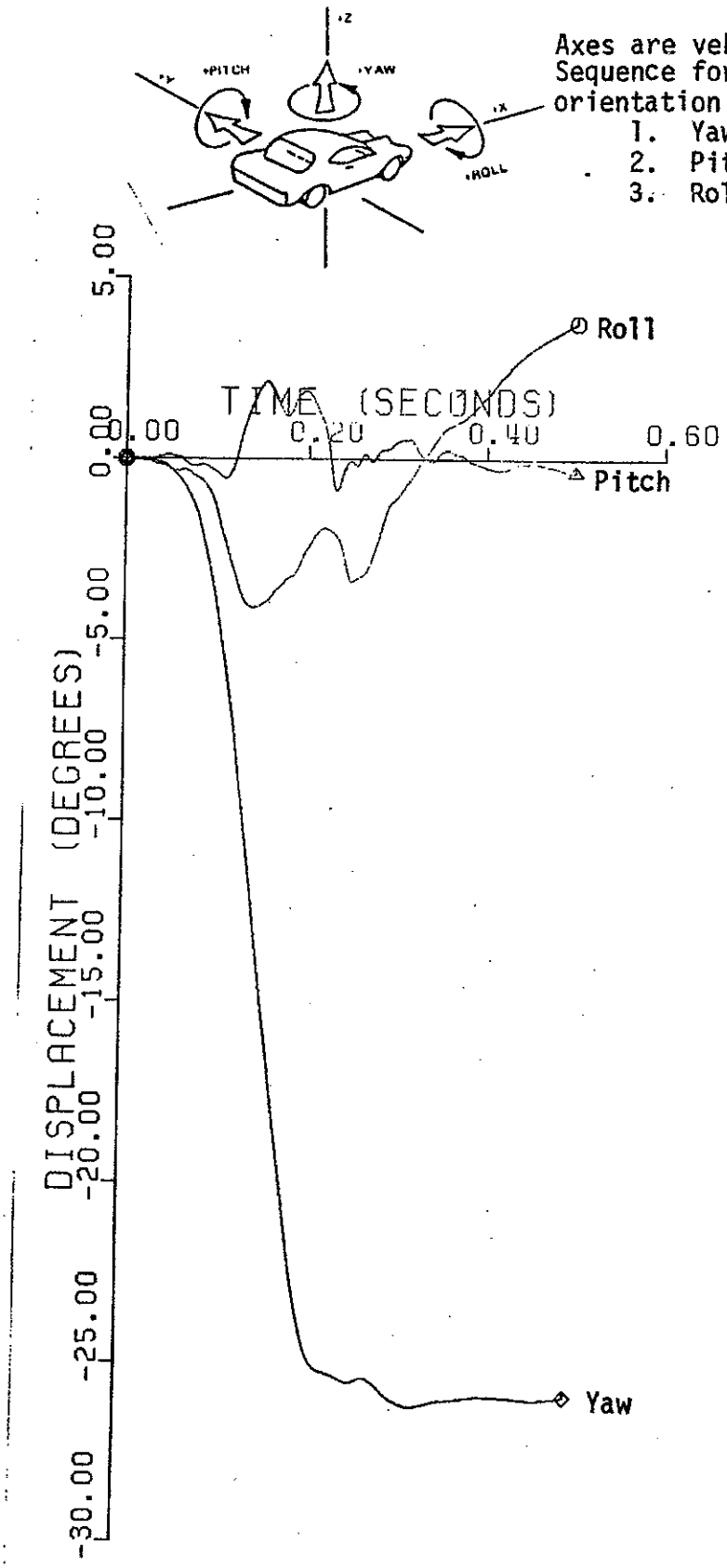

Figure 59. Vehicle angular displacements for test 2417-2.

REFERENCES

1. Cain, J. C., "Development and Testing of A Low-Maintenance, Energy-Absorbing Bridge Rail," Thesis presented to Texas A&M University, College Station, Texas, August 1985, in partial fulfillment of the requirements for the degree of Master of Science.
2. Michie, J. D., "Recommended Practices for the Safety Performance Evaluation of Highway Appurtenances," NCHRP Report 230, March 1981.
3. Beason, W. L., and Ross, H. E., "Development of a Truck-Mounted Portable Maintenance Barrier," Research Report 2262-5, Texas Transportation Institute, Texas A&M University, May 1984.
4. Strybos, J. W., Morgan, J. R., and Ross, H. E., "Emergency Opening System for an Authorized Vehicle Lane," Research Report 105-1F, Texas Transportation Institute, Texas A&M University, March 1984.
5. Powell, G. H., "Barrier VII: A Computer Program for Evaluation of Automobile Barrier Systems," FHWA-RD-73-51, Federal Highway Administration, Washington, D.C., March 1973.
6. Cain, J. C., Beason, W. L., and Hirsch, T. J., "Development of A Low-Maintenance, Energy-Absorbing Bridge Rail," Research report in preparation, Texas Transportation Institute, Texas A&M University.
7. Arnold, A., "Bridge Deck Designs for Railing Impacts," Research Report 295-1F, Texas Transportation Institute, Texas A&M University, Jan. 1984.
8. Buth, C. E., et al., "Safer Bridge Railings," Report FHWA/RD-82/072, Federal Highway Administration, June 1984.
9. Hirsch, T. J., et al., "Energy Absorbing Bridge Rail (Fragmenting Tube)," Technical Memorandum 505-8, Texas Transportation Institute, Texas A&M University, Feb. 1970.
10. Hirsch, T. J., and Buth, C. E., "Testing and Evaluation of Bridge Rail Concept," Final Report on Project RF 3053, Texas Transportation Institute, Texas A&M University, May 1975.
11. Kimball, C. E., et al., "Development of a Collapsing Ring Bridge Rail System," Report RD-76-39, Federal Highway Administration, Jan. 1976.
12. Stoughton, R. L., "Vehicle Impact Testing of a See-Through, Collapsing Ring, Structural Steel Tube, Bridge Barrier Railing," Calif. Dept. of Transportation, Office of Transportation Laboratory, Sacramento, June 1983.